(1)

Volume I

Optimization Study Report
on
Base Level Analyzer

Contract No. AF 33(657) 13866

Prepared for

Air Force Systems Command
U. S. Air Force
Wright Patterson Air Force Base, Ohio

5 January 1965

181

5322-FR

This document contains ____ pages
Copy # ____ of ____ copies

Volume I

Optimization Study Report
on
Base Level Analyzer

Contract No. AF 33(657) 13866

Prepared for

Air Force Systems Command
U. S Air Force
Wright Patterson Air Force Base, Ohio

6 January 1965

Prepared by: Peter N. Dadeney
Peter N. Dadeney
Program Manager

Approved by: William G. Langton
William G. Langton
Vice President,
Science & Engineering

BAIRD-ATOMIC, INC.
33 University Road
Cambridge, Massachusetts 02138

VOLUME I

TABLE OF CONTENTS

VOLUME I

TABLE OF CONTENTS (Cont.)

TABLE OF CONTENTS (Cont.)

VOLUME II AD 687 480

TABLE OF CONTENTS

VOLUME II

TABLE OF CONTENTS (Cont.)

VOLUME I

LIST OF TABLES

VOLUME II AD 687 480

LIST OF TABLES

VOLUME I

LIST OF ILLUSTRATIONS

LIST OF ILLUSTRATIONS (Cont.)

VOLUME I

LIST OF ILLUSTRATIONS (Cont.)

VOLUME II AD 687 480

LIST OF ILLUSTRATIONS

1. INTRODUCTION

This Optimization Study Report is submitted as deliverable Item I of Aeronautical Systems Division contract AF 33(657)-13866. The report establishes the specification and design of a simplified Base Level Analyzer (Lubricant - Contamination) that is capable of repeatable high accuracy when operated by Air Force personnel under all anticipated service conditions. The report includes a complete analysis of the proposed design, which is supported by data, graphs, drawings, and illustrations for clarification.

2. OBJECTIVES OF THE OPTIMIZATION STUDY

The prime objectives of the optimization study were to:

a. Establish the feasibility of meeting the detailed requirements of Exhibit "A" AF 33(657)-13866 dated 25 May 1964. The feasibility to be supported by analytical and experimental data.

b. Generate realistic, attainable specifications for a Base Level Analyzer (that deviate by a minimum amount) from the requirements of Exhibit "A".

c. Provide design information for two (2) prototype Base Level Analyzers capable of meeting the specifications generated under (b), the design being such that it can advantageously embody a growth capability while being economical to produce in quantity lots.

d. Establish a Reliability Plan for a total program.

e. Provide a Reliability Prediction for the optimized design based upon a detailed analysis.

f. Establish a Maintainability Plan for the total program.

g. Establish a Safety Plan for the total program.

3. SUMMARY

3.1 General Discussion

This report is best started by stating the basic requirements of the Base Level Analyzer system.

Paraphrased from section 3.0 Exhibit "A" these are:

a. The equipment must be capable of detecting contamination elements in lubricating oil in concentrations of between one and 500 parts per million.

b. The elements to be detected are: iron, lead, tin, silver, copper, chromium, nickel, silicon, magnesium, and aluminum.

c. The accuracy and precision of the instrument shall be such that the deviation from the true amount of any element present in a Standard Reference Specimen shall not exceed ± two parts per million or 10 percent, whichever greater.

d. The design shall be such that minimum training, calibration and maintenance will be required and that the equipment can be operated by airmen of the prescribed skill level.

e. The equipment shall be self-supporting and readily transportable and any recalibration necessary shall be performed by (Air Force) maintenance personnel.

f. The equipment shall be such that it can be readily maintained by Air Force personnel, i.e., the total maintenance hours for the equipment over its operating life shall not exceed 120 hours.

g. The design must be reliable and have an MTBF of not less than 150 hours.

h. There will be minimum safety hazard for operating personnel.

i. The operating temperature range of the equipment is 32°F to 130°F.

j. The analyzer design shall be such that environmental specification MIL-STD-810 Class III can be met.

k. The design shall meet the radio frequency interference specification MIL-I-26600.

The results of the optimization study show that the design that most closely meets all the Base Level Analyzer requirements is a 1-meter emission grating spectrometer that uses a constant digital reference technique, digital data processing, and all solid state electronics (figures 3-1, 3-2, and 3-3).

Some unique features of the design are:

a. All environmental conditions can be met.

b. Automatic line position adjustment to compensate for temperature, and humidity effects in the optical system.

c. Automatic focus adjustment to compensate for linear expansion in the optical head.

d. Dark current cancellation.

e. Manual control to compensate for pressure changes.

f. Double electrostatic shielding around all radio frequency interference generators, with the outside console being a complete continuous shield with gasketing on all removable parts.

g. Hermetic sealing of all humidity sensitive components.

h. Thermal isolation of the complete optical system.

i. Capable of rapid alignment.

j. Digital readout.

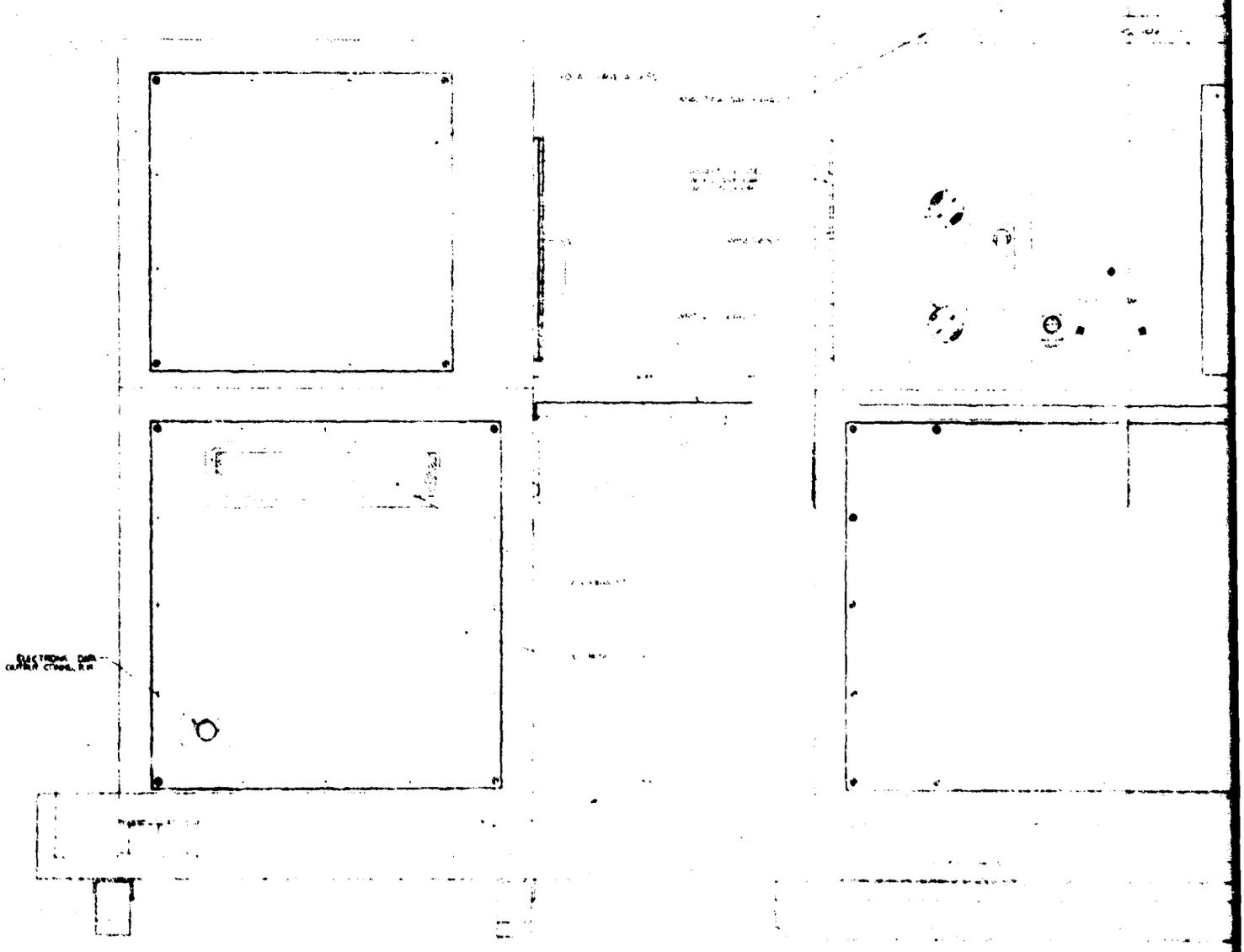

A

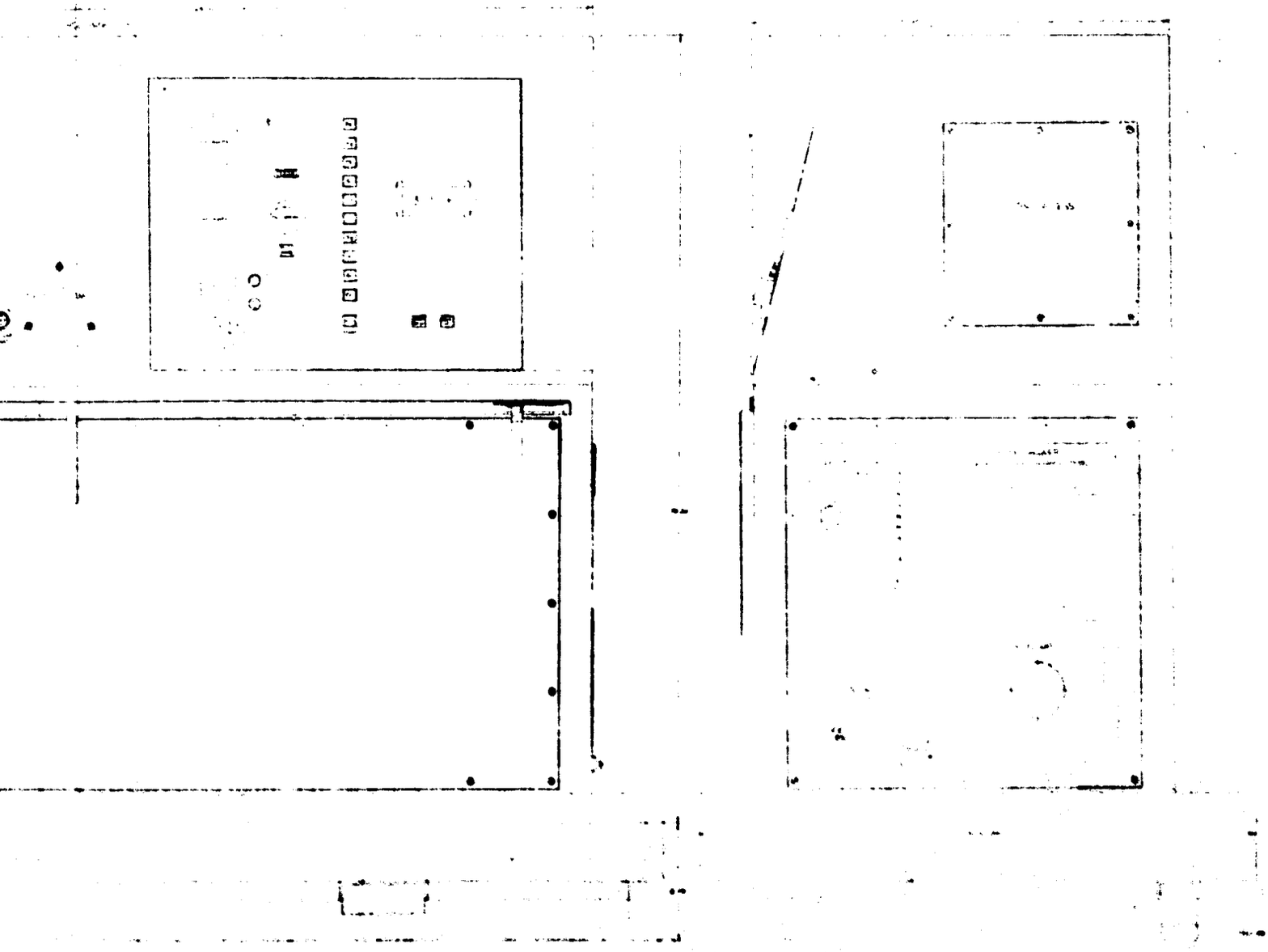

Figure 3-1. Base Level Analyzer Assembly

B

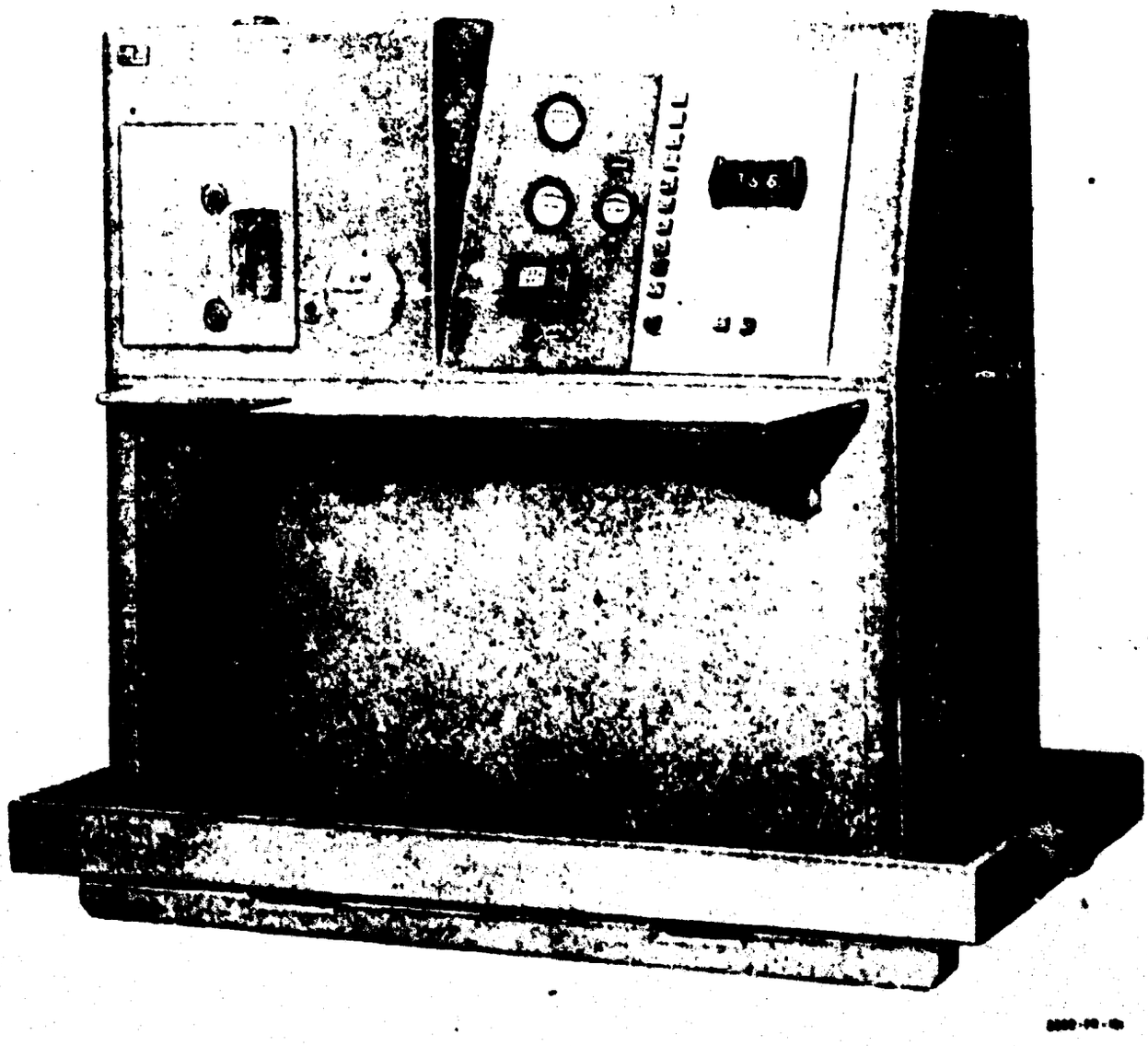

Figure 3-2. Base Level Analyser, Artist's Concept

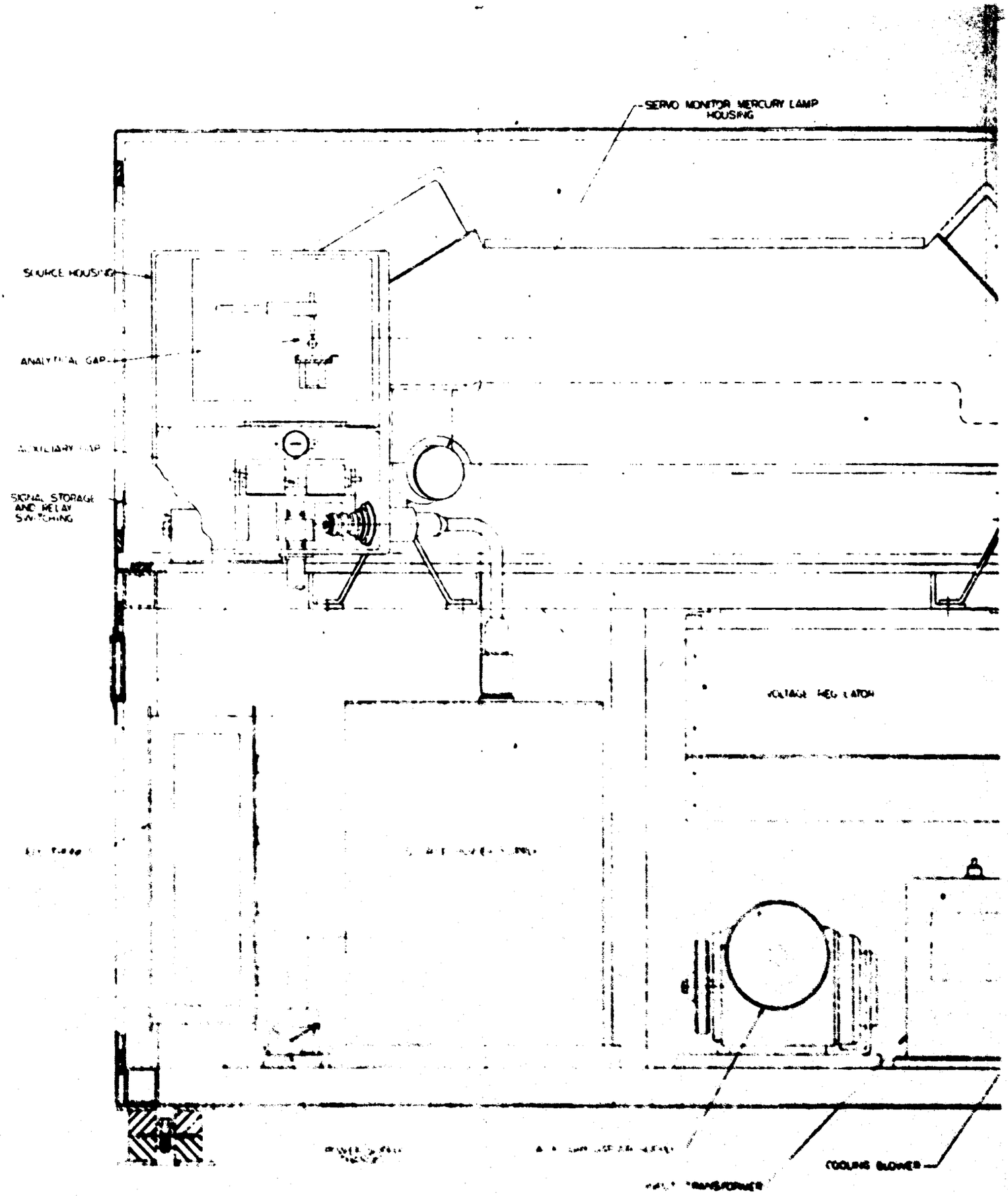

Figure 3-3. Base Level Analyz

A

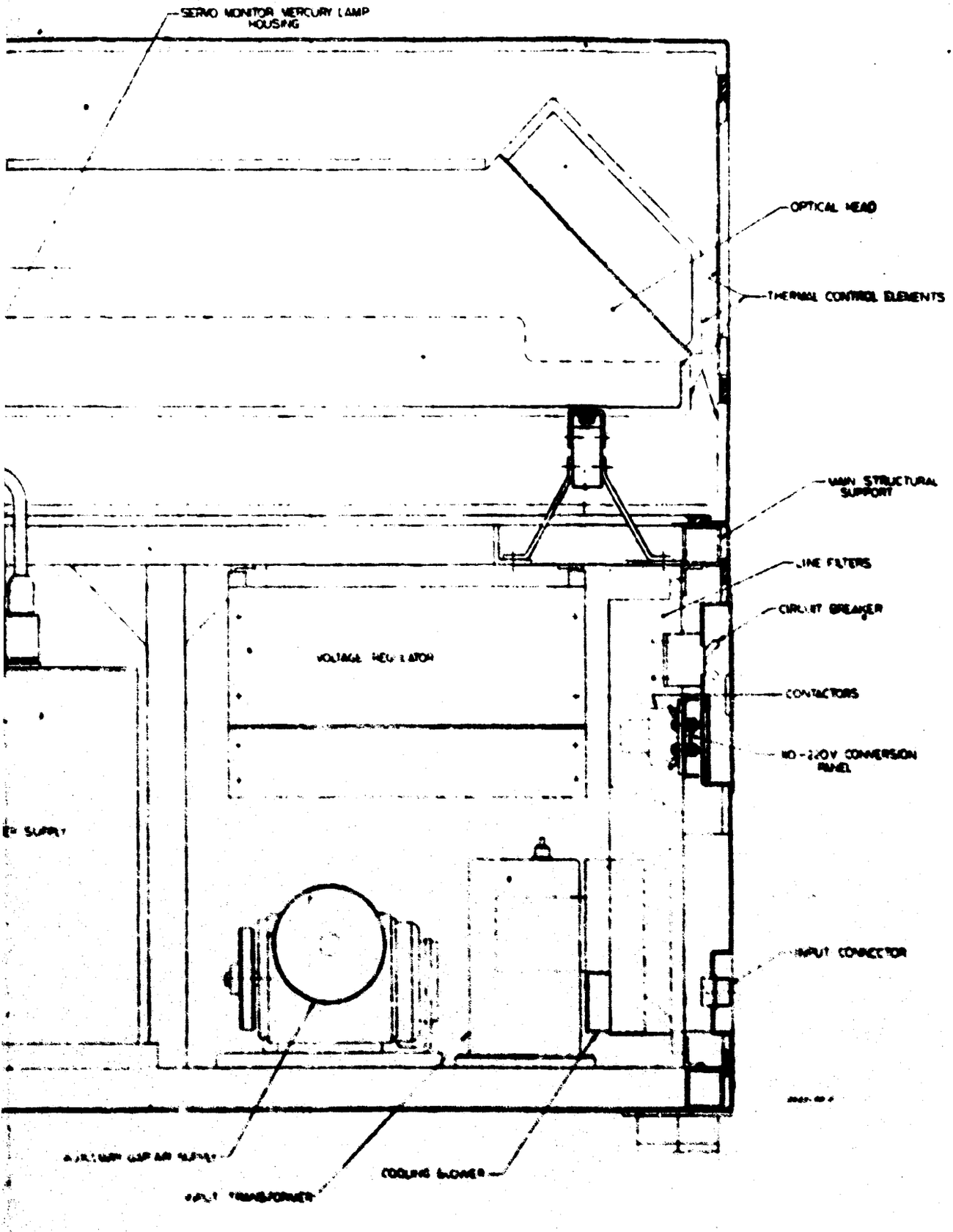

B

Figure 3-3. Base Level Analyzer, (Front View Cross Section

The physical characteristics of the equipment, including the transit case ready for shipment, figure 6-38, are:

Height	71 inches
Width	72 inches
Depth	40 inches

And the total weight is 993 pounds.

This study was started based upon the premise that a 1-meter emission spectrometer was capable of meeting the design requirements of a Base Level Analyzer. This premise has, with a few exceptions, been fully substantiated and proven. The only area where the requirements of Exhibit "A" cannot be met is concerned with basic oil chemistry and lack of oil standards and is completely independent of instrument technique or design. No attempt has therefore been made to consider other analysis techniques (atomic absorption, etc.) or designs.

In relating this study to the existing state of the art, it is perhaps well to make a direct but informal comparison between a commercial spectrometer and the specific Base Level Analyzer. A commercial emission spectrometer is a specialized instrument operated by a skilled technician in a controlled environment, whereas the specified Base Level Analyzer is a tool to be operated by semi-skilled personnel under extremes of environment while having equal or better accuracy than that currently available.

The design of a 1-meter spectrometer for use under standard commercial conditions (air conditioned room) presents no major difficulties, except for oil chemistry limitations; however, the design of such an instrument to meet the specified shock, vibration, radio frequency interference, and environmental conditions presents major design problems

To preclude the possibility of "re-inventing the wheel", a literature search was conducted to ascertain what had previously been accomplished with similar instruments under the specified conditions. The search revealed that a design of this nature had never before been attempted.

In the specification of the equipment, considerable emphasis has been placed on accuracy (repeatability), not just over a short period (day) but over extended periods (months). Additionally, it is a requirement that it be possible to fabricate replica equipments having identical accuracy characteristics. The submitted design will meet these objectives and will make it possible to measure an oil sample (on separate equipments) in either Florida (hot and humid) or Colorado (cold and dry) and get identical results within the accuracy limits specified thus providing the basis of a well correlated engine analysis and maintenance program using contaminant trend analysis techniques. In addition, it opens up the real possibility of oil standardization and the establishment of oil contaminant standards, neither of which exist at the present. It is not inconceivable to believe that in the future manufacturers of new engines will be required to provide contaminant trend analysis data as part of final acceptance material.

Once the full impact of the environmental specifications had been fully analyzed in terms of system performance, and design criteria had been established, the necessary control and compensations systems were developed and the design concluded. It is to be noted that the subject design is based to the maximum amount possible upon techniques that have been proven by many years of experience with commercial instruments. New techniques have been utilized only when significant improvement in system performance can be achieved, where cost can be reduced, and only when the technique has survived a rigid performance analysis.

The total design has been the subject of a complete reliability analysis and the predicted Mean Time Between Failure (MTBF) is 15 times better than that specified, resulting in a high degree of confidence both in the ability of the system to perform and in low maintenance costs. In order to summarize in more detail the salient point of the study, the following aspects will be discussed separately:

a. Contaminant Analysis

b. Environmental Effects

c. Reliability, Maintainability, Safety

3.2 Contaminant Analysis

In considering the problem of oil contaminant analysis as related to designing equipment to meet the requirements of Exhibit "A" where it is stated "that the equipment shall measure the true amount of an element contained in a Standard Reference Specimen" (paragraph 3.2a) it is necessary to obtain answers to a number of basic questions namely -- What is the contaminant purity of a base oil and to what standard is it made? Are there approved contaminant standards available and what is their accuracy? Is there an approved method for generating such standards? In order to obtain the necessary answers, a survey was made of Government, industry, and academic institutions with the following results:

a. The contaminant purity of base oils (including medicinal mineral oil) is unknown except in a most general manner.

b. Oils are produced to gross standards well outside the limits specified for the Base Level Analyzer.

c. There are no nationally approved oil contaminant standards in existence.

d. There is no nationally approved method for producing such standards.

In addition to the survey, Baird-Atomic solicited samples of "Standard Reference Specimens" from a number of highly respected laboratories, namely, Pensacola, Analysts Incorporated, Analyst of Puerto Rico, and Dr. Ice, University of California. These specimens were analyzed and they showed a complete lack of correlations between published and measured contamination levels. Further, Baird-Atomic manufactured many standards to the method outlined in National Bureau Standard Monograph 54 and obtained similar varied results.

From the above it can only be concluded that, at this time, it is impossible to measure "the true amount of an element contained in a Standard Reference Specimen". Baird-Atomic, therefore, takes exception to paragraph 3.2a, Exhibit "A".

It should be noted that this is the only fundamental exception in the submitted design, all other deviations are in limits and tolerances, as will be explained. As an alternative to paragraph 3.2a, Baird-Atomic recommends that the design be based on a standard deviation about the average value (for ten analyses of a single sample) of the specified contaminants where Baird-Atomic will provide the necessary standards prepared according to the National Bureau of Standards procedure using 7808 oil as a base.

It is to be noted that this alternate specification in no way destroys the accuracy (repeatability) requirements of the specification. Based on the above specification (which was discussed with Wright Patterson Air Force Base personnel and received verbal technical approval), a statistical analytical study and a mathematical system error analysis were performed to establish the feasibility of meeting the alternate requirement. The statistical study involved the production of three groups of the aliquot specimens which were analyzed (on the Baird-Atomic Research Direct Reader Spectrograph) ten times per specimen for a total of three hundred data points. This

data was then processed on an IBM 1620 computer to establish the standard deviation about the average, resulting in the graphs, to be found in appendix A. These graphs together with the mathematical error analysis and National Bureau of Standards information are the basis for the performance specifications to be found in section 5.0.

National Bureau of Standards is referred to as an authority that claims that not more than 200 parts per million of silicon can be placed in solution.

Where limits and tolerances have been redefined with respect to Exhibit "A", it will be the aim of Baird-Atomic to meet the original specification but as a design goal only.

3.3 Environmental Conditions

A detailed analysis of the effects of the applicable environmental conditions specified in both Exhibit "A" and MIL-STD-810 sheltered equipment showed that the three environmental conditions that most effect the accuracy and performance of the system are temperature, pressure, and humidity. The portion of the system that is most severely affected by these conditions is the optical head, the heart of the system, where each condition produces both a lateral shift and a dispersion shift in the optical path. In addition, temperature produces another undesirable effect, namely defocusing. All of these effects cause considerable system degradation and must be compensated for if specified performance is to be achieved.

To compensate for lateral shifts, a closed servo monitor system has been included in the design. This system monitors the position of a reference emission line, and as this line shifts laterally, an error signal is developed which rotates a deflector plate and drives the reference line back to its correct position, hence correcting the entire spectrum. Focus changes are controlled by an open loop focus servo system which alters the optical pathlength by inserting varying thicknesses of calcium fluoride in the path of the emitted light where the calcium fluoride thickness depends on the mean temperature of the optical head.

The compensation for pressure requires that the grating be moved 0.003 inch down the mean dispersion axis of the optical system for a change in altitude of 0 to 10,000 feet. Since it is not necessary to adjust the position of the grating mount continuously due to ambient pressure changes, this system has not been made automatic. Compensation is achieved by means of a manual control to which there is ready access from the side of the console. In addition to its effect on the optical head humidity presents a problem in the main console where it can cause leakage in high impedance circuits (integrator capacitor) and arc over in the high voltage supply. These effects have been reduced to insignificant levels by the simple expedient of hermetically sealing all high impedance circuits and by ensuring that the interior of the equipment is operated at a higher temperature than the incoming air thereby preventing condensation. It is to be noted that no exceptions will be taken to the environmental conditions.

3.4 Reliability, Maintainability, Safety

A detailed reliability analysis and subsequent prediction for the system shows that the MTBF of the system is 19 times better than that specified for 8.4 samples per hour and 6.3 times better for 60 samples per hour. The reliability for 60 samples per hour was calculated in order to establish that the system met or exceeded the specification even if automatic electronic readout were added to the system. All reliability information has been based on:

a. Published Reliability Data
b. Failure Rates Quoted by Suppliers
c. MIL Handbook 217
d. Best Engineering Estimates

Since the reliability of the system is substantially better than that specified, it is anticipated that there will be no problem to meeting the maintainability goals. Every effort has been made to build in maximum maintainability, i.e.,

test points, panel meters, and oscilloscope. In addition all circuitry is constructed on plug in printed board where there is access to all sides.

4. SYSTEM ANALYSIS

4.1 General System Discussion

This portion of the report describes the functional operations which must be performed in an oil analysis system having a direct readout. It also outlines the methods that Baird-Atomic, Inc., has chosen to instrument each operation. Reasons for some of the more important design decisions are presented.

In brief, the operation of the Base Level Analyzer is as follows:

a. Excite the impurity atoms in the oil sample

b. Collect, disperse, and measure the emitted radiation at selected and representative wavelengths

c. Convert the voltage measure of emitted radiation to a voltage measure of impurity concentration

d. Convert the latter voltage to a form suitable to the user

The functional block diagram of the Base Level Analyzer is presented in figure 4-1. It shows the emission source, consisting of oil sample, analytical gap, and source power supply; the optical head including the fore optics, entrance slit, diffraction grating, exit slits, photodetectors and integrators; the data converter which changes integrated emitted light data to impurity concentration data; and the readout which presents the impurity concentration data to the user in convenient form. Also shown is the Analyzer's brain, the program timer, which regulates all other functions

The spectrometric source is discussed in paragraph 4.1.1, while paragraph 4.1.2 describes the optical head. The basic data handling approach, using a constant digital reference followed by analog data conversion is explained in paragraph 4.1.3. Paragraph 4.1.4 covers the digital data readout.

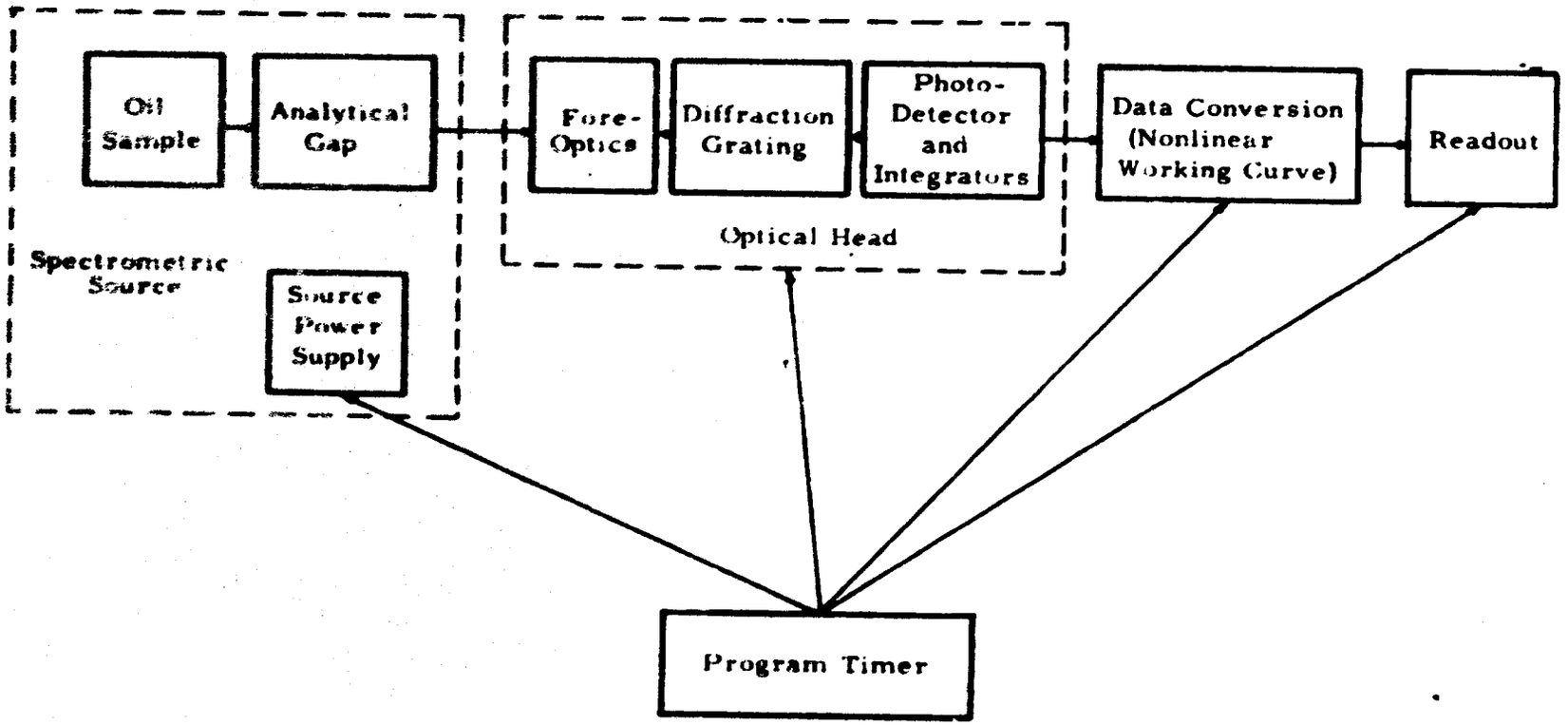

5322-FR-102

Figure 4-1. Base Level Analyzer, Functional Block Diagram

4.1.1 Spectrometric Source

The Base Level Analyzer employs a spectrometric light source consisting of oil sample, analytical gap, and source power supply. The oil sample is contained in a porcelain boat and is carried to the analytical gap by the lower electrode, a graphite disk rotating through the oil in the boat at 30 rpm. Spaced 3 millimeters from the disk is the upper electrode, a 1/4-inch graphite rod. As the oil passes through the gap, its impurity content is excited by a high inductance a-c spark, the characteristics of which have been experimentally selected for maximum excitation of the difficult elements to detect, such as lead and tin, while avoiding ignition or splashing of the oil. Burn times are kept reasonably short, of the order of 20 seconds, and the reproducibility obtained is good.

A detailed discussion of the source and the experimental work leading to selection of the source parameters is given in paragraph 4.2.2.

4.1.2 Base Level Analyzer Optical Head

The source energy is imaged on the diffraction grating by the fore optics, a plano-convex quartz lens. The lens parameters are chosen so that the image of the source is smaller than the active area of the grating and so that the entrance slit is well within the illuminated solid angle. This method of partially-coherent illumination insures that minor optical misalignments will not affect the detected signal level.

The diffraction grating itself has a 1-meter radius and has 1667 lines per millimeter (42,400 lines per inch). It is mounted in a modified Eagle mount and gives 6A per millimeter resolution. Spectral coverage is 2200 to 4300A in first order.

A 1-meter grating has been selected for the Base Level Analyzer primarily because it leads to an instrument only about one third the size of that using the

conventional 3-meter optics and hence is much more convenient. The use of the smaller optics is possible primarily because the oil analysis problem presents a simpler and less crowded spectrum than is encountered in iron and steel analyses where 3-meter instruments are conventional. The simpler oil analysis spectrum can easily be handled with linear resolution at the focal curve of 6A per millimeter and the increased resolution of a longer focal length instrument is not required.

The actual resolution of the Base Level Analyzer has been determined from photographic and other data to be 0.4A (paragraph 4.2.4). This resolution requirement is exceeded by the Analyzer which, with a 50-micron entrance slit and 25-micron exit slit, has calculated resolution of 0.225A. Again the widely different choice of widths for entrance and exit slits gives some immunity to changes in optical alignment.

The exit slits are 14 in number, 10 being 25 micron slits for the 10 elements being analyzed, one 25 micron slit for the tilt-normal, two special 1000 micron slits for the optical alignment servo and a 200 micron slit for the reference line. These slits are arranged on a segment of the Rowland circle and are all backed by 1P28 photomultiplier tubes.

The optical head also includes the integrating capacitors charged by the photomultipliers plus switching relays associated with the capacitors. These electronics have been made part of the optical head in order to better control the surrounding environment and to keep the low level signal connections short.

The reference line chosen for the Base Level Analyzer is background at 3897A. The 200-micron slit represents 0.75A at this wavelength and contains no interferences. More than half of the total background light at this wavelength comes directly from the oil itself, rather than from the graphite electrodes. Hence, the chosen reference is a good measure of the amount of oil carried to the electrodes. Its purpose is discussed in paragraph 4.1.3

In addition to the basic optics so far described, there are several control devices and monitoring devices in the optical head which have been included to allow the instrument to function properly throughout the wide range of environmental conditions specified. These control devices are the optical alignment servo, the grating pressure correction adjustment, the focus servo, the tilt-normal mechanism, and photomultiplier dark current cancellation.

Of all the environmental conditions specified, the effect of atmospheric pressure is most severe. Pressure variations change the density and hence the refractive index of air. The result is a lateral shift of the spectrum, the magnitude of which depends on wavelength. A total shift of a spectral line at the focal curve of as much as 50 microns is possible. This shift must be corrected and an optical alignment servo is provided for this purpose. The servo operates only when the instrument is not analyzing oil and accurately aligns the 3126A line of mercury, obtained from an auxiliary mercury lamp source, with its exit slit. An alignment correction of ± 100 microns is provided by a tilting calcium fluoride plate at the entrance slit.

Since 3126A is near the center of the spectral coverage, little error occurs near the center of the spectrum. However, since the pressure induced shifts are wavelength dependent, a large dispersion change also occurs and this is not corrected by the alignment servo. Consequently, the grating is made to move along a line through its center and the center of the focal curve. The correct dispersion adjustment is made manually by the operator in accordance with average atmospheric pressure at his location

Temperature, humidity, and carbon dioxide concentration changes also affect the refraction index of the air, but to a lesser extent than pressure changes. Their dispersion errors are negligible and no compensation is needed. Temperature changes, however, also affect the grating spacing and the size of the optical supporting structure. The grating spacing changes tend

to compensate the refractive index changes in the air and consequently are beneficial. Structural changes do not affect the angular alignment provided one material is used throughout and it is maintained at a uniform temperature. Serious focus changes, however, do occur as the structural dimensions change. Correct focus must be maintained in order to avoid output errors and a servo is provided for this purpose. The focus servo inserts a variable thickness of calcium fluoride in the optical path, the thickness inserted being a function of temperature.

In order to monitor the performance of the optical alignment servo and to check optical alignment generally, a tilt-normal mechanism is provided. This mechanism adjusts the tilt angle of a quartz plate in front of the exit slit for the 3650A line of mercury. Two positions are provided: normal incidence and a tilted angle of incidence. The ratio of the 3650A photomultiplier output is the normal position to that in a tilt position is a known value which is indicative of the alignment of the 3650A line with its slit. Any misalignment of the spectral line decreases the tilt-normal ratio.

The final error correcting system which is included in the optical head of the Base Level Analyzer is for photomultiplier dark current cancelation. Dark current can produce a significant error in the readout, especially at the higher operating temperatures, since photomultiplier dark current increases rapidly with temperature. The cancellation system alternately shutters the source and reverses the integrating capacitor polarities so that the net integral of dark current is zero while the source produced current integral is unaffected.

4.1.3 Data Conversion

The optical head of the Base Level Analyzer has 10 signal and one reference outputs. These outputs are the voltages accumulated on integrating capacitors at the end of the source burn and are functionally related, through what is

known as the working curve, to the concentrations of the various elements in the sample. A data conversion procedure is required o ransform the capacitor voltages to values proportional to concentration.

The first step in the conversion is the selection of a method of controlling the length of the source burn time. Two procedures are commonly employed, constant time and fixed reference. The latter will be employed in the Base Level Analyzer. In the fixed reference method, the reference capacitor voltage is converted to a digital number and is compared to a fixed digital reference. When the digital reference is exceeded, the source is shuttered. In effect, the reference voltage is normalized and does not appear in the nonlinear working curve function. Therefore, a nonlinear amplifier can be used for the conversion process, its gain characteristic having the same form as the working curve.

Some of the advantages of the constant digital threshold approach stem from the fact that it is the ratio of unknown to reference voltage which is important. All system variations which produce the same percentage variation in both unknown and reference channels cancel out of the final result. A typical example is the variation of the capacitance of the integrators with temperature. If the temperature coefficients of reference and unknown capacitors are identical, no error will result from a temperature shift. This is not true of the constant burn time approach.

A major advantage of the constant digital threshold data conversion method is the possibility of using analog, rather than digital, conversion techniques. The Baird-Dow technique, a constant burn time method, uses the time required to discharge the reference capacitor voltage to the impurity capacitor voltage as a logarithmic measure of the ratio of the impurity voltage to reference voltage. Although times can easily be measured with great accuracy in digital form, this method is not convenient because of the

complexity of a digital working curve conversion. A digital computer and memory are required where only a single operational amplifier suffices with a constant digital reference. In addition the accuracy of the logarithmic Baird-Dow system is poor when the discharge times become long (low impurity voltages).

To sum up the advantages of the constant digital reference approach: the error cancelling abilities of an unknown-to-reference voltage ratio measurement are combined with the ability to use a simple analog working curve conversion.

4.1.4 Readout

Following the analysis of a sample, the data obtained is stored in analog form on the integrating capacitors. Under the control of the program timer each capacitor voltage is then sampled and converted, using a nonlinear amplifier incorporating the working curve, to a voltage directly proportional to impurity concentration. The voltages at the output of the nonlinear amplifier are connected sequentially to an analog-to-digital converter, the same converter used initially to establish the constant digital reference, and changed to digital format. Each digital number is stored in a separate 9-bit register. The complete operation, including analog sampling, analog-to-digital conversion, and digital storage, requires only 100 milliseconds for 10 channels and is completely automatic so that the leakage of the integrating capacitors is negligible.

The operator is free to interrogate any or all of the digital storage registers at will immediately following the completion of the sample burn by pushing the proper buttons on the control console The concentration of any one of the ten impurity elements may be displayed in decimal form on three Nixie tubes. Because of the digital nature of the data storage at this point there is no danger of error from variations in readout technique or timing and the same element concentration may be repeatedly read out without error.

4.2 Oil Contaminant Analysis

4.2.1 General Discussion

As there was no available performance information on an instrument similar to the Base Level Analyzer, it was necessary to establish the answers to a number of basic questions before the design could be satisfactorily concluded. An experimental program was therefore initiated to obtain the necessary data. The data required, involved the optimization of

a. Emission Lines for Each Specified Element
b. Source Conditions
c. Reference Emission Line
d. Entrance/Exit Slit Dimensions

In addition, information was required on the quality of available standard, and the performance of an instrument under the environmental conditions specified.

The Baird-Atomic Emission Instrumentation Laboratory was therefore used to simulate the known parameters of the Base Level Analyzer and to arrive at some of the missing parameters of the design.

The instrument, chosen to carry out the investigative task, was the Baird-Atomic Research Direct Reading Spectrograph (RDRS). This instrument is a basic 3-meter modified "Eagle" mount to which direct reading capabilities have been added. The 20-inch photographic camera was replaced with a direct reading head which can accommodate up to 16 photomultipliers. The greatest advantage of the instrument is the rapidity with which slits can be set (utilizing an electronic slit setting device). The RDRS is, therefore, ideally suited to the particular problem. In conjunction with the RDRS, a Baird-Atomic NB-1 Spectrosource was used. This is probably the most versatile source available, having four excitation modes with an infinite number of variable parameters available.

The particular grating chosen for the experiment was a 15-thousand-line-per-inch pyrex grating blazed for 5500A first order. In order to approximate the 6A-per-millimeter dispersion of the Base Level Analyzer, this grating was employed in the first order at a mean dispersion of 5.56A per millimeter. This presented a problem in that the blaze angle of this grating is far from ideal for this particular application especially at the lower wavelengths where lead, the most difficult element to analyze is located. A grating with a 3200A first order blaze would be much more efficient.

The RDRS is susceptible to temperature changes of the order of ±5°F, especially with the small 50 microns to 25 microns ratio of the slits. The Emission Instrumentation Laboratory, is not temperature controlled and during the statistical analysis runs which took place over a period of three days, there were noticeable temperature effects on the samples.

Additionally, the slits that were used on the RDRS were not all at the correct angle (the entering light normal to the slit face). As a result, there was scattered light which presented both sensitivity and reproducibility effects.

The capacitors chosen to store the charge were the normal 1.0 microfarad for the reference and 0.1 microfarad for all the unknowns. Due to the great sensitivity of magnesium the spread of clock divisions for the range of concentrations was over 80, which is beyond the accurate reading limits of the Baird-Dow RC discharge. As a result, readings below 5 parts per million of magnesium were impossible and some of the lower values of other elements (for example copper) were susceptible to poor precision due to the nature of the RC logarithmic readout.

4.2.2 Reference Line Determination

The reference line chosen must be one that is free of extraneous influences and yet is representative of the oil sample investigated.

Several possible selections presented themselves and each in turn was evaluated. The first lines to be investigated were two hydrogen lines which through possible breakdown of the oil might be excited into emission. After both photographic and photoelectric study, it was determined that with the source conditions employed neither the H 4861 A or the H 4340 A line were being excited. Use of the H 4861 A would have been doubtful primarily due to focal curve physical limitations.

The next element to be investigated as a suitable reference was carbon which can be excited in sparking of the oil. However since carbon electrodes were employed in the analysis, it was anticipated that there would be considerable contribution from the electrodes. To estimate the amount of carbon excitation actually coming from the oil, the carbon electrodes were replaced by a copper disk and counter electrode. Using these electrodes, there was some difference in the sample excitation due to the differing electrical properties of the two substances, but by neglecting these small differences it was ascertained that there was approximately 10 percent contribution to the carbon line from the oil itself. This was considered too small a contribution to render it useful as a reference line. Another carbon line at 2296 A was evaluated. But this C III line, due to its high excitation potential, did not lend itself to use as a reference.

The next area of reference that presented itself was the amazing reproducibility of the background in certain regions of the spectrum regardless of what type oil was analyzed. With this observation a search was made of photographic plates, spectral charts, and tables to see if an area within the spectral coverage of the system could be found that was free of element interference. One region which satisfied the above requirements was in the

vicinity of 3897 A. In this region there are no element interferences and there is a good light level. However, there is also some weak cyanogen band structure which is due to the electrodes. By running the electrodes without oil, it was determined that 60 percent of the background plus cyanogen structure was coming directly from the oil itself. This is a much greater contribution by the oil to the reference line than all other lines examined.

Total light and central image were also evaluated but BKD 3897 A was found to be superior in all cases and was therefore selected as the reference.

4.2.3 Element Line Selection

The major task in the element line selection is to choose the most sensitive analytical line that is free of interference, and falls within the physical limitations of focal curve and slit sizes. Most of the lines chosen are well documented in previous Baird-Atomic instruments; but, due to a difference in dispersion between the Base Level Analyzer and other Baird-Atomic spectrometers, it was necessary to carry out a literature search to verify the data found with actual curves

Oil spectra were photographed first to verify the freedom of interfering lines, since the oil spectrum is quite simple and informative.

In order to optimize the light output, several lines were investigated for some elements, the most notable being lead and tin Figure 4-2 shows a study of the three different lead lines, before lead 2203 A was finally chosen. Also an evaluation of two tin lines is shown in figure 4-3. Three lines (copper above 200 parts per million, silver above 150 parts per million, and magnesium above 200 parts per million) show reversal, this is a natural phenomena and does occur in all instruments.

The following lines, therefore, represent the best compromise when all the factors mentioned above are considered and they are adequate to perform the task requested of them

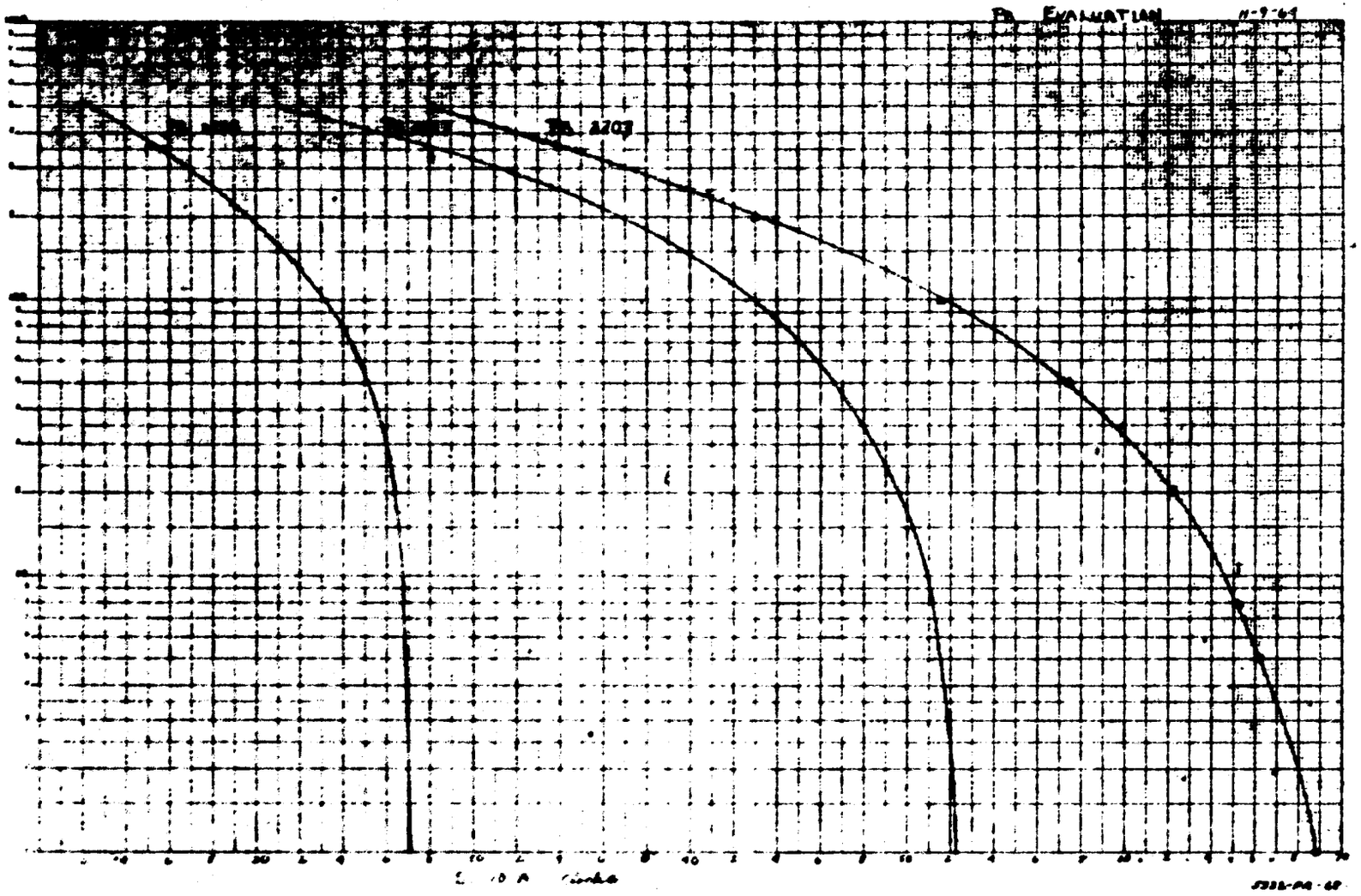

Figure 4-2. Lead Evaluation

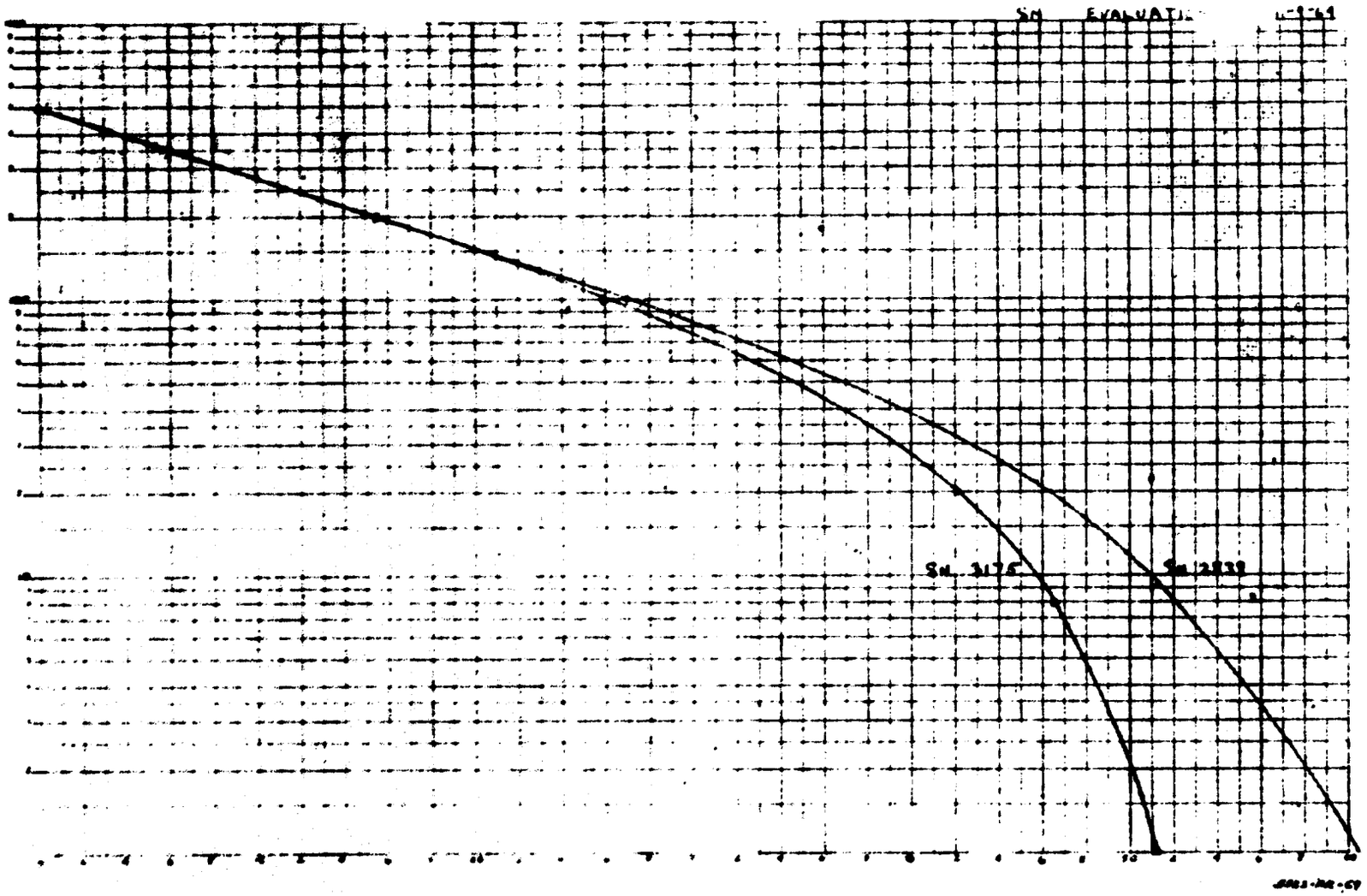

Figure 4-3. Tin Evaluation

Lead	2203 A	Silver	3382 A
Iron	2599 A	Nickel	3414 A
Magnesium	2802 A	Mercury	3650 A (master monitor)
Tin	2839 A	Background	3895 A (ref)
Silicon	2881 A	Aluminum	3961 A
Mercury	3126 A (servo)	Chromium	4254 A
Copper	3274 A		

4.2.4 Entrance/Exit Slit Determination

The prime factors that govern both extrance and exit slit sizes are closely allied to those of element line selection as well as the optical components chosen. The resolution must be sufficient to resolve the element lines from all line interferences. The resolution necessary was determined to be 0.4 A. Since the dispersion of the Base Level Analyzer is 6 A per millimeter, optimum slit width may be calculated from the following.

$$\text{resolution} = \frac{\text{entrance width} + \text{exit width}}{2} \times \text{dispersion}$$

$$\text{resolution} = \frac{50\,\mu + 25\,\mu}{2} \times 6\ \text{A/mm}$$

$$\text{resolution} = 0.225\ \text{A}$$

Due to line broadening, the actual resolution is probably closer to 0.3 A, sufficient to resolve the chosen element lines.

The combination of entrance and exit slit widths may be seen to be a constant. The entrance and exit slit widths can never be the same, otherwise there would be no room for any spectrum line movement Any slight shift in spectrum position would result in different data

A question now arises as to whether the entrance or exit slit should be the larger. If the exit slit is chosen to be the smaller, it is possible to look at only the central portion of a 50-micron spectrum line with the 25-micron exit slit and therefore eliminating the background associated with the spectrum line. This gives the maximum signal-to-noise ratio and therefore the greatest sensitivity. The use of a wider exit than entrance slit was evaluated on lead 4057 A as depicted in figure 4-4. The loss in sensitivity is due mainly to background since no line interference is present within the calculated resolution of the 50-micron and 150-micron combination.

Going to a narrower exit slit could result in a problem of the light level becoming too low for efficient operation of the system. With a 50-micron entrance slit and a 25-micron exit slit combination there is sufficient light level and adequate resolution. These slit combinations were used on the RDRS evaluation and the analytical results support this selection.

The width of the reference slit on background 3897 A is 200 microns. By use of previous equations the resolution is found to be 0.75 A. There are no interferences present within this area. This was confirmed by monitoring the reference line on all sample evaluations. The larger width of the reference slit is necessary to get the best sampling possible and to have as little variation as possible with different samples.

Two other slits which are involved only with optical alignment, and not with the analytical data, are a special offset mercury slit for use in the automatic servo system and a 25-micron regular slit to be used for the tilt-normal system.

4.2.5 Optimum Source Conditions

Under source conditions, the analytical timing sequence, the electrical parameters and the physical spacing will be discussed

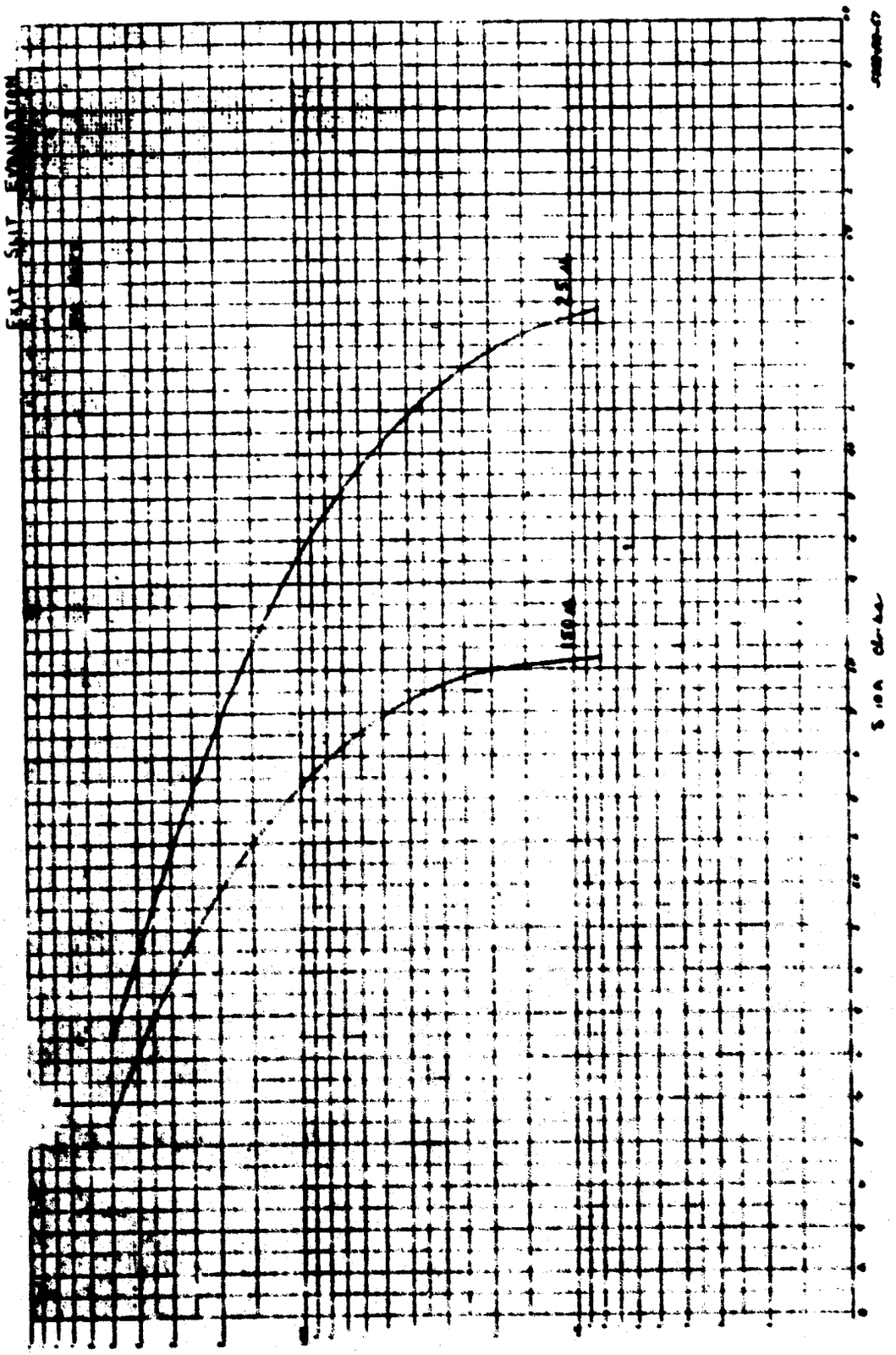

Figure 4-4. Exit Slit Evaluation

The prime aim in this area is to establish the most sensitive source embodying the necessary accuracy. As sensitivity is increased there is a loss of accuracy. A high inductance a-c spark was chosen as the most efficient source. The spark has the following parameters:

4.0 RF amperes	5 breaks per half cycle
0.005 microfarad capacitance	400 microhenries inductance
3-millimeter analytical gap	30 rpm rotating disk
160-degree 1/4-inch graphite electrode	h-4072 disk electrode
8-second preburn	21-second exposure

The addition of secondary inductance lessens the air lines in the spark and as a result increases sensitivity, especially for lead and tin. Without inductance it is impossible to read below 100 parts per million for lead and tin

A rotating electrode speed of 30 rpm was chosen, since with this speed there was a large and hence more representative sampling. A speed in excess of this would tend to spatter the oil too much.

The counter electrode is a standard purity 1/4-inch graphite rod (National AGKS) shaped with a 160° included angle (ASTM C-2). High purity counter electrodes such as National L-3957 were tried and no increase in sensitivity or curve shifts resulted The disk electrode is a National L-4072 AGKSP grade

The preburn and exposure times were also determined after much investigation The preburn time of eight seconds is sufficient to precondition the sample and stabilize the discharge Preburn times of up to 45 seconds were timed with no improvement in either precision or detectability. The 21-second exposure period was found to be the time after which there was

no improvement in analytical results. Light is actually only integrated for one-half this time due to a dark-current correction system. Exposure times of up to 60 seconds have been tried, and the only results are reduced load capability and the possibility of the oil flashing.

The oil to be sampled is held in a no. 2 Coors porcelain boat. The boats are free of contamination, are easily cleansed for reuse, and require a minimum amount of oil for an analysis.

Another source condition tried was the low-voltage rectified arc. On most analytical runs the flash point of the oil was surpassed and a fire resulted in the boat.

4.2.6 Oil Standard Preparation

The key to the entire oil contaminant analysis program lies in the preparation of reliable standards. The spectrometer is nothing more than a good comparator and is only as good as the data fed into it, namely reliable standards.

An immediate question that can be asked is: are there such things as true or absolute standard? Many people have tried to arrive at such standards, but as yet there have only been close approximations. It was the function of an ASTM study group to try and arrive at an absolute standard, using Standard of Indiana. (LF-1954) base oil. They produced standards with errors from the "true" amount of up to 43 percent. The problem of an absolute standard is therefore very real.

This was further accentuated when oil standards from Naval Air Station, Pensacola, Florida; McDill Air Force Base, Tampa, Florida; Analysts of Puerto Rico, San Juan, Puerto Rico; Analysts Inc., Torrance, California; Professor Ice, Belmont, California; and those prepared by Baird-Atomic were run in a test program. There were concentrations within one set of standards that differed by 30 parts per million and standards among different

laboratories that differed by over 120 parts per million. Some standards were more reproducible than others, with the ones showing the best precision also plotting the most linear curve. One set of standards which were over two years old had silver plated out on the bottle which points out one of the stability problems.

The standards prepared by Baird-Atomic follow very closely the method outlined in National Bureau of Standards Monograph 54. This report gives in detail how the National Bureau of Standards organo-metallic salts were made and how with proper solubilizing compounds stable additions in lubricating oils can be formulated. The National Bureau of Standards does state that silicon above 200 parts per million is doubtful and also that these solutions "are stable for several weeks". Whether or not these standards are compatible with the various additives that may be in the oils to be analyzed is another unanswered question. The Baird-Atomic standards were prepared for the ten elements of interest with the exception of silicon in the concentrations of 500, 400, 300, 200, 100, 50, 20, 10, 5, 1 and the base oil. Silicon had a maximum concentration of 200 parts per million and was diluted in the same proportion. As of the date of this report, the standards are clear and homogeneous and give good repeatability. A continuing check of their stability will be made.

The first attempt at preparing Baird-Atomic standards, (while solubilizing compounds were or order) was to add the organo-metallics to the selected 7808 base directly, and blending the additions for 24 hours in a blender. After a period of three days, salts started to precipitate out and precision studies were poor. Upon the receipt of solubilizing agents the procedure outlined in National Bureau of Standards Monograph 54 was followed with excellent results. One note of interest was that the lead curves plotted with the first 7808 standard and the new 7808 standards with solubilizers were identical.

The four basic oil types with which this study are concerned were procured (7808 from Mobil) and the 23699, 1065, and 1100 from Esso. The two reciprocating types (1065 and 1100) per unit burn time (due to their greater viscosity) gave about 10% more reference light, but also each of the unknown was also receiving more light by an equal factor.

The end result is that all four base oils gave results within one part per million. This is to be expected from the very nature of the spectrographic internal standard method.

4.2.7 Statistical Analysis

In order to establish and identify some of the variables contributing to the overall system performance, and to obtain "real" accuracy data a statistical analysis was performed.

A set of three series of standards labeled A, B, and C were formulated with concentrations of 500, 400, 300, 200, 100, 50, 20, 10, 5, 1 and 0 parts per million present. using a 7808 base oil and to the procedure outlined in National Bureau of Standards Monograph 54. By successive dilutions of the 500-parts per million standards all other values were obtained. It is to be noted that the 500- and 0-parts per million standards though labeled A, B, and C are one and the same oil. This is especially noteworthy when one takes a critical look at the data in appendix A. With a few minor exceptions which can be attributed more to the instrument than to the standards, the spread of voltages is as great for these two values as it is for the formulated standards.

The curves* were arrived at by normalizing the values from the Baird logarithmic readout to a predetermined reference voltage which is the principle under which the Base Level Analyzer will operate. The middle curve represents a plot of the mean value determined from seven runs which were made over a period of three days. The two outer curves represent the

*Appendix A

deviation from the mean. An enlarged plot is at the right to show the same curves in the critical 0 to 20 parts per million range. By choosing one voltage one is able to read three values of the concentration in parts per million and hence can get a feel for the accuracy of the equipment under the conditions elaborated upon in paragraph 4.2.1.

By overlaying the three series of standards one is able to compare the accuracy of one standard to another. It will be noted that for aluminum Baird-Atomic has but standards B and C and only up to a maximum concentration of 400 parts per million. This was a result of an instrument problem associated only with aluminum which could not be corrected until after the statistical analysis had been run. A rerun of aluminum was made but due to depleted samples, all the values were not available. This statistical analysis consisted of 330 burns and provides a reasonable statistical profile of Base Level Analyzer performance.

4.3 Optical Analysis

The optical system for the Baird-Atomic Base Level Analyzer is capable of performance which is well within the limits necessary to meet the specification requirements. The quality of the slit images at the exit slit curve on the Rowland circle is influenced by two factors:

a. Diffraction

b. Grating Resolution

4.3.1 Diffraction Resolution

The diameter of the minimum spot size in the image of a point can be calculated by the following formula.

$$d = f\lambda$$

where

d = effective diameter of diffraction image

f = f/number of optical system

λ = wavelength

If

f = f/20

λ = 0.430 micron (4300 A)

d = 20 x 0.43 = 8.6 microns

4.3.2 Grating Resolution

The resolving power of the grating ($\Delta\lambda$) or its ability to separate wavelengths of light is determined by the formula:

$$\Delta\lambda = \frac{\lambda}{Nd \cos \theta}$$

N = number of grating lines

d = line spacing of grating

θ = angle of diffracted light, measured from grating normal (4300A)

$$\Delta\lambda = \frac{0.430}{50 \times 10^{-3} \times 0.95595} = 8.9 \text{ microns}$$

Since the formula for the grating is based on the minimum diffraction pattern, the two effects are not additive. However, this confirms the fact that the resolving power of the system is more than adequate for good imaging of a 50-micron wide slit.

4.3.3 Spectral Line Image Quality

4.3.3.1 Discussion of Image Quality -- The image quality of the spectral line used in a direct reading spectrometer can in some cases be the limiting parameter of instrument accuracy. By far, the most important image quality aberration is that of spectral line curvature.

It is a characteristic of direct reading spectrometers that when a straight entrance slit is used, curved spectral lines result, and the degree of the curvature is a function of the angles involved in producing the image, entrance slit height, and radius of curvature of the grating.

The obliqueness of the angles of diffraction with respect to the grating normal are dictated by the dispersion required for a specific application and the radius of curvature of the diffraction grating. The entrance slit height is dictated by the minimum energy requirement of the system.

Spectral line curvature is important to optical stability, due to the fact that a curved image superimposed on a straight aperture exit slit will result in a more critical slit alignment and less allowable relative movement between

the image and aperture if constant photomultiplier energy is to be received. If any energy change is observed by the photomultiplier tube, the result will be an apparent concentration change in the oil and thus an incorrect concentration reading.

If the spectral line curvature is sufficient, it can also limit the signal-to-background ratio and, therefore, limit the minimum detectable concentration. In addition, it can increase the wavelength separation requirements of the optical system due to close characteristic radiation from another element (interference).

4.3.3.2 Experimental Measurement Study -- In order to evaluate the effects of spectral image quality on the Base Level Analyzer design, an experimental measurement study was initiated to obtain spectrograms based on varying the separate parameters which govern image quality.

The equipment used for this study was a 1-meter optical breadboard and an experimental grating. The particular grating used had a 1-meter radius of curvature with 1440 grooves per millimeter. It should be noted that this is not the same as the grating proposed in the design (1666.7 grooves per millimeter) and that it was only used due to the long delivery time of the correct grating.

The experimental parameters used for the study were as follows:

angle of incidence = 25.90

various angles of diffraction observed = -4°, +0.7, +5°, +11°, +17°

grating = 1 meter, radius of curvature with 1440 groove per millimeter

The various angles of diffraction observed were defined by the low pressure mercury lamp source. The wavelengths and their respective diffraction angles are given in table 4-1.

Table 4-1

Wavelengths and Their Respective Diffraction Angles

Wavelengths (Angstroms)		Diffraction Angles (Degrees)	
2536.52	first order	-4.1	
3125.66	first order	+0.7	-3.5
3650.15	first order	+5.1	Base Level Analyzer Range
4358.35	first order	+11.0	
2536.42	second order	+17.0	16.3

The measuring technique employed was to take two spectrograms with each individual variable setting. By placing the emulsion side of one film, with wavelength increasing to the right, against the emulsion side of an equivalent film, with wavelength decreasing to the right, the displacement due to curvature was easily measured with 30X microscope (figure 4-5).

A number of films were taken separately varying the three parameters at our disposal, namely the entrance slit height, grating width, and grating height.

4.3.3.3 Displacement Due to Curvature versus Grating Width -- All of these measurements (table 4-2) were taken over a spectrum height of 25 millimeters with the full entrance slit height of 24 millimeters, and the full grating height aperture of 30 millimeters. These measurements of displacement due to curvature are in microns (1 micron = 10^{-3} millimeters).

The results of this study are graphically represented in figure 4-6. It should be noted that extreme care was taken to ensure that these displacements due to curvature were real and not the result of an oblique ray intersecting a curved surface. This possibility was checked using a reference straight edge to measure the displacement of a single line on a single spectrogram. From figure 4-6 it can be seen that the displacement due to curvature is not a function of grating width.

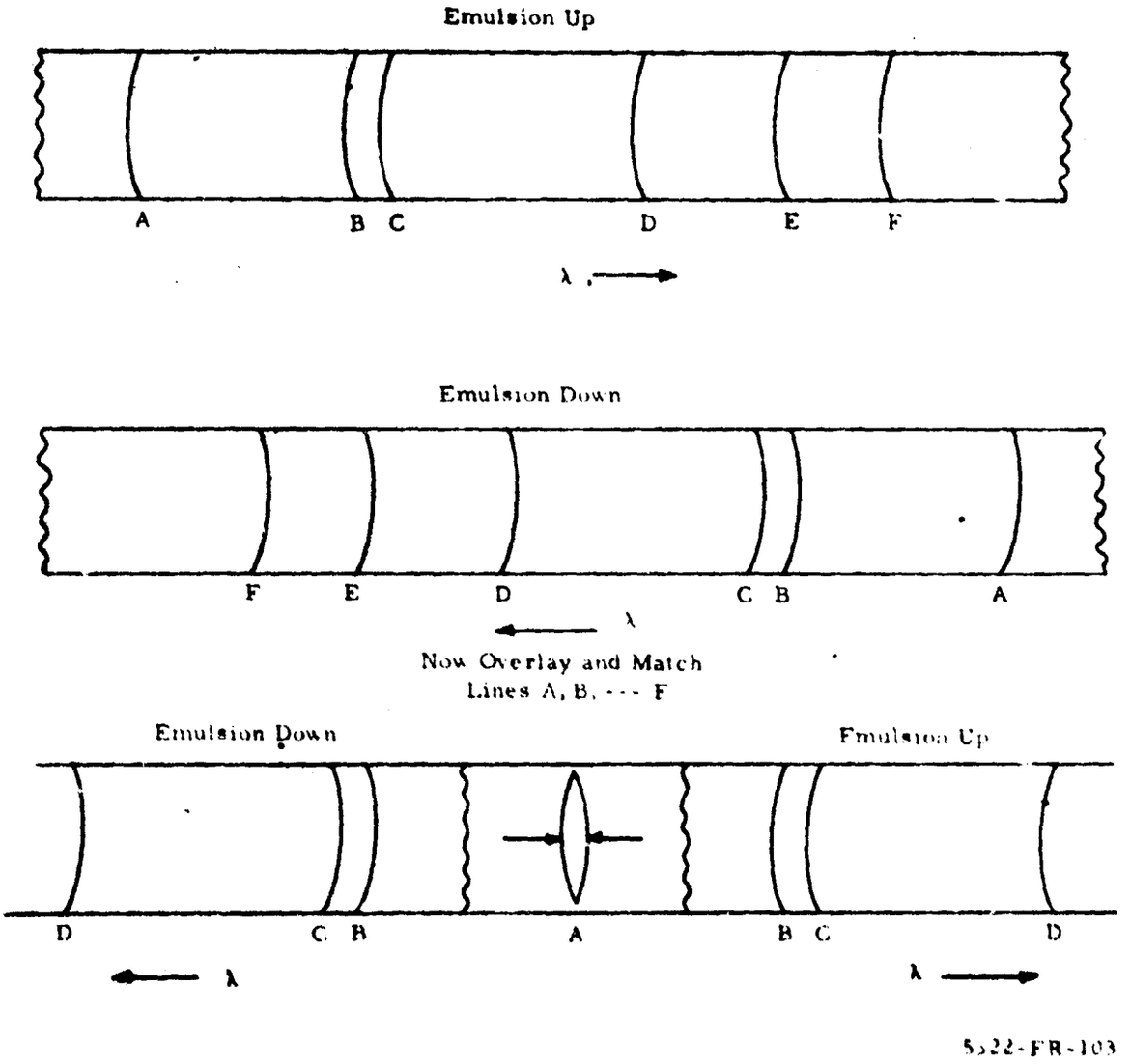

Figure 4-5. Method of Measuring Displacement using Two 35-millimeter Films

Table 4-2

Measurements of Curvature versus Grating Width

Film Number	Exposure Time (seconds)	Grating Width (millimeters)	Displacement due to Curvature B = -4.1 degrees (microns)	+5.1 degrees (microns)	+17.0 degrees (microns)
86	0.050	50	72	72	85
91	0.067	40	70	72 (76)*	93
92	0.085	30	70	72 (74)	89
93	0.125	20	72	72 (76)	89
94	0.250	10	60	68	91

*Measurements in parenthesis are repeat measurements to indicate degree of accuracy obtained.

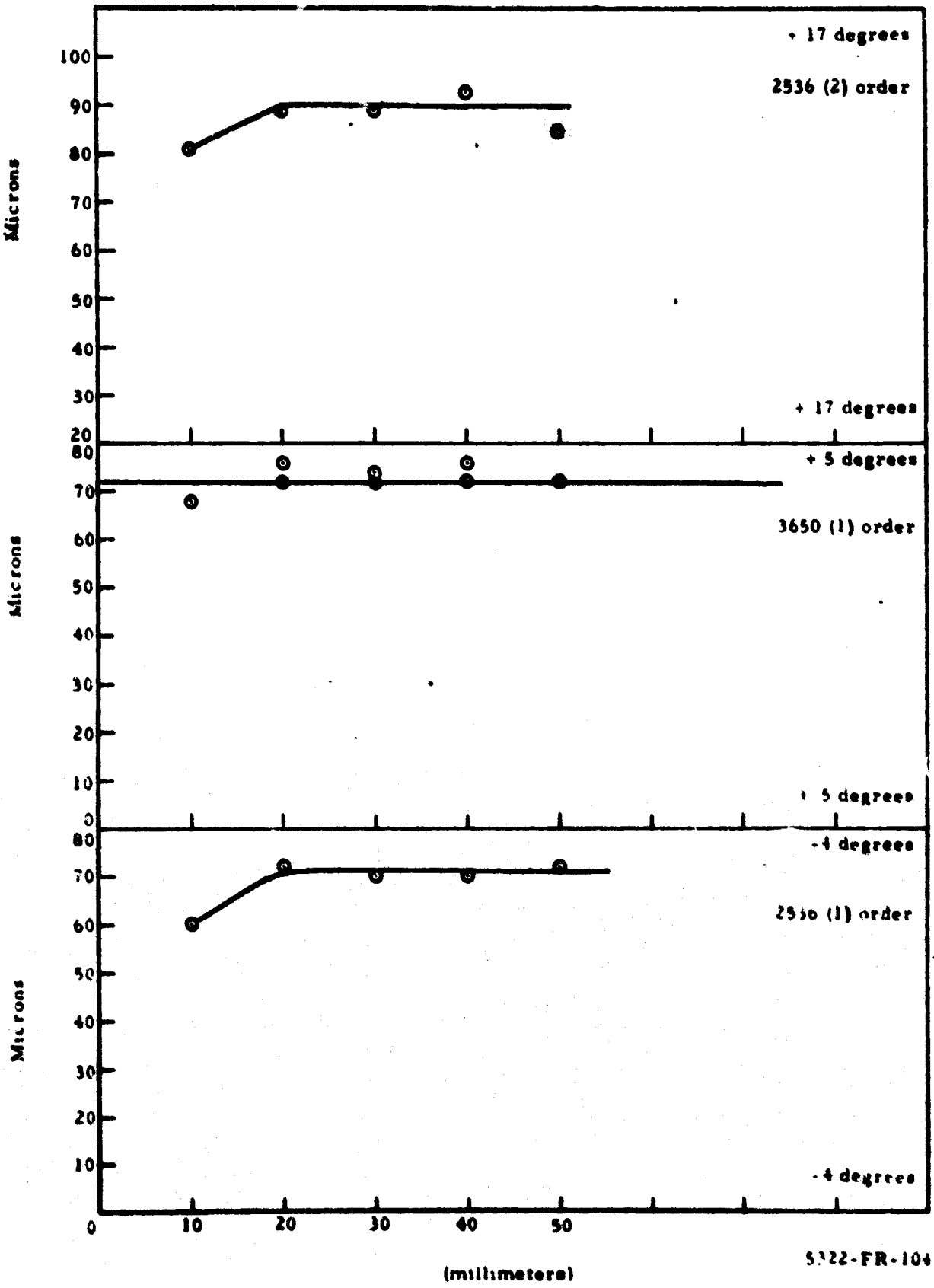

Figure 4-6. Displacement Due to Curvature versus Grating Width

4.3.3.4 Displacement due to Curvature versus Grating Height -- All of these measurements were taken over a spectrum line height of 25 millimeters, with the full entrance slit height of 24 millimeters, and the full grating width aperture of 50 millimeters (table 4-3).

The results of this study are graphically represented in figures 4-7 and 4-8. Figure 4-7 indicates that the displacement due to curvature is a relatively small function of grating height. The order of this function is defined by the angle of diffraction. Figure 4-8 shows that the displacement due to curvature for a one millimeter high aperture is virtually a linear function of the angle of diffraction.

4.3.3.5 Displacement due to Curvature versus Entrance Slit Height -- All these measurements were taken over a spectrum line height equal to the entrance slit height, with the full grating aperture 30 by 50 millimeters (table 4-4).

Figure 4-9 graphically exhibits the displacement due to curvature as a relatively strong function of the entrance slit height. In fact, when the data is plotted as displacement due to curvature versus (entrance slit height)^2, the relationship is essentially linear at all three angles of diffraction.

4.3.3.6 Displacement due to Curvature versus Optimum Optical Parameters for Basic Level Analyzer -- A spectrogram was taken with a vertical aperture of 10 millimeters placed at Sirks focus. The resulting spectrum lines were 10 millimeters in height and the displacement due to curvature measurements were recorded over the 10-millimeter height. The results of this film are shown in table 4-5.

Table 4-3

Measurements of Curvature versus Grating Height

Film Number	Exposure Time (seconds)	Grating Height (millimeters)	Displacement due to Curvature				
			B = -.4 degrees (microns)	+0.7 degrees (microns)	+5.1 degrees (microns)	+11.0 degrees (microns)	+17.0 degrees (microns)
86	0.050	30	72	no meas.	72	no meas.	85
95	0.067	24	66 (68)*	no meas.	72	no meas.	85
96	0.085	18	72 (68)	no meas.	60	no meas.	85
97	0.125	12	55 (56)	no meas.	61	no meas.	93
98	0.250	6	42 (42)	no meas.	51	no meas.	83
99	2.000	1	34	36	49 (48)**	61	77

*Again, measurements in parenthesis are repeat measurements.

**Denotes measurement with respect to reference straight edge.

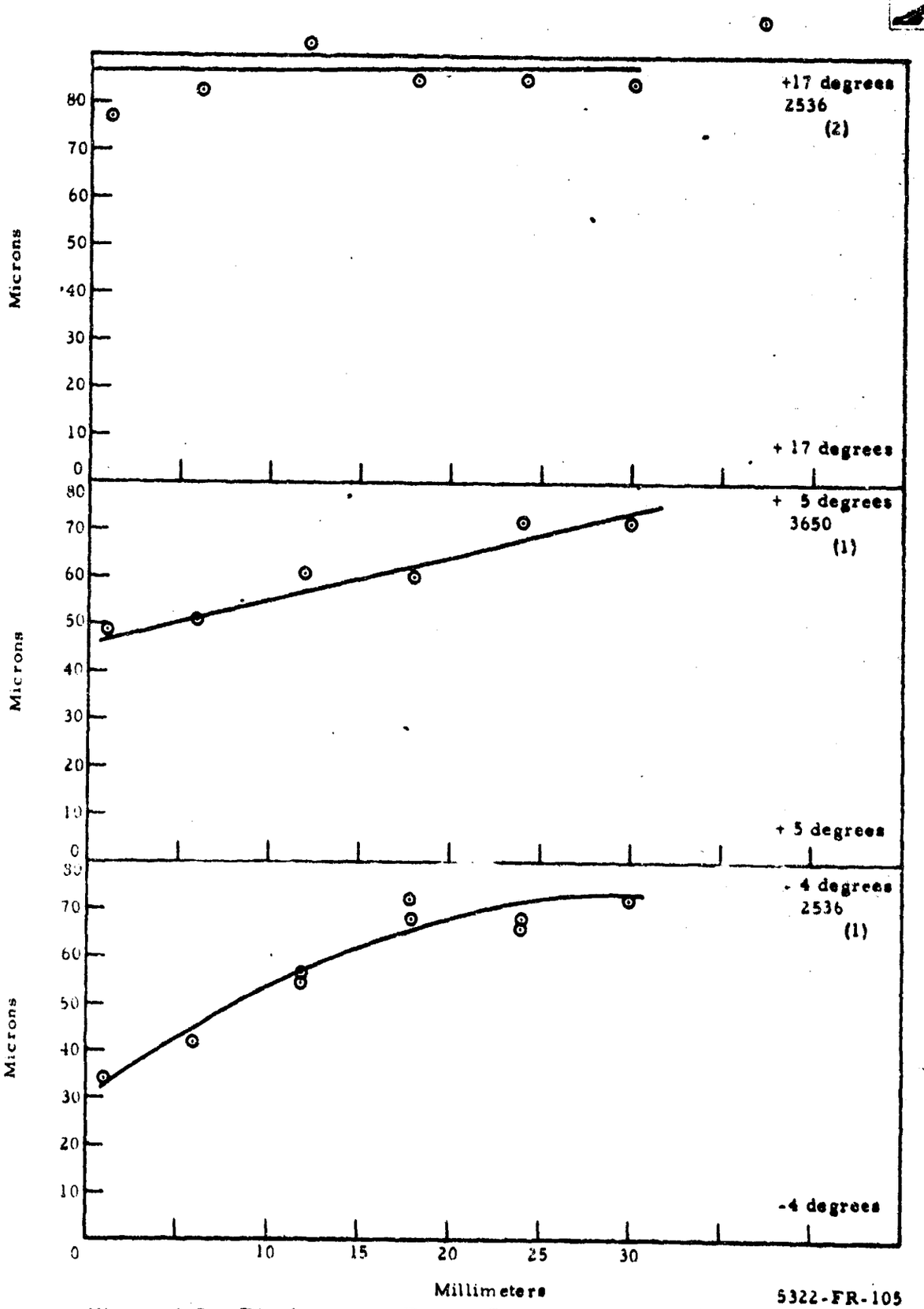

Figure 4-7. Displacement Due to Curvature versus Grating Height

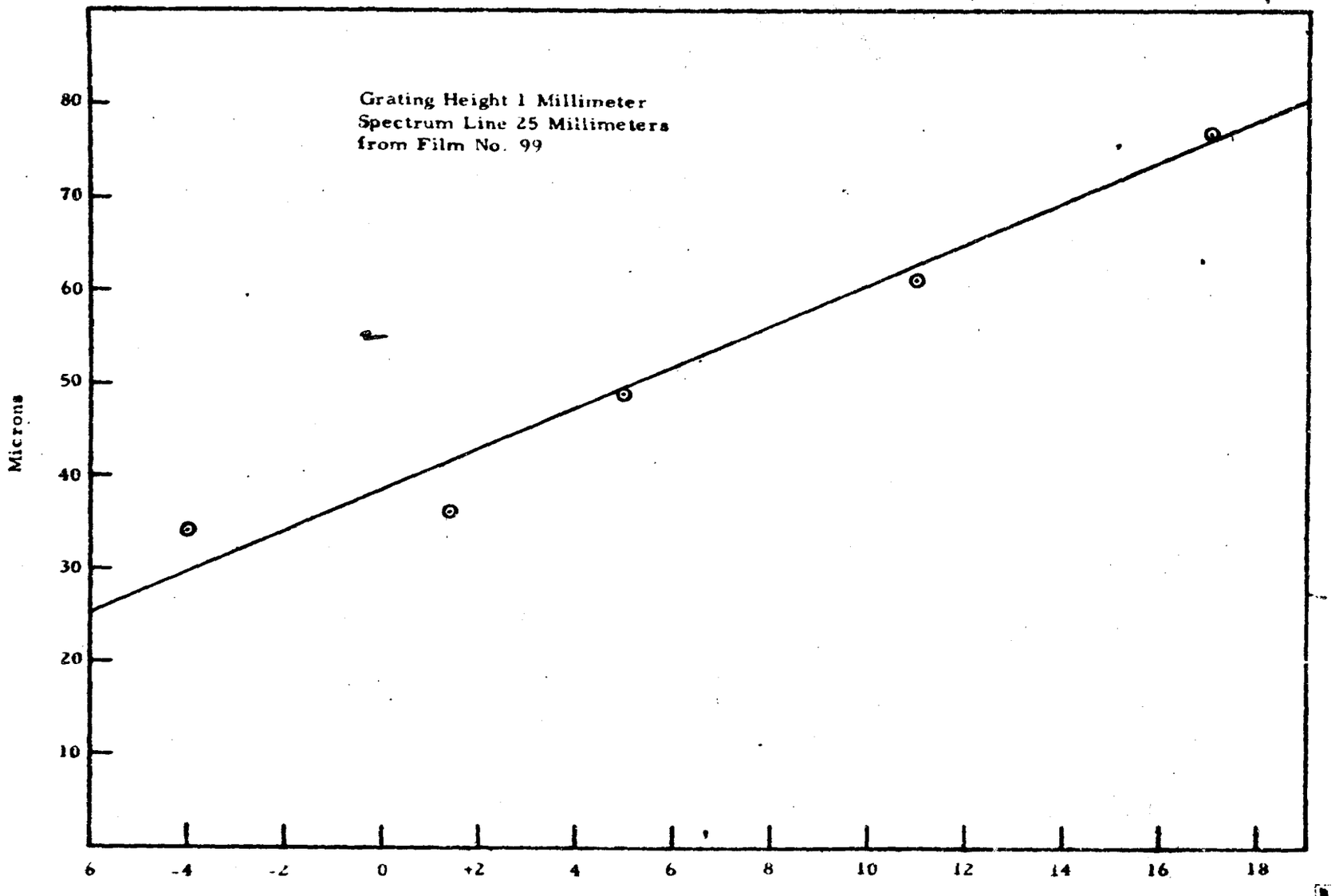

Figure 4-8. Displacement Due to Curvature versus Angle of Diffraction

Table 4-4

Measurements of Curvature versus Entrance Slit Height

Film Number	Exposure Time (seconds)	Entrance Slit Height (millimeters)	Entrance Slit (Height)^2 (square millimeters)	Displacement due to Curvature B = -4.1 degrees (microns)	+5 degrees (microns)	+17 degrees (microns)
86	0.050	24	576	72	72	85
87	0.050	20	400	51	51	51
88	0.050	15	225	25 (30)*	30	25 (29)*
89	0.050	10	100	21	17	17
90	0.050	5	25	12	12	12
101	0.050	1	1	0	0	0

*Denotes measurements taken with respect to reference straight edge.

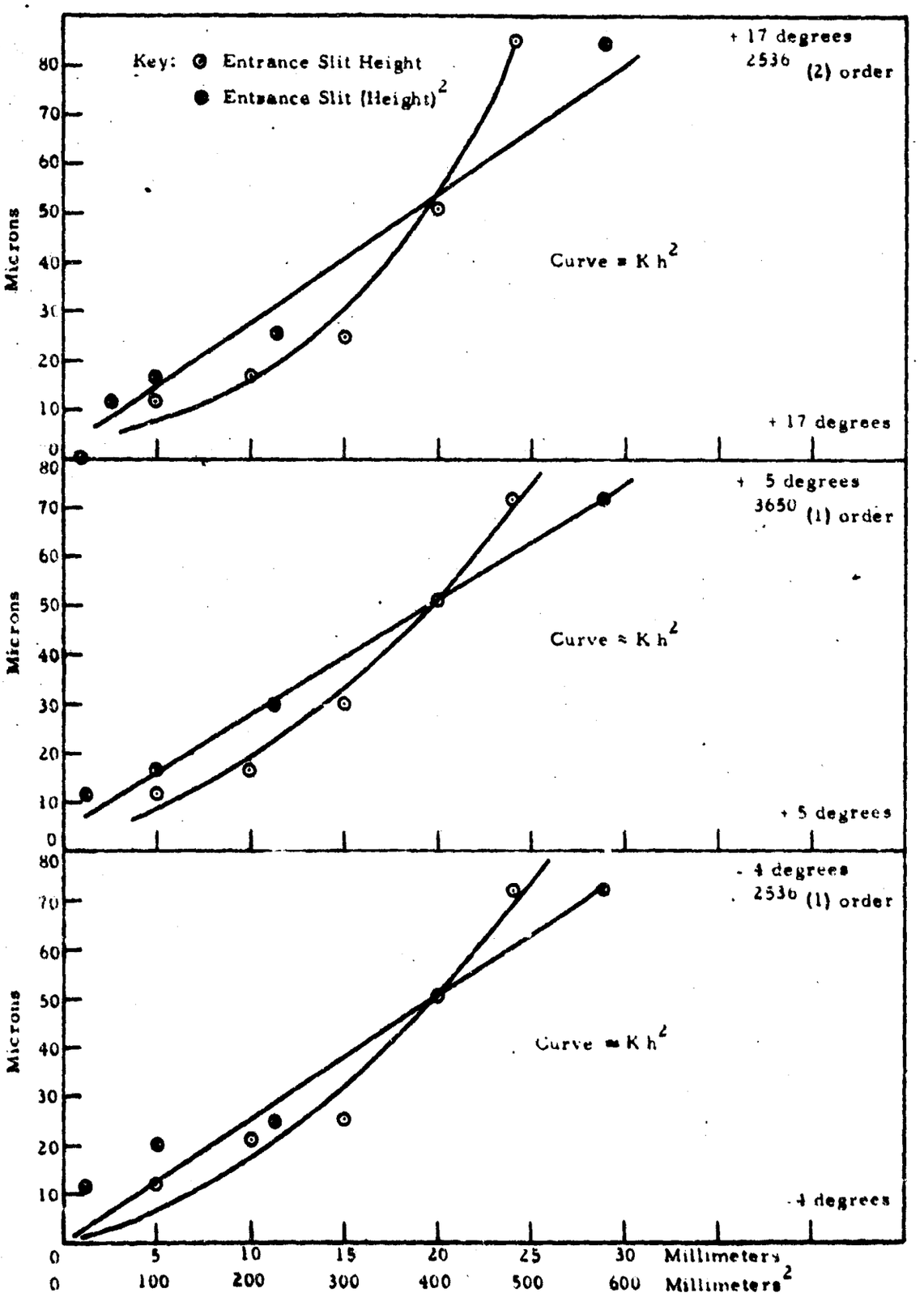

5322-FR-107

Figure 4-9. Displacement Due to Curvature versus Entrance Slit Height and versus Entrance Slit (height)^2

Table 4-5

Measurements of Curvature versus Optimum Parameters

Film Number	Exposure Time	Displacement due to Curvature B = -4.1 degrees (microns)	+5 degrees (microns)	+17 degrees (microns)
215		23	17	13

Note: Within the limits of experimental error, these are identical to the film number 89 (table 4-4).

4.3.3.7 Conclusions -- The linear reciprocal dispersion recommended for the Base Level Analyzer is 6A per millimeter when a 50-micron entrance slit and a 25-millimeter exit slit are used. With these parameters, the theoretical wavelength separation is 0.225A. Under these conditions, the displacement due to curvature must be less than 25 microns. When the slit setting accuracy (± 5 microns) is subtracted from this, the resulting unused portion of the line is 15 microns. This value of 15 microns is the maximum allowable curvature.

With the data from table 4-5, film number 215, and remembering that the displacement due to curvature increases with the square of exit slit height, the maximum height of the exit slit can be calculated to be 8 millimeters. Therefore for the Base Level Analyzer the optimum height of the exit is 8 millimeters with the height of spectrum line limited to 10 millimeters at Sirks focus. Limiting the aperture at Sirks focus minimizes the effect of scattered light observed by the photomultiplier.

4.3.4 Location of Exit Slits

The approximate location of the exit slits of the Base Level Analyzer can be obtained from the equation

$$m\lambda = \frac{A}{N} (\sin i + \sin \theta) \qquad (4\text{-}1)$$

where

m = order of diffraction

λ = wavelength of line

A = width of grating

N = total number of grating lines

i = angle of incidence (figure 4-10)

θ = angle of diffraction

Equation (4-1) can be solved for the diffraction angle

$$\theta = \sin^{-1} \left[m\lambda \left(\frac{N}{A} \right) - \sin i \right] \qquad (4\text{-}2)$$

Equation (4-2) can be evaluated for the Base Level Analyzer case with

$m = 1$

$i = 24.1$ degrees

$\frac{N}{A} = 1666.7$ lines per mm

and with the wavelengths given in table 4-6 . The results also appear in table 4-6

A convenient measure of exit slit location is the linear dispersion at the focal curve, $\frac{ds}{d\lambda}$

$$\frac{ds}{d\lambda} = R \frac{Nm}{A \cos \theta} \qquad (4\text{-}3)$$

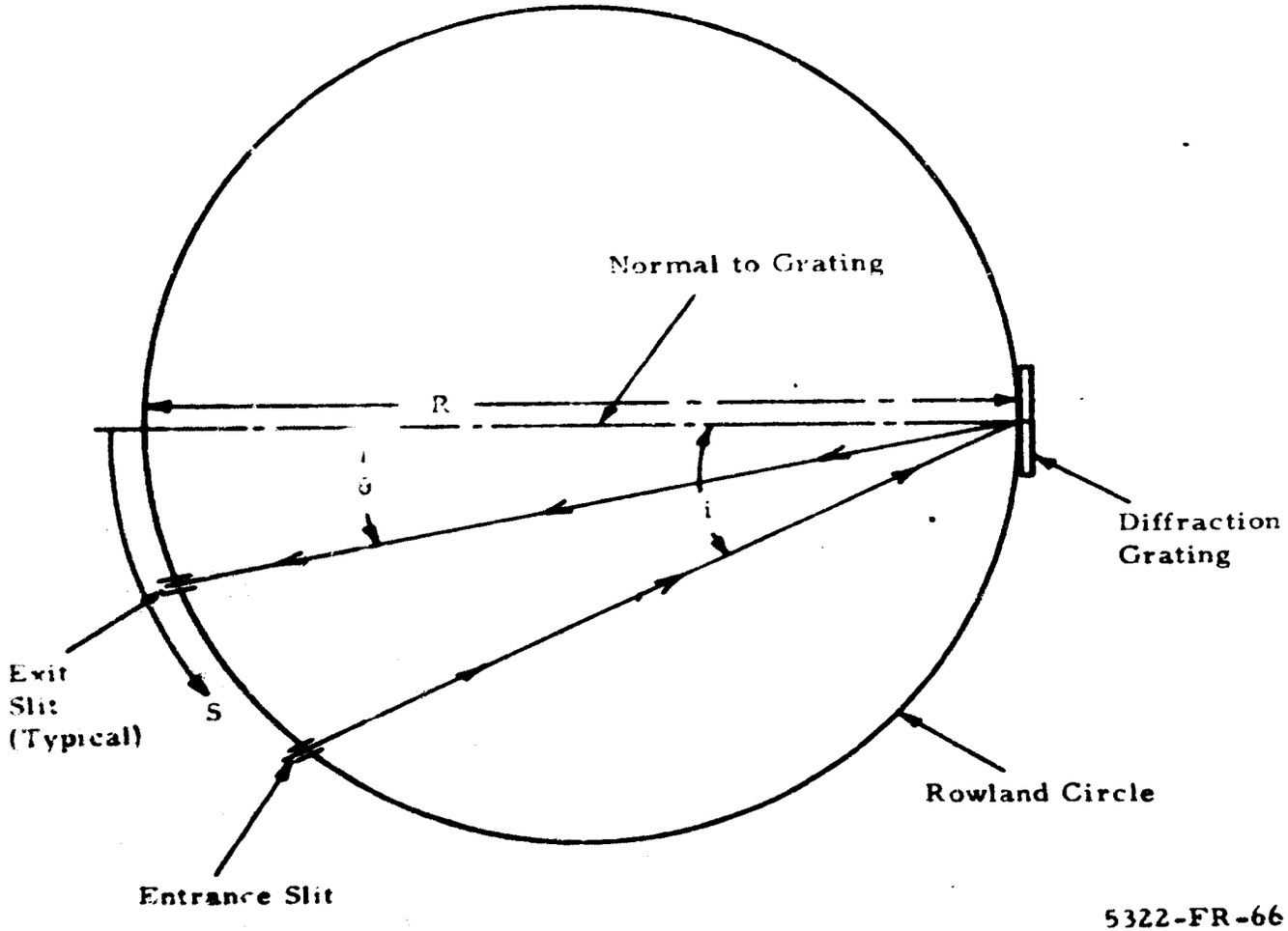

Figure 4-10. Layout of Grating Spectrometer

where

R = the focal length of the grating

For a 1-meter grating of 1666.7 lines per millimeter at normal incidence in the first order

$$\frac{ds}{d\lambda} = \frac{1 \text{ millimeter}}{6\,A} \qquad (4-4)$$

Table 4-6
Location of Exit Slits

Element	λ(A)	θ (degrees)
Iron	2599	1.433
Silver	3382	8.940
Copper	3274	7.898
Chromium	4254	17.462
Nickel	3414	9.248
Silicon	2881	4.123
Magnesium	2802	3.365
Aluminum	3961	14.590
Mercury	3126	6.470
Mercury	3650	11.538
Tin	2839	3.719
Lead	2203	2.358

4.3.5 Effect of Temperature, Pressure, and Humidity on Exit Slit Position

The design of the Base Level Analyzer takes into account the effect of variations of temperature, pressure, and humidity on the required exit slit locations. Compensation for these environmental effects is provided wherever

the amount of shift is such that it is appreciable compared to the width of the exit slits. Each of the three environmental variables (pressure, temperature, and humidity) affects the index of refraction of air and hence the wavelength of the radiation in the air. Additionally thermal variations change the line spacing on the quartz diffraction grating.

A fourth variable, the amount of carbon dioxide gas in the air, can also be considered since it also affects the refractive index of the air.

The angles in the Base Level Analyzer diffraction spectrograph are all reasonably small (between 0 and 24 degrees). Hence the small angle approximation, $\theta \simeq \sin \theta$, can be used without great error and the grating equation can be written

$$\theta \sim \frac{Nm \lambda_v}{A n} - i \qquad (4-5)$$

The value λ_v is the wavelength of the radiation in vacuum. The total differential gives approximately

$$\Delta\theta = \frac{\partial \theta}{\partial T} \Delta T + \frac{\partial \theta}{\partial P} \Delta P + \frac{\partial \theta}{\partial f} \Delta f \qquad (4-6)$$

where

T = temperature

P = atmospheric pressure

f = partial pressure of water in the air

Considering only pressure variations

$$\Delta\theta = \frac{\partial \theta}{\partial P} \Delta P = - \frac{Nm \lambda_v}{A n^2} \frac{\partial n}{\partial P} \Delta P \qquad (4-7)$$

The index of air varies with pressure according to the equation

$$n - 1 = \left[\frac{(n-1)_{P_o}}{P_o} \right] P \qquad (4\text{-}8)$$

where

P_o = a reference pressure

Therefore

$$\Delta\theta = - \frac{Nm\,\lambda_v}{A} \frac{(n-1)_{P_o}}{n^2} \frac{\Delta P}{P_o} \qquad (4\text{-}9)$$

The linear shift of the position of the line is ΔS

$$\Delta S = R\Delta\theta = - \frac{Nm\,\lambda_v}{A} \frac{(n-1)_{P_o}}{n^2} \frac{\Delta P}{P_o} R \qquad (4\text{-}10)$$

The actual shift experienced by the Base Level Analyzer, using an optical alignment servo monitor designed to keep a line at the center of the spectral band centered on its slit is a dispersion change. The shift experienced by the lines at the highest (or lowest) wavelength is

$$\Delta S = - \frac{Nm}{A} (\lambda_{v_{max}} - \lambda_{v_{avg}}) \frac{(n-1)_{P_o}}{n^2} \frac{\Delta P}{P_o} R \qquad (4\text{-}11)$$

This equation can be evaluated for

$$\frac{N}{A} = 1667 \text{ lines mm}^{-1}$$

$$m = 1$$

$$\lambda_{v_{max}} - \lambda_{v_{avg}} \simeq + 900 \text{ A}$$

$$(n-1)_{760 \text{ mm Hg}} = 280 \times 10^{-6}$$

P_o = 760 millimeters mercury

R = 1 meter

n = $\simeq$ 1.00

ΔP = -238 millimeters mercury (the pressure change from 0 to 10,000 feet altitude)

The result is that ΔS is a maximum of + 16 microns for a line at the high wavelength end of the focal curve for the high altitude case as compared with the sea level case. ΔS for a line at the low wavelength end of the focal curve is -13.7 microns.

Returning now to equation (4-6), consider now only the temperature variations. If all of the structure is of the same material and is insulated from external sources of heat so that it is isothermal then

$$\frac{\partial i}{\partial T} = 0 \qquad (4\text{-}12)$$

and

$$\Delta\theta = \frac{\partial \theta}{\partial T} \Delta T \qquad (4\text{-}13)$$

where

$$\frac{\partial \theta}{\partial T} = - \frac{Nm \lambda_v}{A^2 n^2} \left[A \frac{\partial n}{\partial T} + n \frac{\partial A}{\partial T} \right] \qquad (4-14)$$

The value of $\partial A / \partial T$ for the grating can be obtained from the expression for thermal expansion of quartz.

$$A = A_o \left[1 + \partial_q T \right] \qquad (4-15)$$

and

$$\frac{\partial A}{\partial T} = A_o \partial_q \qquad (4-16)$$

where

A_o = the original grating width at 0°C

∂_q = the coefficient of thermal expansion of quartz

The index of refraction of air varies with temperature according to the equation

$$(n-1) = \frac{(n-1)_o}{1 + \alpha T} \qquad (4-17)$$

so that

$$\frac{\partial n}{\partial T} = - \frac{(n-1)_o \alpha}{(1 + \alpha T)^2} \qquad (4-18)$$

Consequently

$$\Delta S \simeq R \Delta T \frac{Nm (\lambda_{v_{max}} - \lambda_{v_{avg}})}{A n} \left[\left(\frac{n-1}{n} \right) \frac{\alpha}{(1+\alpha T)^2} - \vartheta_q \right] \qquad (4\text{-}19)$$

Equation (4-19) can be evaluated for the following parameter values in addition to those noted above.

$\Delta T = \pm 30°C$ (the maximum deviation from room temperatures)

$\alpha = \frac{1}{273} °C^{-1}$

$\vartheta_q = 0.5 \times 10^{-6} °C^{-1}$

For a temperature increase of 30°C above nominal room temperature a line at the maximum wavelength end of the focal curve shifts + 2.2 microns. A negative shift is obtained for a temperature decrease.

Now consider only the effects of humidity variations. Equation (4-6) becomes

$$\Delta\theta = \frac{\partial \theta}{\partial f} \Delta f \qquad (4\text{-}20)$$

where

$$\frac{\partial \theta}{\partial f} = - \frac{Nm \lambda_v}{A n^2} \frac{\partial n}{\partial f} \qquad (4\text{-}21)$$

The index of refraction of air varies with humidity approximately according to the expression*

$$n = n_d - \frac{41 f \times 10^6}{760} = n_d - Kf \qquad (4\text{-}22)$$

*Taken from International Critical Tables

In this equation

n_d = index of dry air

f = partial pressure of H_2O (mm Hg)

Differentiating equation (4-22) we can find the value of $\frac{\partial n}{\partial f}$.

$$\frac{\partial n}{\partial f} = - K \qquad (4-23)$$

The shift of a line at the maximum wavelength end of the focal curve with respect to its nominal slit position, assuming again the optical alignment servo operating on a line in the center of the spectral band, is

$$\Delta S = R K \Delta f \frac{Nm (\lambda_{v_{max}} - \lambda_{v_{avg}})}{A n^2} \qquad (4-24)$$

This equation can again be evaluated using the standard parameter values plus

$$K = \frac{41 \times 10^{-6}}{760} \text{ (mm Hg)}^{-1}$$

and

$\Delta f = 10^2$ millimeter mercury

The last value is obtained as being a maximum change in partial pressure of water vapor. The minimum is, of course, 0 millimeter mercury; the average, 15 millimeter mercury (for 23°C and 72 percent relative humidity); and the maximum, about 120 millimeter mercury (55°C and 100 percent relative humidity). The resulting shift is + 0.8 micron.

The effect of the partial pressure of carbon dioxide gas in air on the index of refraction can be neglected. The International Critical Tables indicate that doubling the normal amount of carbon dioxide (0.03 percent) in air will increase the index by less than one part in 10^7. This compares with a change of 92 parts in 10^7 for the anticipated pressure change from 0 to 10,000 feet altitude.

The effects of all the variables considered above are summarized in table 4-7. It is apparent that for a 50-micron entrance slit and 25-micron exit slits that only the pressure change presents a problem. An optical adjustment must be provided to compensate for altitude changes.

Table 4-7
Summary of Environmental Changes in Line Position

Variable	Range of Variable	Shift of Line at $\lambda_{v\,max}$ Relative to Line at λ_{avg} (microns)
Pressure	0 to 10,000 feet altitude ΔP = -238 mm Hg	+ 13.7
Temperature	ΔT = + 30°C	+ 2.2
Humidity	23°C and 72% RH to 55°C and 100% RH Δf = + 10^2 mm Hg partial pressure of water	+ 0.8
CO_2 Concentration	negligible	

4.3.6 Effect of Temperature, Pressure and Humidity on Line Position

In addition to the dispersion shifts analyzed in paragraph 4.3.5 spectral emission lines are also displaced laterally when subjected to the temperature, pressure, and humidity conditions specified in Exhibit "A" An analysis of lateral shift on a 3400 A line follows.

Now

$$\theta \simeq \frac{Nm\,\lambda_v}{A\,n} - i$$

and

$$\Delta\theta = \frac{\partial\theta}{\partial T}\,\Delta T + \frac{\partial\theta}{\partial P}\,\Delta P + \frac{\partial\theta}{\partial f}\,\Delta f$$

where

f = partial pressure of water

P = atmospheric pressure

T = temperature

Now for pressure variations only,

$$\Delta\theta = \frac{\partial\theta}{\partial P}\,\Delta P = -\frac{Nm\,\lambda_v}{A\,n^2}\,\frac{\partial n}{\partial P}\,\Delta P$$

where

$$n - 1 = \left[\frac{(n-1)_{P_o}}{P_o}\right] P$$

so that

$$\frac{\partial n}{\partial P} = \left[\frac{(n-1)_{P_o}}{P_o}\right]$$

Therefore,

$$\Delta\theta = -\frac{Nm\,\lambda_v}{A\,n^2}\left[\frac{(n-1)P_o}{P_o}\right]\Delta P$$

and

$$\Delta S = R\Delta\theta = -\frac{Nm\,\lambda_v}{A\,n^2}\left[\frac{(n-1)P_o}{P_o}\right]R\,\Delta P \qquad (4\text{-}25)$$

Substituting the same values used to evaluate equation (4-11) and $\lambda_v = 3400$ A in this equation, the total pressure induced shift is found to be $\Delta S = 50$ microns.

Considering the lateral shift of line position produced by temperature variations only

$$\Delta\theta = \frac{\partial\theta}{\partial T}\,\Delta T$$

It has been assumed that selection of materials in the spectrograph is such that

$$\frac{\partial\iota}{\partial T} = 0$$

Then

$$\frac{\partial\theta}{\partial T} = -\frac{Nm\,\lambda_v}{A^2 n^2}\,\frac{\partial(A\,n)}{\partial T} = -\frac{Nm\,\lambda_v}{A^2 n^2}\left[A\,\frac{\partial n}{\partial T} + n\,\frac{\partial A}{\partial T}\right]$$

This equation can be evaluated using equations (4-17, 4-18, 4-15, and 4-11) The result is

$$\Delta S = R\Delta\theta = + R\Delta T \frac{Nm \lambda_v}{A^2 n^2} \left[A \frac{(n-1)_o \alpha}{(1+\alpha T^2} - A_o \theta_q \right]$$

and

$$\Delta S \simeq R\Delta T \frac{Nm \lambda_v}{A n} \left[\left(\frac{n-1}{n} \right) \frac{\alpha}{(1+\alpha T)^2} - \theta_q \right] \quad (4-26)$$

Substituting the parameters previously used in equation (4-19) and a value of 3400 A for λ_v, the lateral shift produced by a 30°C temperature change is $\Delta S = 6.6$ microns.

Finally considering humidity variations only

$$\Delta\theta = \frac{\partial\theta}{\partial f} \Delta f$$

where

$$\frac{\partial\theta}{\partial f} = \frac{\partial}{\partial f} \left[\frac{Nm \lambda_v}{A n} - 1 \right] = - \frac{Nm \lambda_v}{A n^2} \frac{\partial n}{\partial f}$$

Substituting equations (4-22 and 4-23) in this equation, the lateral shift from humidity

$$\Delta S = R\Delta\theta$$

$$= RK\Delta f \frac{Nm \lambda_v}{A n^2} \qquad (4-27)$$

Substituting the parameter values previously used in equation (4-24) plus 3400 A for λ_v, the humidity produced lateral shift is found $\Delta S = 3.05$ microns.

The total lateral shifts produced by environmental changes in the center of the focal curve are summarized in table 4-8. These shifts are completely corrected by the optical alignment servo and hence indicate the range of correction required of that servo.

Table 4-8
Summary of Environmental Changes in Line Position
(for 3400 A Line)

Variable	Range of Variable	Lateral Shift (microns)
Pressure	0 to 10,000 feet altitude ΔP = -.238 mm Hg	50
Temperature	ΔT = + 30°C	6.6
Humidity	23°C and 72% RH to 55°C and 100% RH	3.05
	Δf = + 10^2 mm Hg partial pressure of water	

4.3.7 Temperature Effects on Focus

Since all critical optical elements on the Rowland circle, entrance slit, grating, and exit slits are connected together by means of a mechanical structure, it is necessary to evaluate the performance of the structure over the temperature extremes. In the following analysis, one assumption has been made, that is, that the grating is thermally inert. This is a valid assumption because the grating blank is made of fused quartz which has a thermal coefficient of expansion of 0.28×10^{-6} inches per inch per °F.

Now considering a condition where the grating is fixed, and only the entrance and exit slits are free to move (figure 4-11), the change in optical path length can be expressed

$$\Delta L_{(a+b)} = K (L_a + L_b) \Delta t$$

where

K - linear coefficient of expansion

Δt = temperature change

L_a = distance from grating to exit slit

L_b = distance from entrance slit to grating

Now if the optical head is machined and aligned at 80°F the maximum temperature change in either direction is 50°F and with L_a = 39 inches and L_b = 36 inches and using 11.5×10^{-6} inches per inch per °F.

$\Delta L_{(a+b)}$ = 0.044 inch for a 50°F temperature change or a total out of focus of 0.088 over the specified temperature range. With an f/20 optical system, this represents a ± 0.002-inch or ± 50-micron emission line broadening at the exit slit. This line broadening represents a major energy loss (see paragraph 7.4.2 for detailed calculations.)

Rowland circle diameter	39.37 inches
Grating to exit slit distance	39.0 inches
Grating to entrance slit distance	36.0 inches

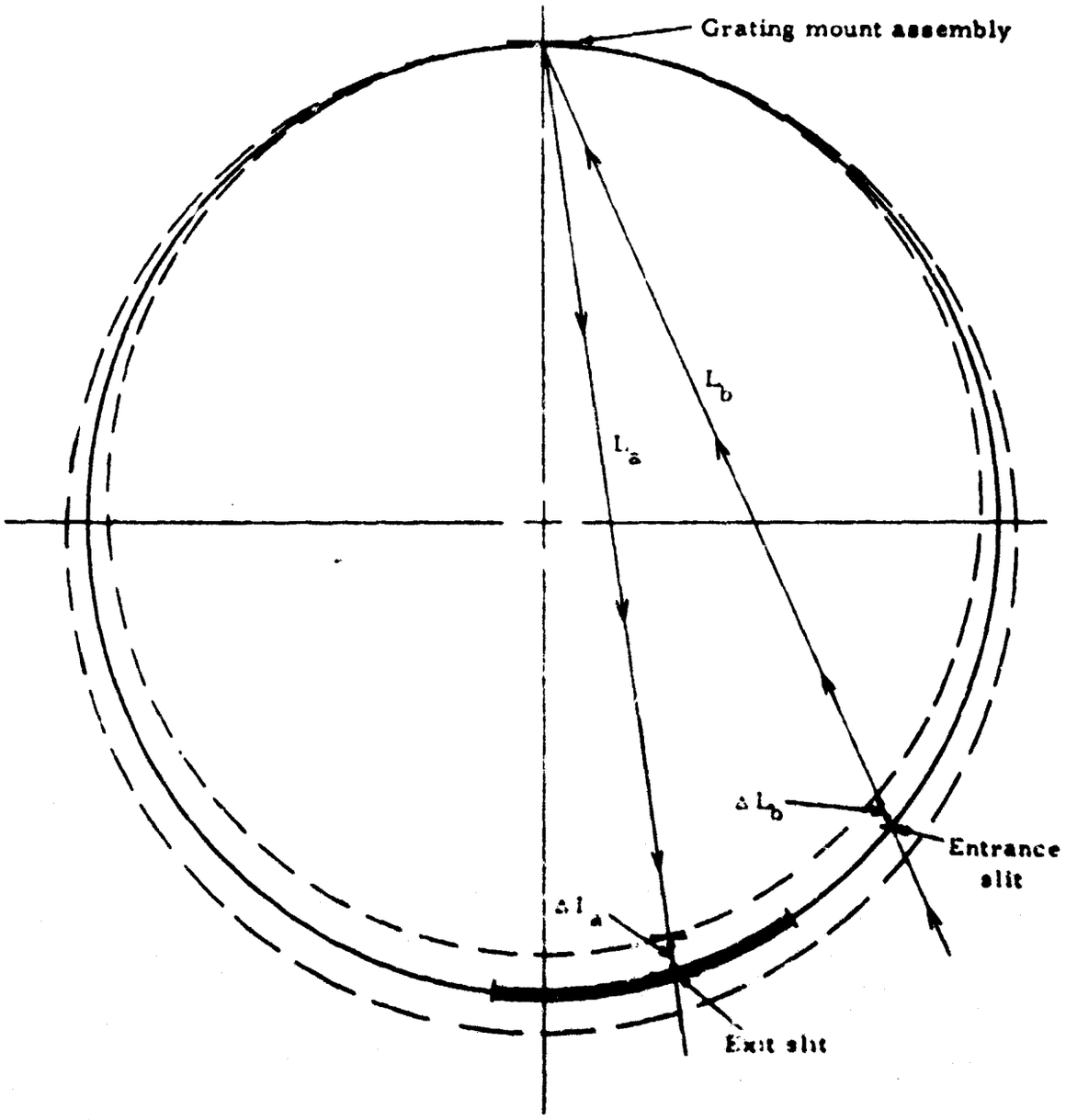

LEGEND

Rowland circle normal ——————

Rowland circle expanded — — —

Rowland circle contracted — — — —

Focal curve area ▬▬▬

Optical path ——→

Figure 4-11 Rowland Circle

5322-FR-108

4.3.8 Light Level

Since all direct reading spectrometers used for spectrochemical analysis record relative rather than absolute energy, the logic used to show sufficient energy at the phototube will be based on past experience. It is to be shown that this energy with the Base Level Analyzer is at least as great as that of current commercial oil analysis instrumentation and is more than adequate.

The energy gathering power of an optical system is the f/number which in the case of an optical spectrometer is the distance from the grating to the focal curve (approximately the radius of curvature of the grating) divided by the mean aperture.

$$f/no. = \frac{R}{\bar{A}}$$

where

$$\bar{A} = 2\left[\frac{W \times H}{\pi}\right]^{1/2}$$

Therefore

$$f/no. = \frac{R}{2\left[\frac{W \times H}{\pi}\right]^{1/2}}$$

where

W = width of the ruled area

H = height of the ruled area

Now the energy ratio being diffracted by two gratings (1-meter versus 3-meter) at a particular wavelength, is the ratio of the square of the f/numbers. This is assuming that the entrance optics and the blaze of the grating are equally efficient. Therefore, comparing the Pensacola Naval Air Station 3-meter f/42.1 spectrometer with the Base Level Analyzer 1-meter f/22.9, 1-meter system will gather approximately 3.4 times as much energy per unit entrance slit height as the 3-meter system.

Now the Pensacola system has a 22-millimeter entrance slit height compared to the 8 millimeter used in the Base Level Analyzer, therefore the total energy advantage of the 1-meter system is 23 percent.

4.4 Radio Frequency Interference

Since the Base Level Analyzer contains two active spark gaps (broadband radio frequency radiator, considerable attention was addressed to the problem of making the design meet the requirements of MIL-I-26600 Class II. A review of all internal (Baird-Atomic) interference data was conducted and an external literature search was made in order to determine the practiced state of the art in spectrograph radio frequency interference suppression. All information gathered showed that no serious attempt had ever been made to design, construct, or qualify a spectral emission instrument to MIL-I-26600.

It was therefore decided that a breadboard should be constructed and subjected to the specified tests, so that design criteria could be established.

The breadboard was constructed using components that would most closely approximate the final design (figure 4-12). These components were, with one exception, layed out such that the excitation source could be completely enclosed, the only exception being the 12 kilovolt transformer primary. This is shown diagramatically in figure 4-13. In order to minimize the capacity coupling between the primary and secondary of the transformer a Faraday shield plane was placed between them. This shield plane also acted as the base plate of a fine mesh copper enclosure (figure 4-13). Since at frequencies in excess of one gigacycle the attenuation of a copper mesh shield starts to deteriorate. Provision was made to enclose the total breadboard, (including copper mesh shield) in a further continuous galvanized steel enclosure, thereby effecting double shielding. The steel enclosure was made large enough to hold line suppression filters in the event that they were required. Both shields (copper mesh and steel) were pierced so that adjustments could be made to the control gap and such that air could be ducted into the system (figures 4-14, 4-15, and 4-16).

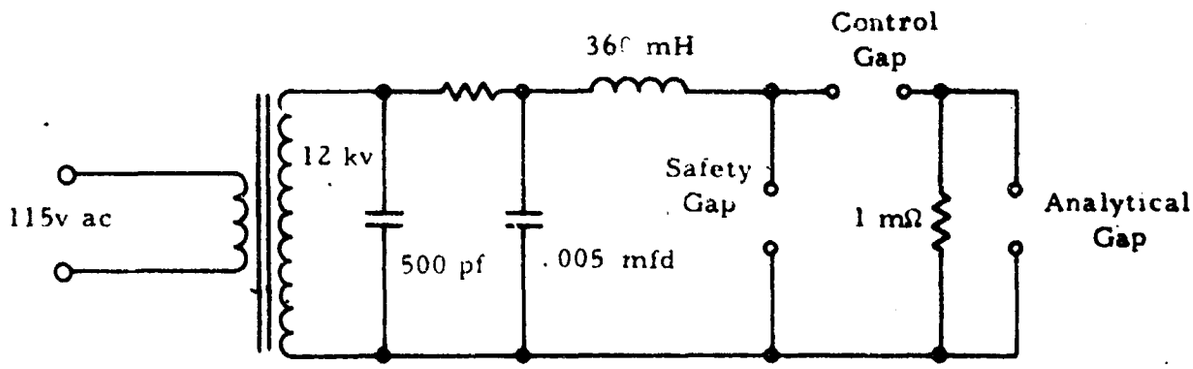

Figure 4-12. Breadboard. Schematic Diagram

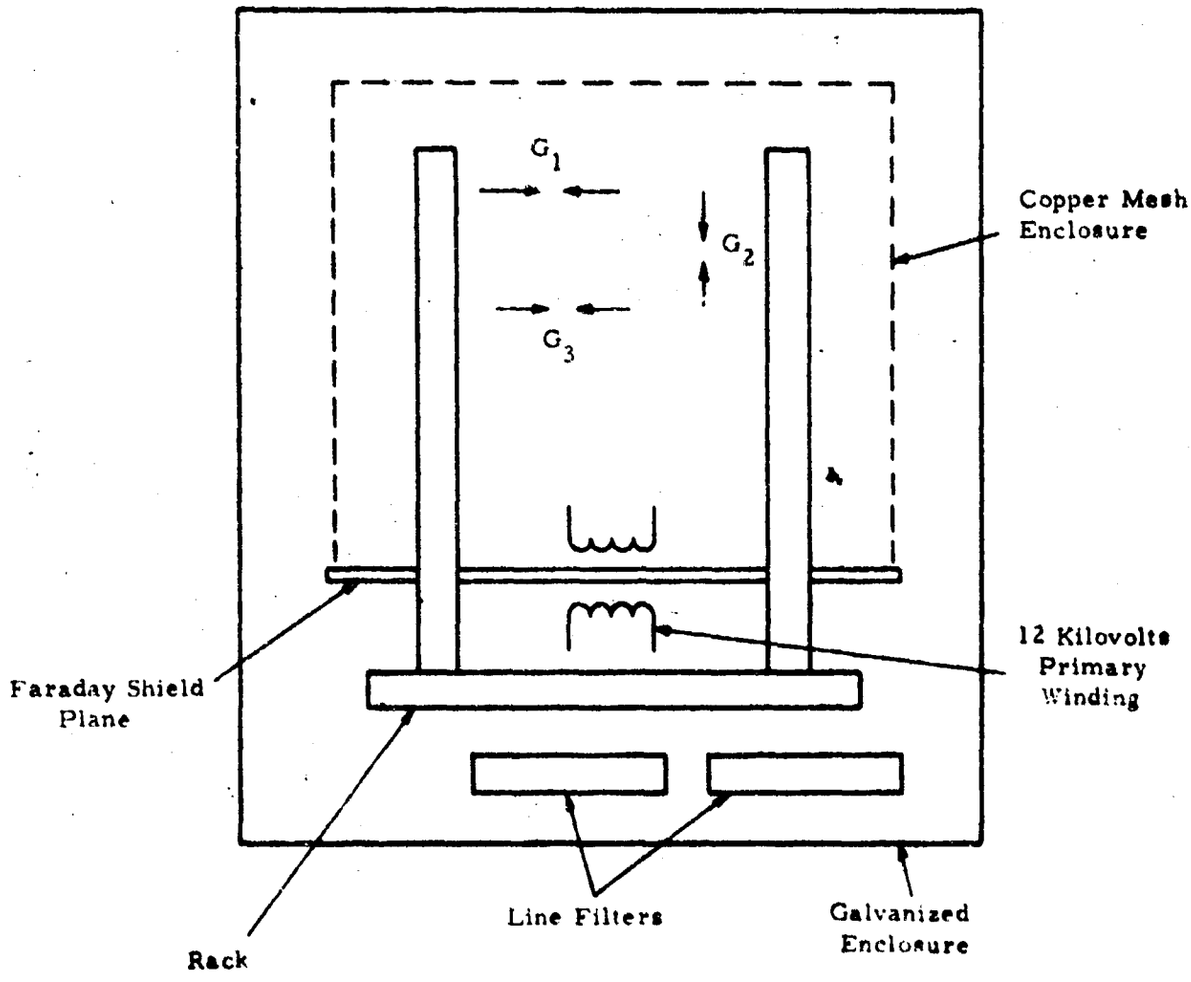

G_1 = control gap
G_2 = analytical gap
G_3 = safety gap

5322-FR-88

Figure 4-13. Breadboard Layout

Figure 4-14. Breadboard Without Shields

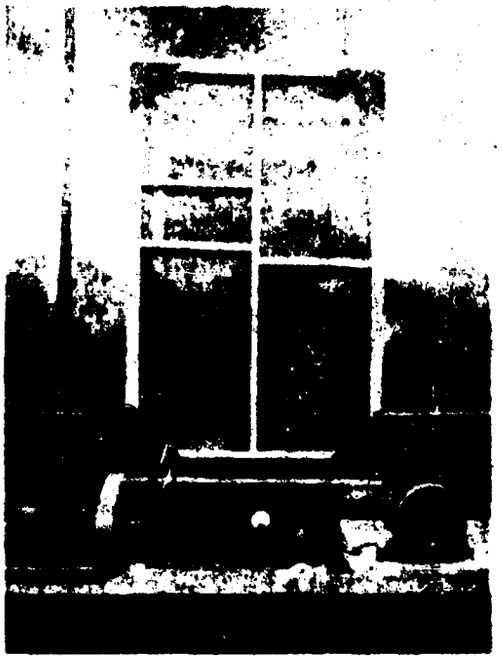

Figure 4-15. Breadboard With Copper-Mesh Shield

5322-FR-92

Figure 4-16. Breadboard With Copper-Mesh and Galvanized Steel

The configuration of the breadboard and the associated shields gave rise to a test program based on progressive shielding, namely

a. Test of breadboard without shields or filters.

b. Test of breadboard with copper mesh shield and without filters.

c. Test of breadboard with both copper mesh and steel shields and without filters.

d. Test of breadboard with all shields and filters.

All tests (both conducted and radiated) were performed to MIL-I-26600 Class III and were performed by Sanders Associates, Inc., Nashua, New Hampshire (figure 4-17). It is to be noted that radiation tests to Class III are more severe than to Class II by a factor of seven. The test results and report prepared by Sanders are to be found in appendix B.

Tests showed that it is possible to design a Base Level Analyzer to MIL-I-26600 Class II providing the following criteria are met.

a. All radiating sources must be double shielded and the external shield must be both solid and continuous.

b. All external openings (windows, air ducts, etc.) must be shielded.

Note: It is undesirable to have rectangular openings in the outershield due to the possibility of wavelength propagation.

c. Line suppression filters must be used and must have at least 70db attenuation at 0.11 megacycles.

d. Faraday shields must be placed between the primary and secondary of all excitation source transformers.

e. Shielded cable and/or conduit must be used for all interconnections.

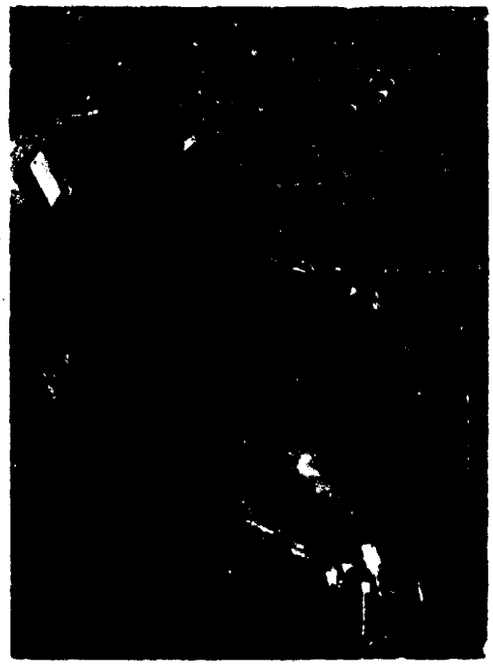

(a) 9322-FR-03

(b) 9322-FR-04

(c) 9322-FR-00

Figure 4-17. Various Views of Test Setup

f. The equipment must be grounded with a solid 3-inch ground strap.

All of the above criteria have been met or exceeded in the subject design and no interference problems are anticipated.

5. SYSTEM SPECIFICATIONS

5.1 Capability

The Base Level Analyzer shall be capable of routinely detecting trace elements in lubricating oil over the range of concentrations specified for each element in table 5-1. The equipment will discriminate in respect to the ten elements -- iron, lead, tin, silver, copper, chromium, nickel, silicon, magnesium, and aluminum.

5.2 Accuracy

The accuracy of the instrument shall be such that the deviation from the average measured amount of any specified element present in the Standard Reference Specimen shall not exceed the limits set forth in table 5-1. The deviation (D) is expressed in the following formula.

$$D = \frac{\sqrt{d_1^2 + \cdots\cdots d_{10}^2}}{(10)^{1/2}}$$

where the differences of the ten analyses from the average measured value d(average) are shown as d_1 through d_{10} and the average amount of an element, d(average), contained in a Standard Reference Specimen is expressed

$$d(\text{average}) = \frac{\quad}{10}$$

where d_{a_1} through $d_{a_{10}}$ are the actual measured values of the element as displayed on the Base Level Analyzer readout.

Table 5-1

Accuracy Specifications

Element	Low Concentration Accuracy (ppm)	Low Concentration Range (ppm)	High Concentration Accuracy (percent)	High Concentration Range (ppm)	Concentration Range (ppm)
Magnesium	± 2	1 to 20	± 10	20 to 500	1 to 500
Chromium	± 2	1 to 20	± 10	20 to 400	1 to 400
Lead	± 7	1 to 70	± 10	70 to 500	1 to 500
Silicon	± 3	1 to 30	± 10	30 to 200	1 to 200
Silver	± 3	1 to 20	± 15	20 to 300	1 to 300
Nickel	± 2	1 to 20	± 10	20 to 500	1 to 500
Iron	± 3	1 to 30	± 10	30 to 500	1 to 500
Copper	± 4	1 to 26.6	± 15	26.6 to 300	1 to 300
Tin	± 2	1 to 20	± 10	20 to 500	1 to 500
Aluminum	± 2	1 to 20	± 10	20 to 300	1 to 300

5.2.1 Standard Reference Sample

The Standard Reference Sample shall be prepared by the contractor and shall be formulated (using 7808 oil as a base) in accordance with National Bureau Standards Nomograph 54 and shall contain contaminant levels of 8, 20, 50, 100, 200, 300, 400, and 500 parts per million up to the maximum level of each element as specified in table 5-1.

5.2.2 Temperature Range

The accuracy specified in paragraph 5.2 shall not be exceeded over a temperature range of 32°F to 130°F.

5.3 Configuration

The configuration of the Base Level Analyzer shall conform to figure 3-2.

5.3.1 Size

The dimensions of the equipment (including transit case) shall not exceed the following:

Height	71 inches maximum
Width	72 inches maximum
Depth	40 inches maximum

5.3.2 Weight

The weight of the equipment (including transit case) shall not exceed 1100 pounds.

5.4 External Connections

The equipment shall require only the following external connections:

a. Electrical Power
b. Exhaust Gas Ducting
c. Ground Connection
d. Incoming Air Duct (Note: only when there is a local explosion hazard)
e. Electrical Readout Signal to Auxiliary Equipment

5.4.1 Electrical Power

The equipment shall operate from

a. Single phase 60-cps, 115 volts ± 10 percent

b. Single phase 50 cps, 235 volts ± 10 percent

Peak power shall not exceed 4000 watts.

5.5 Readout

The equipment shall have two readouts; one visual, the other electrical.

5.5.1 Visual Readout

The visual readout shall be a 3-digit Nixie display and (for 7808 oil only) shall present the analysis of the contimant directly in parts per million. The readout will be directly under the control of the operator by means of a front panel switch.

5.5.2 Electrica. Readout

The electrical readout shall be a 10-line (9 wires plus ground) 9-bit parallel binary output. Each active line shall be capable of feeding a 10,000-ohm load. The output level shall be 0 to + 10 volts where zero volts is logic "zero" and + 10 volts is logic "one."The readout will be directly under the control of the operator by means of a front panel switch.

5.6 Maintenance Manhours

Based on a quantitative prediction, the maintenance manhours shall not exceed 0.04 of the operating hours where the total operating hours equals 3000.

5.7 Reliability

The Mean Time Between Failure shall not be less than 150 hours and the reliability shall not be less than 0.9989 for a 10-minute operating use period over a total of 3000 operating hours.

5.8 Electromagnetic Interference

The analyzer shall conform to the requirements of MIL-I-26600 Class II.

5.9 Environmental Conditions

The analyzer shall meet MIL-T-21200 Class III and shall conform to the requirements of the sheltered equipment category as specified in MIL-STD-810.

5.10 Safety

Provision for the safety of personnel shall be incorporated to the maximum extent possible with regard to anticipated operating conditions and capability of operating personnel.

6. SYSTEM DESIGN

6.1 General

As discussed in paragraph 4.1 the Base Level Analyzer is comprised of three major systems (figure 3-3).

a. The Optical Head Assembly

b. Excitation Source and Power Control System

c. Electronic Signal Processing System

The purpose of this section is to discuss in detail the design of each major system showing the rationale for choosing a particular design, the functional operation of the design, and the method of implementation.

In addition, this section contains a description of the mechanical design which shows the mechanical interrelation of the three major systems.

6.1.1 Optical Head Assembly

As discussed in section 4, the optical head assembly (figure 6-1) contains six functional systems as follows.

a. Main Optical System

b. Servo Monitor System

c. Tilt-Normal Subsystem

d. Focus Servo System

e. Sample Stand Assembly

f. Relay Network and Integrator Subassembly

It is to be noted that item (f) is not in itself a complete system and that it has only been included in this assembly because of its physical location. It is, in fact, a functional part of the electronic signal processing system and its relation to that system will be discussed in paragraph 6.1.3.

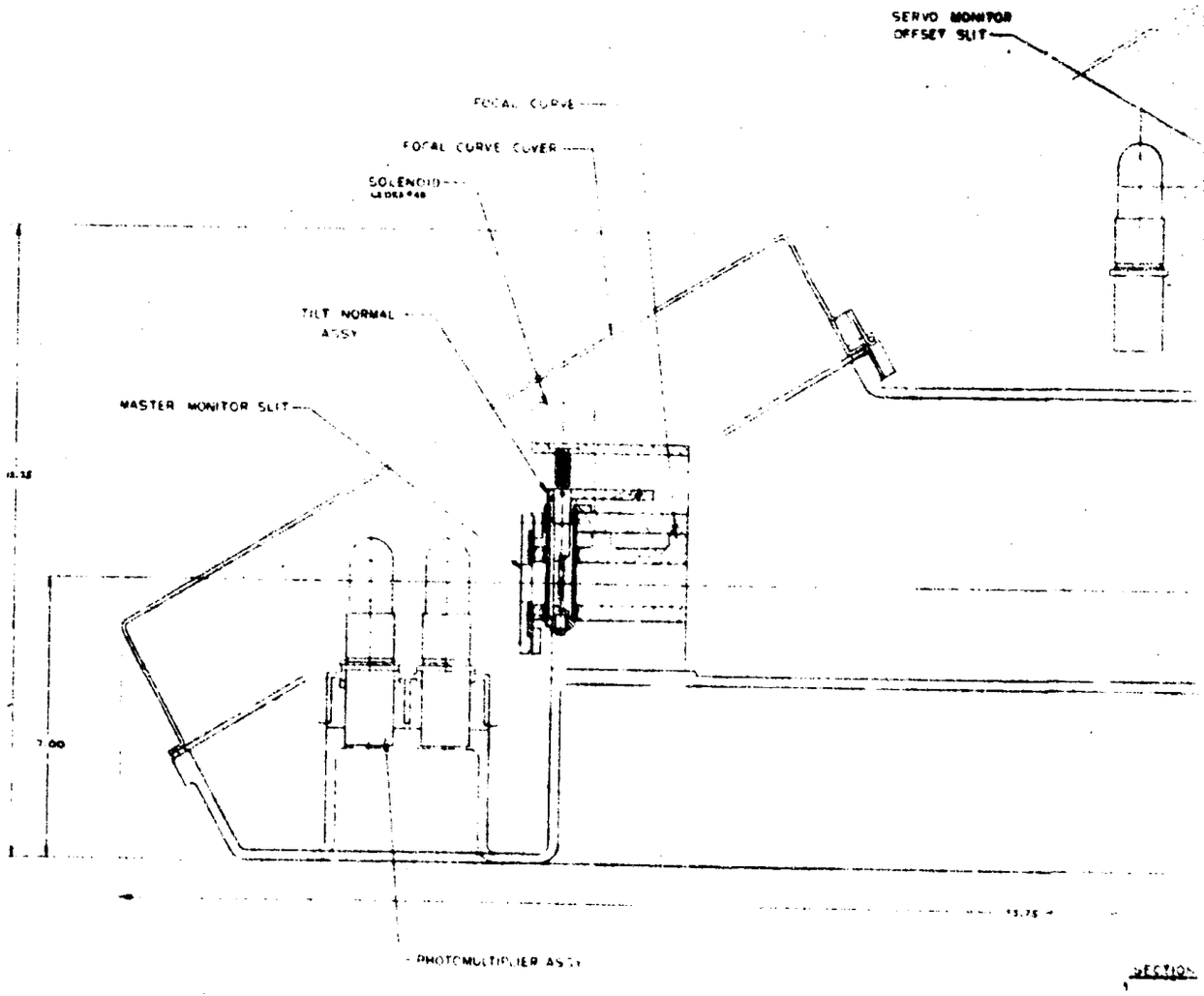
SERVO MONITOR
OFFSET SLIT
FOCAL CURVE
FOCAL CURVE COVER
SOLENOID
TILT NORMAL
ASSY
MASTER MONITOR SLIT
PHOTOMULTIPLIER ASSY

A

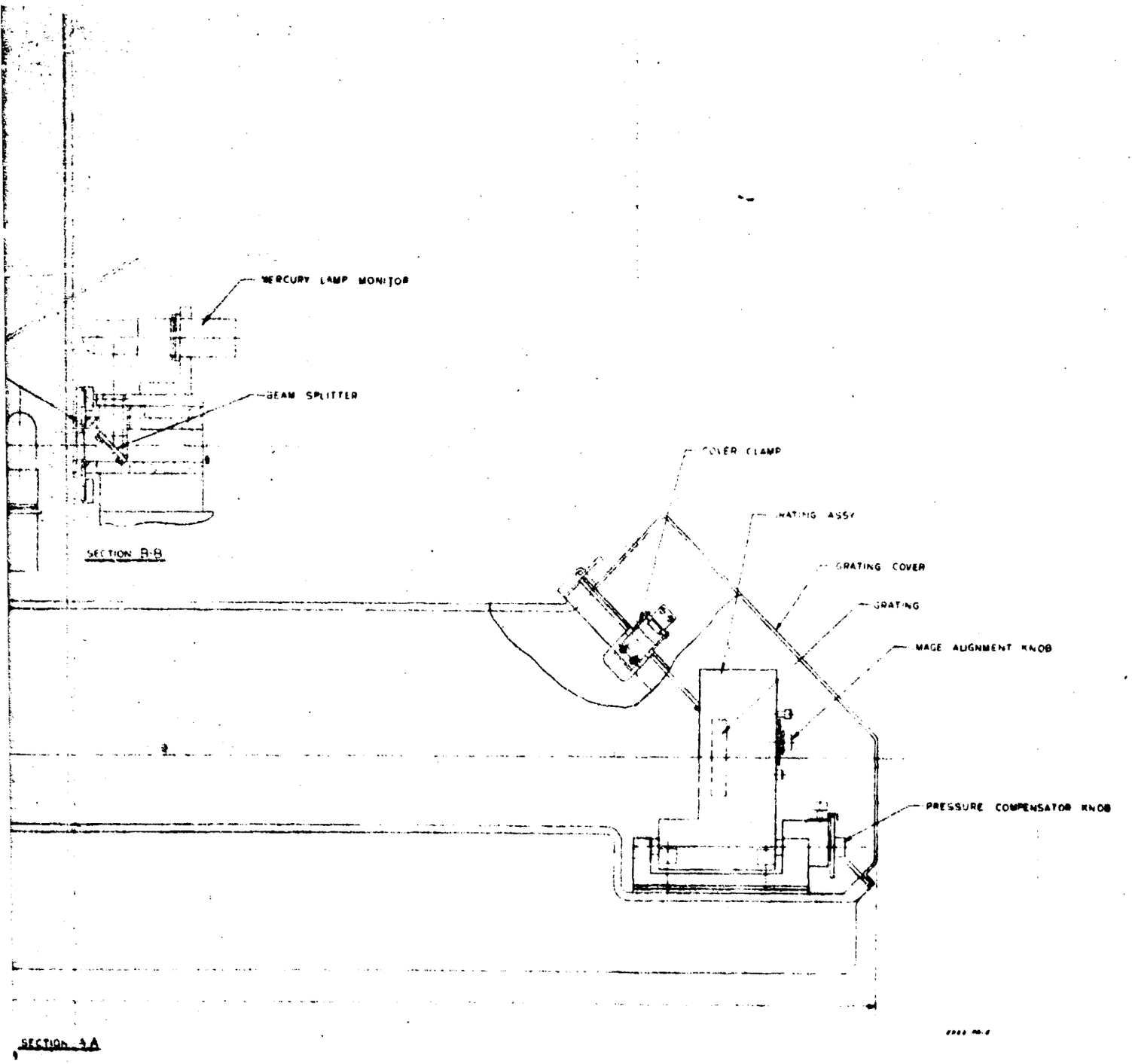

Figure 6-1. Optical Head (Cross Section through Focal Plane and Tilt-Normal System

B

6.1.1.1 Main Optical System -- The main optical system is illustrated schematically (figure 6-2). It consists of:

a. Source or Analytical Gap
b. Entrance Optics
c. Entrance Slit
d. Concave Grating
e. Focal Plane and Exit Slits
f. Folding Mirrors and Phototubes

6.1.1.1.1 Entrance Optics -- The analytical gap, where the oil is excited, has an effective size, when viewed by the entrance optics of 6 millimeters in width by 3 millimeters in height. The radiation from this source is picked up by the entrance (or condenser) lens and directed into the spectrometer proper. A concave mirror located behind the analytical gap reimages the gap on itself in the manner common to film projectors and gives more energy and more uniform distribution of the energy.

The condenser lens is designed and its location chosen to fill the entrance slit uniformly with energy from the analytical gap, and with a minimum loss. The most efficient optical system can do no more than fill the entrance slit with the brightness, or steradiancy, of the source, minus transmittance and reflectance losses. In other words, when viewed from any point on the grating, the entrance slit should appear uniform in intensity along its length and this intensity should be equal to the maximum intensity of the source, minus unavoidable transmittance and reflectance losses. In this situation, the total energy entering the system is proportional to the open area of the slit.

The two general approaches to accomplishing this are:

a. Image analytical gap directly on the entrance slit
b. Image the analytical gap onto the aperture of the grating

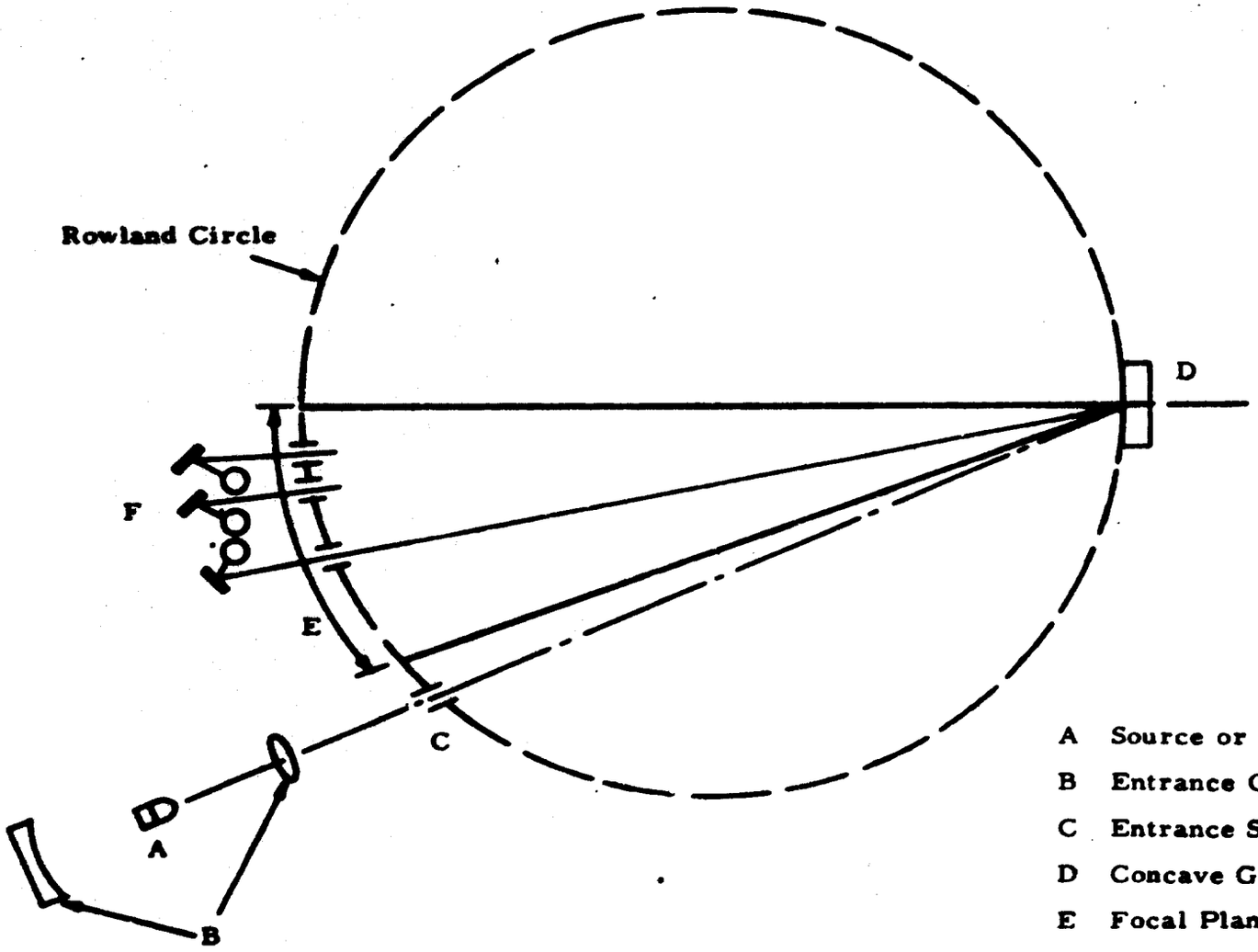

A Source or Analytical Gap
B Entrance Optios
C Entrance Slit
D Concave Grating
E Focal Plane and Exit Slits
F Folding Mirrors and Phototubes

5322-FR-70

Figure 6-2. Main Optical System

When the analytical gap is imaged directly on the entrance slit, the energy getting through the slit is limited to a thin vertical section of the source because the edges of the slit act as a field stop and cut out radiation coming from any portion of the gap that is not on the center line. In a vertical direction, the area of maximum radiance is limited to the portion of the length of the slit covered by the image of the source. If the imaging system is 1 to 1, this limits the effective slit length to 3 millimeters. This limitation can be overcome by increasing the magnification of the condenser system to fill the full slit height. However, this takes an increasing amount of space.

Another important disadvantage is the fact that no radiation is received that originates in areas of the source that are not on the optical axis. Therefore, the total energy measured by the system is not a good average of the radiation over the entire area of the gap.

Now, if the analytical gap is imaged onto the aperture of the grating, the entrance slit is uniformly filled along its length, and in addition, the energy measured by the system is integrated over the entire area of the source gap. For this reason, imaging of the gap on the grating aperture was selected as the optimum method of slit illumination for the Analyzer.

The condenser lens (B) is designed and located to throw an image of the 3 x 6 millimeter analytical gap onto the 30 x 50 millimeter ruled area of the grating. The image is magnified by 7.5 making the image 22.5 x 45 millimeter, or slightly smaller than the ruled area of the grating. This permits a small amount of image wander due to inherent instability of the flame in the arc gap without loss of energy when the image overlaps the edge of the grating aperture.

6.1.1.1.1.1 Sirk's Focus -- In a system where both entrance and exit slits are located on the Rowland circle, the image of the entrance slit is brought to a sharp focus at the exit slit in the plane of the Rowland circle. However,

since the image of the entrance slit, as seen in the image plane where the exit slits lie, is astigmatic, the slit image is astigmatic or stretched out vertically and comes to focus vertically in a different plane. In order to make an object come to focus vertically at the exit slit, it is necessary to place it behind the entrance slit at a point known as Sirk's focus. Objects placed at Sirk's focus will come to focus vertically at the exit slit location on the Rowland circle, but will be out of focus horizontally.

The location of Sirk's focus can be calculated from the formula:

$$S = R\left[\frac{1}{\cos A - \sin B \tan B} - \cos A\right]$$

where

R = radius of curvature of concave grating

A = angle of incidence, measured from grating normal

B = angle of dispersion, measured from grating normal

S = distance from Sirk's focus to entrance slit

It is sometimes desirable to locate the condenser lens of the entrance optical system at Sirk's focus, where the lens aperture is in focus at the exit slit, and the lens is of minimum size. However, considerable space can be saved by moving the lens closer to the entrance slit and making it large enough so that the exit slit aperture is still completely filled by the out-of-focus image of the condenser lens. Since there is no problem in designing a lens of sufficient aperture, the condenser lens in this design is located somewhat closer to the entrance slit than Sirk's focus.

6.1.1.1.2 Grating -- The diffraction grating to be used in the Base Level Analyzer design is a concave grating of 1-meter radius of curvature with 1666.7 grooves per millimeter. The angle of the blaze is 16°48' or a blaze wavelength of 3430 A.

The blaze wavelength is defined as that wavelength which is most eificiently diffracted into the first order. This efficiency is routinely 50 percent of the incident energy. The one meter radius of curvature and 1666.7 grooves per millimeter result in a linear reciprocal dispersion of 6.0 A per millimeter. This dispersion along with a 50-micron entrance-25-micron exit slit combination produces a wavelength separation of 0.225 A.

The grating will be a replica on fused quartz and the ruled area will be 30 x 50 square millimeters. A fused quartz grating substrate has been selected because of its low thermal expansion coefficient. The diffraction grating will be ruled by Bausch and Lomb Incorporated.

6.1.1.1.3 Mechanical Configuration -- The most vital mechanical aspect of the spectrometer design is that, over the range of specified environmental conditions, there be minimum dimensional and angular shift between the entrance slit, grating, and exit slit. Therefore, the prime function of the Optical Head Housing is to provide a dimensionally stable base for the optical elements. Other important requirements are that it be a light-tight enclosure and a reasonably air-tight compartment for humidity control.

These requirements dictated that the configuration of the housing be that of an irregularly shaped tabular structure with a ribbed base, having the minimum envelope required to enclose the optical path (figures 6-3, 6-1, and 6-4). This configuration ensures maximum flatness and torsional rigidity. In considering the material to be used in the design, there are many trade-offs, not the least being the method of fabrication. Two obvious methods of fabrication are weldment and casting.

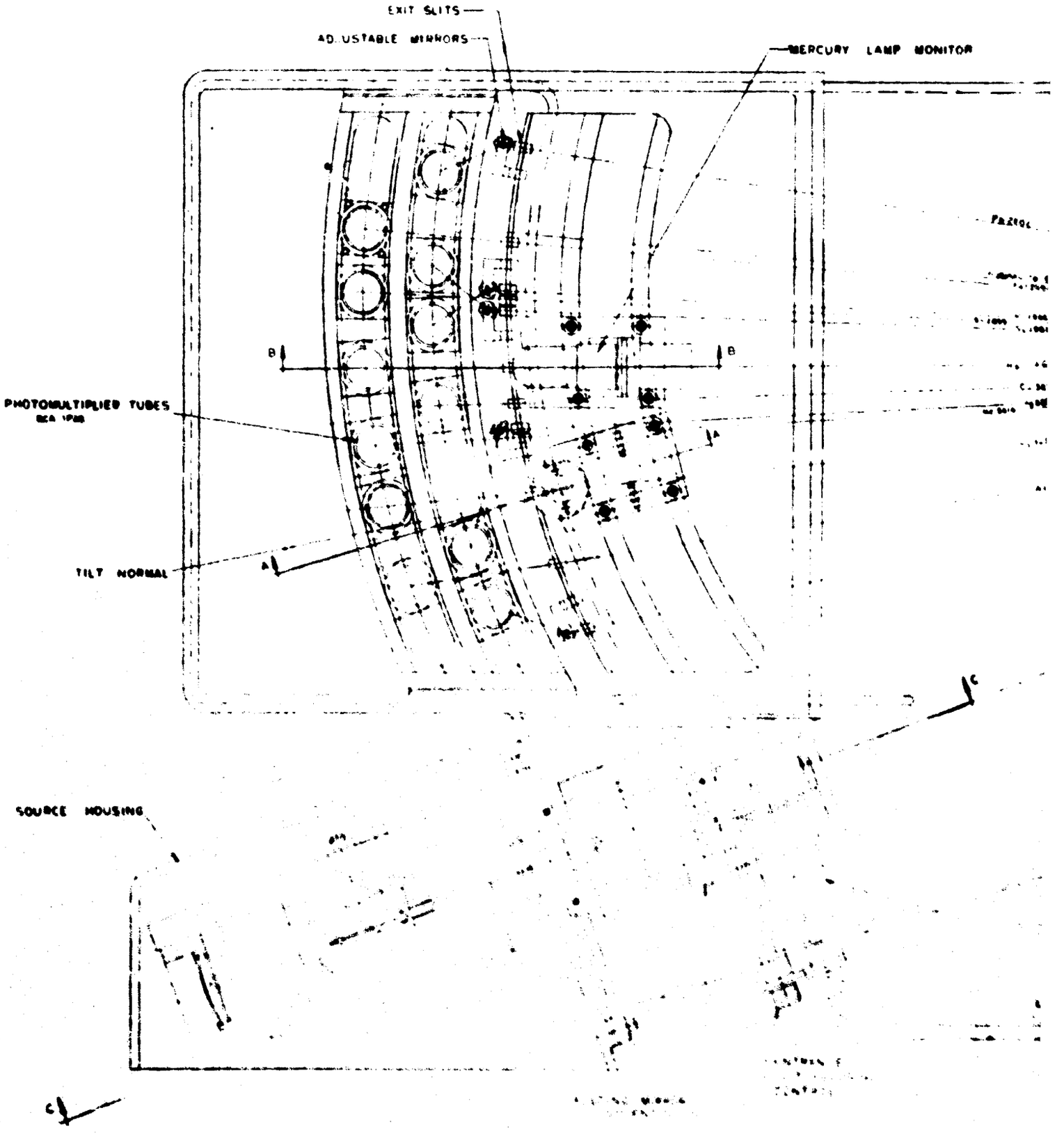
EXIT SLITS
ADJUSTABLE MIRRORS
MERCURY LAMP MONITOR
B
B
PHOTOMULTIPLIED TUBES
TILT NORMAL
A
A
C
SOURCE HOUSING
C

A

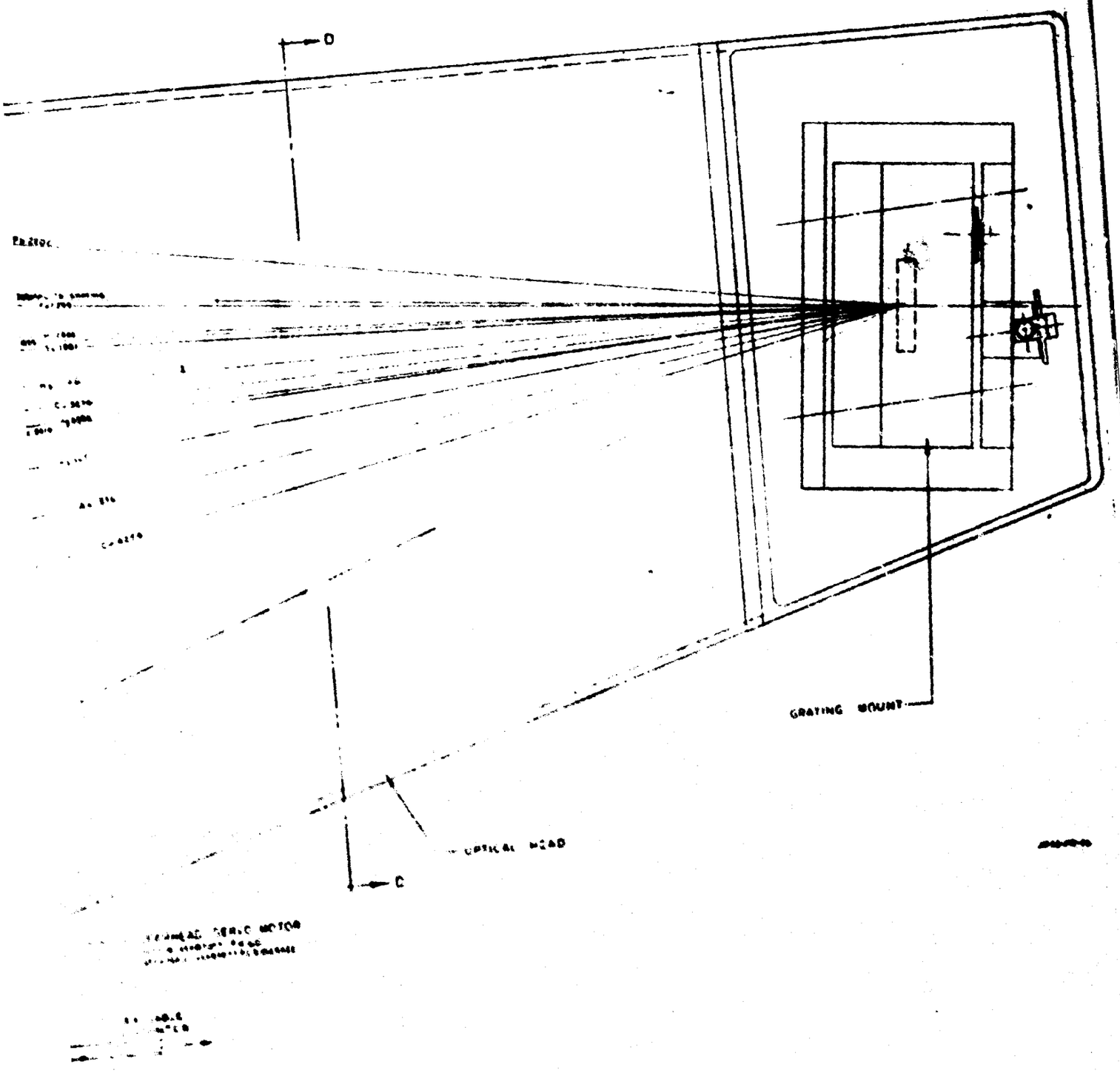

B

Figure 6-3. Optical Head (Top View)

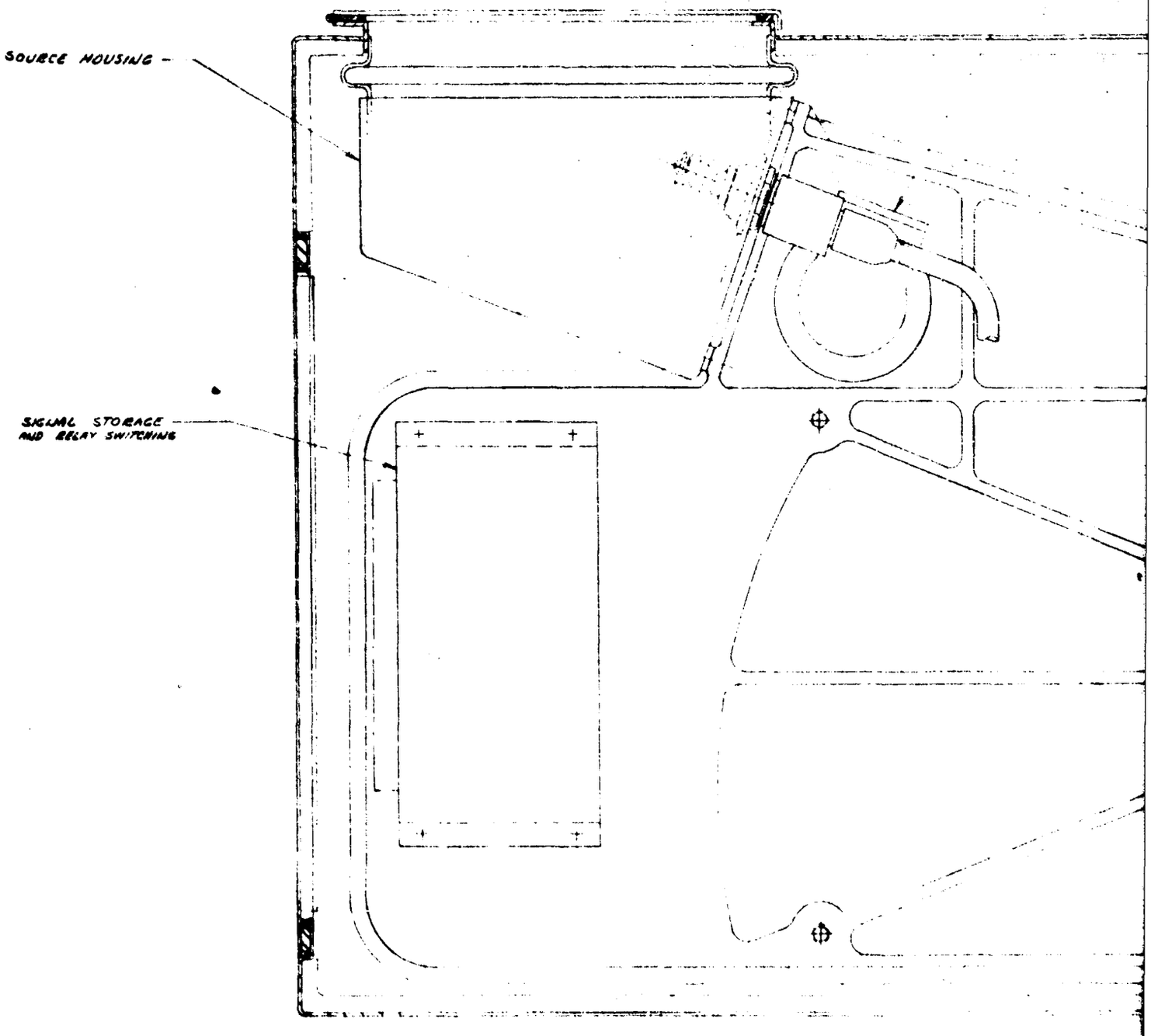

A

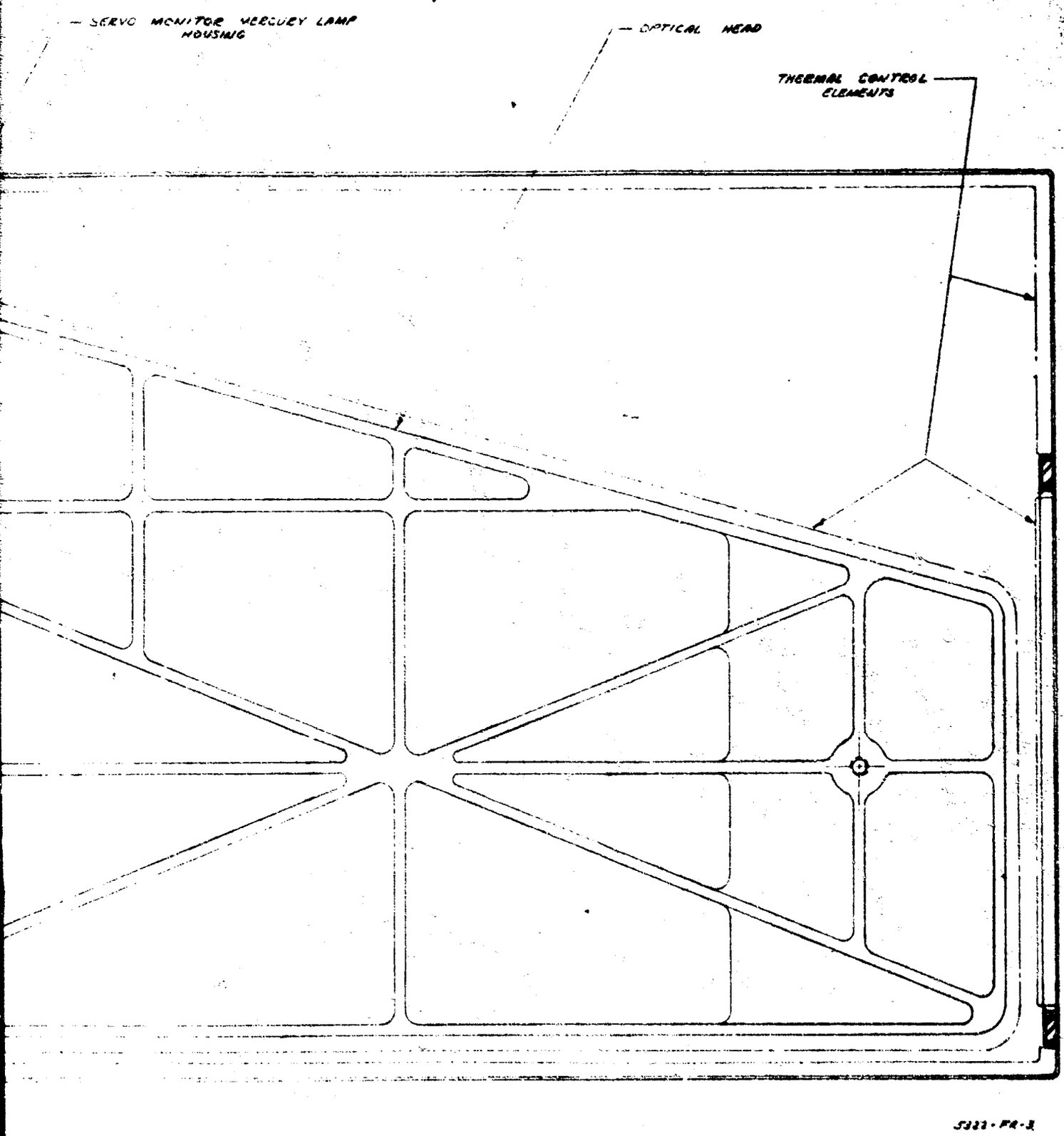

Figure 6-4. Optical Head (Bottom View)

A weldment was rejected on the basis that, with this size of housing, it would be difficult to achieve complete stress relief of the residual stresses caused by welding thereby compromising dimensional stability. Casting on the other hand does not present this problem. From a cost consideration point of view, the tooling required for welding generally equals the pattern cost for an equivalent casting, further the fabrication times for both processes are essentially the same.

In selecting the material from which the casting will be fabricated, the most important considerations are thermal, that is, thermal conductivity and thermal expansion. Conductivity is of great importance since materials having a low figure of thermal conductivity can produce large angular shifts due to differential heating. A low coefficient of expansion is desirable to reduce dimensional shifts. Additional considerations are that the material must have low density for weight reduction and must be castable. The materials considered were:

a. Magnesium
b. Iron
c. Aluminum

Magnesium was rejected due to difficulties in casting and machining. Iron on the other hand is perfectly reasonable in these respects, but presents major weight problems due to the fact that the minimum wall thickness that can be cast is 3/8 inch. This would result in a housing having a weight of 400 to 500 pounds. Aluminum was therefore chosen as the optimum material, the particular grade of aluminum being A 356.

The most significant design feature of the base of the housing is that the focal curve is cast with the base and is actually machined on the casting instead of being attached as a separate piece, as is frequently the case. This greatly reduces the optical alignment complexity and time. It is closely referenced in machining to the grating and entrance slit reference surfaces, thereby

taking advantage of the precision control achievable in machining to attain the highly critical alignment measurements. Other critical mounting surfaces machined on the base are the sample stand mount surface, mounting surface for the entrance slit, servo and, focus mechanism, and optical element mounts. The design is such that all machining operations may be accomplished with standard equipment.

Access doors are provided at three points and are designed to have minimum effect on the structural rigidity. These doors utilize both radio frequency interference and fluid gaskets.

In order to minimize the imposition of external stresses on the housing, it is attached to the main console structure by means of a three point mount (figure 3-3). Thermal isolators are provided between the housing and the main structure to reduce thermal conduction effects.

6.1.1.1.4 Grating Mount -- The function of the grating mount is to provide both a stable base and the necessary precision adjustments that must be made to the grating in order to align the optical system. There are three independent adjustments that must be made to the grating during alignment; these are pitch, roll, and yaw. In addition, an adjustment that provides linear displacement along the mean dispersion angle is required in order to compensate for pressure changes.

The first mount design considered was the much used kinematic mount. This, however, has two major disadvantages:

a. It is not sufficiently rugged to withstand the specified shock and vibration.

b. All the required adjustment motions are interdependent resulting is complex alignment.

The second (final) design that was evaluated was a modified gimbal mount (figure 6-5) where the pitch and yaw motions were provided by flex-pivot bearings. The choice of flex pivots was based on their complete absence of backlash. In essence this bearing is a torsion spring. Both the pitch and yaw motions require precise positioning and this is accomplished by means of precision differential screws using opposing screws for locking. The roll motion is accomplished by rotating the grating about its radius by means of a precision micrometer screw with an opposing screw for locking.

To obtain the linear motion along the mean dispersion angle, two guide rods are used. These guide rods are located in the main base of the mount and are set parallel to the mean dispersion angle. Two "V" grooves ride on one of the rods while a "flat" rides on the other. The "V's" guide the mount and prevent rotation in a horizontal plane, while the "flat" prevents rotation in a vertical plane. A differential screw provides the motion for this adjustment which features two spring-loaded "zero backlash" nuts, which are equally effective for both directions of travel.

A noteworthy feature of this design is that it can be pre-aligned in an alignment jig and placed directly in the optical head with only one further adjustment required. This means that all grating assemblies are interchangeable and results in less maintenance costs.

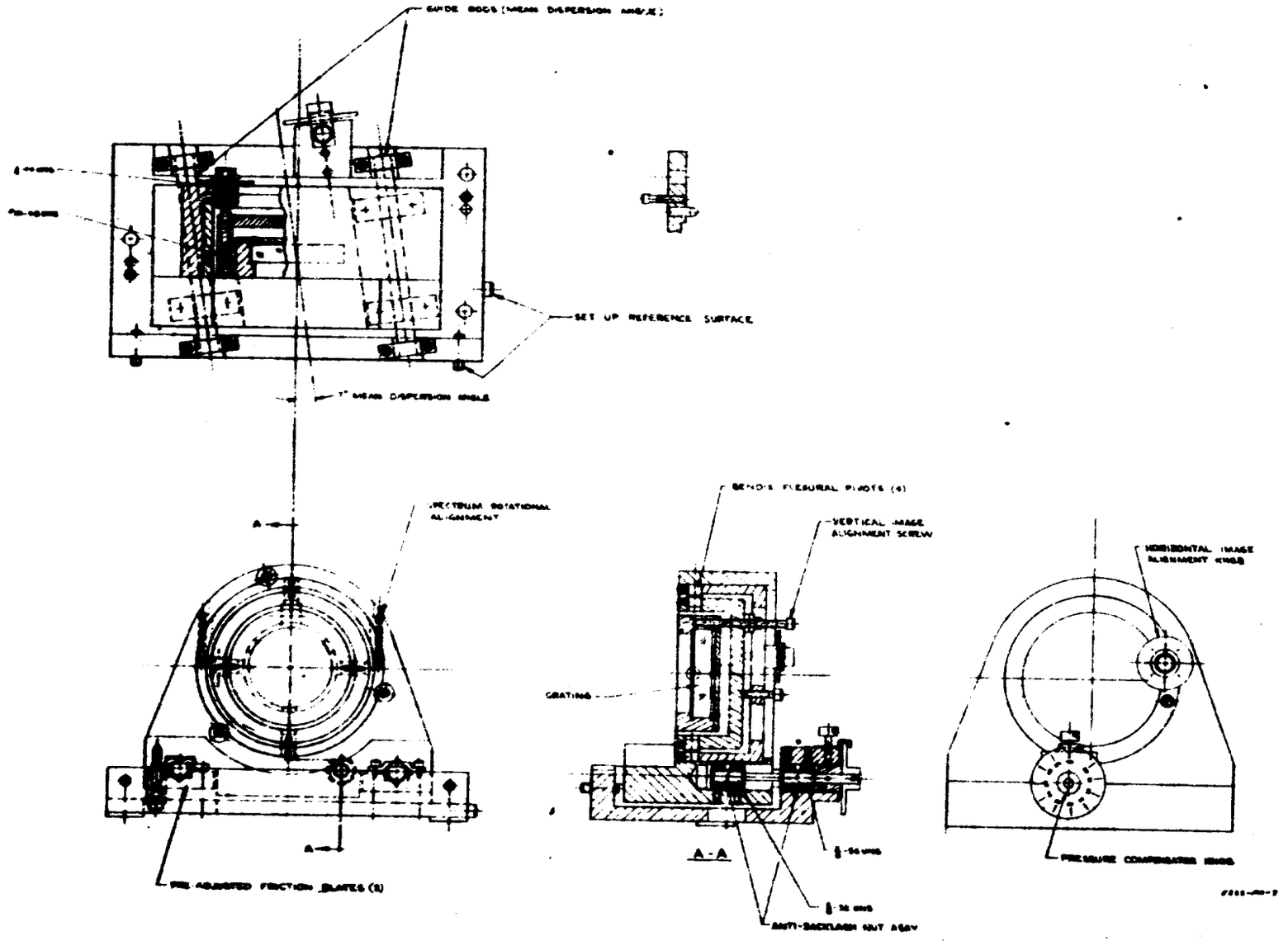

Figure 6-5. Grating Mount Assembly

6.1.1.2 Servo Monitor System

6.1.1.2.1 General -- As discussed in the optical analysis paragraph 4.3.6, there is a spectral line shift due to temperature, pressure, and humidity. The total amount of this shift can be of the order of 60 microns under the worst environmental conditions and can amount to ± 100 microns if mechanical stress and differential heating are considered. Since this degree of line shift results in gross inaccuracies it is necessary to provide an automatic correction system in the design, namely the servo monitor system. This system will have the capability of providing a ± 100 micron correction range with a ± 500 micron acquisition range and an accuracy of ± 1 micron.

The monitor system will only operate between sample burns and will be disconnected during the burn period thus precluding any interference problems. A visual readout will be provided to indicate the amount of line correction being used and to allow the operator to set the monitor system such that it is operating over the ± 100 micron control range. The system operates in the following manner. Light is emitted from an a-c operated monitor reference source (mercury vapor lamp) which is located at Sirk's focus, as calculated for the 3126A mercury line. The light passes through a cylindrical lens, is reflected 90 degrees by means of an electrically actuated 45-degree folding mirror, and is then transmitted through the rest of the optical system, as though it had originated at the analytical gap (figure 6-6). At the grating the mercury light is diffracted, causing characteristic spectrum lines of mercury to appear on the focal curve.

Because the reference source is a-c operated, there will be two glow regions that are excited on alternate half cycles of the 60-cps line voltage. These glow areas are confined to the ends of the tungsten filaments. At the 3126A line location on the focal curve, the two glow areas of the source are in focus and separated vertically (Sirk's focus). Therefore, the upper section of the focal curve receives light from one glow area during one half cycle and the lower section receives light from the other glow region during the next half cycle.

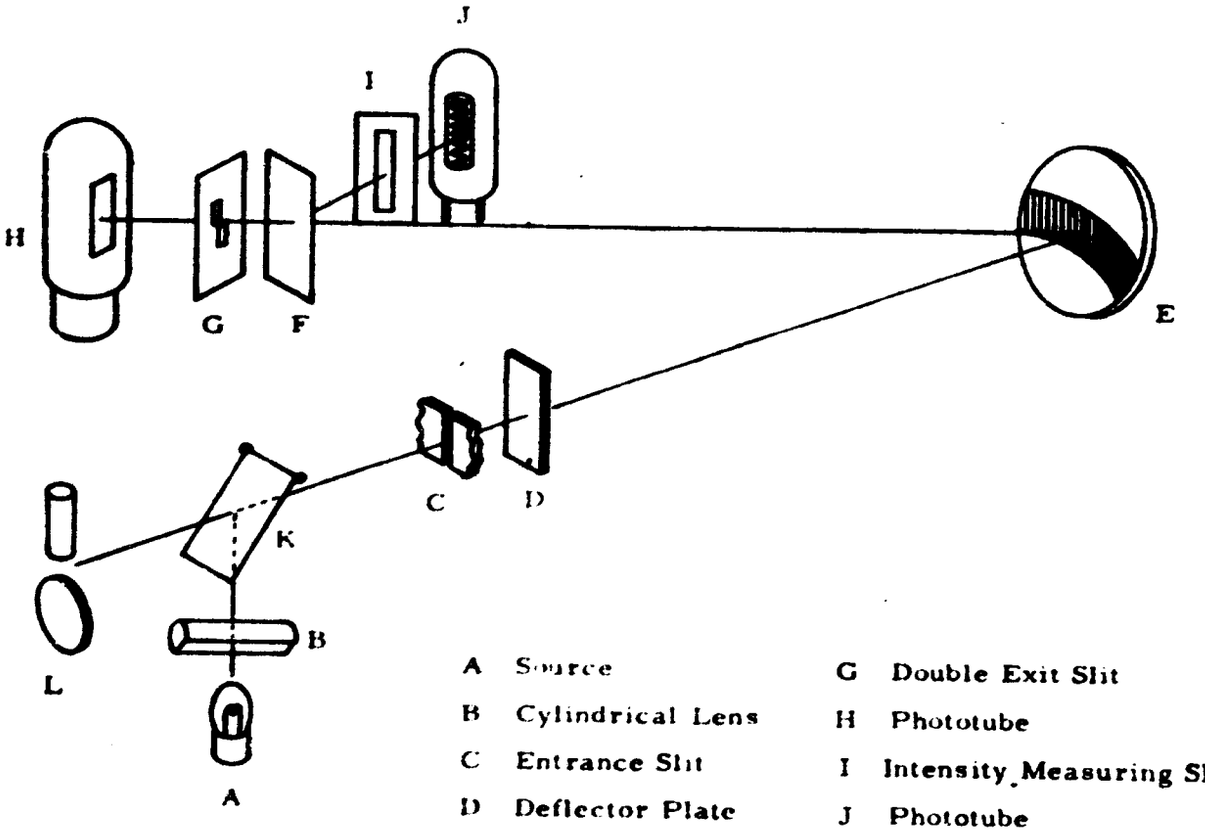

A	Source	G	Double Exit Slit
B	Cylindrical Lens	H	Phototube
C	Entrance Slit	I	Intensity Measuring Slit
D	Deflector Plate	J	Phototube
E	Concave Grating	K	Folding Mirror
F	Beam Splitter	L	Analytical Source

5322-FR-71

Figure 6-6. Servo Monitor Optics

A special offset exit slit is placed on the focal curve to accommodate spatially modulated mercury light. The upper opening of the offset slit passes half the 3126 A spectrum line's top portion while half of the spectrum line's lower portion is passed by the lower opening of the offset slit.

As long as this alignment of spectrum line and offset slit is maintained, a photomultiplier tube placed behind the offset slit "sees" equal amounts of light on each half cycle, and the tube's output current contains no a-c component with the same frequency as the mercury vapor lamp supply (figure 6-7).

If an optical misalignment causes the mercury line to move laterally, however, more light from one half cycle will strike the phototube. Light striking the tube during the other half cycle will be diminished. The difference in light intensities on alternating cycles causes an a-c component to flow in the phototube circuit (figure 6-8). This signal is amplified by a phase-sensitive servo amplifier and causes the servo motor to rotate a transparent, refractive deflector plate which optically shifts the entrance slit laterally until the 60-cps photomultiplier output is driven to zero. The calcium fluoride plate is rotated about an axis parallel to the length of the entrance slit.

In the design of such a servo monitor, three areas are of extreme importance.

a. Choice of Reference Line

b. Material used in the Deflector Plate

c. Differential Light Output Characteristics of the Glow Areas in the Mercury Vapor Reference Source

Note: Areas (a) and (b) are intimately related and will be discussed together.

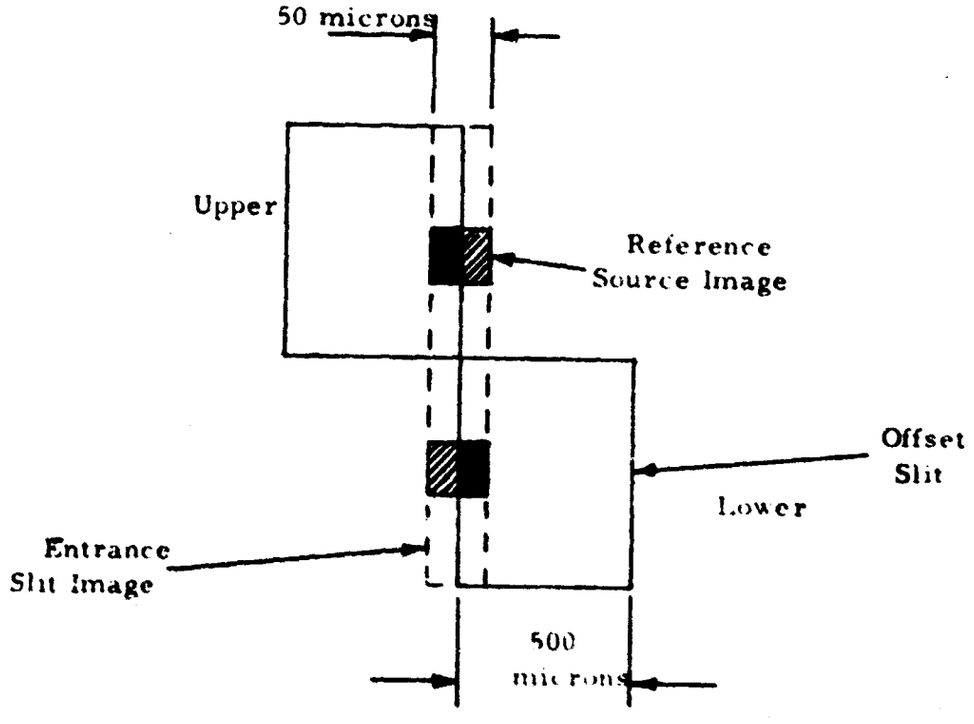

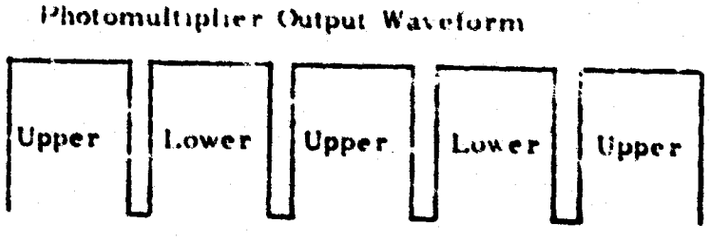

5322-FR-72

Figure 6-7. Offset Slit with Entrance Slit Image and Source Images Superimposed

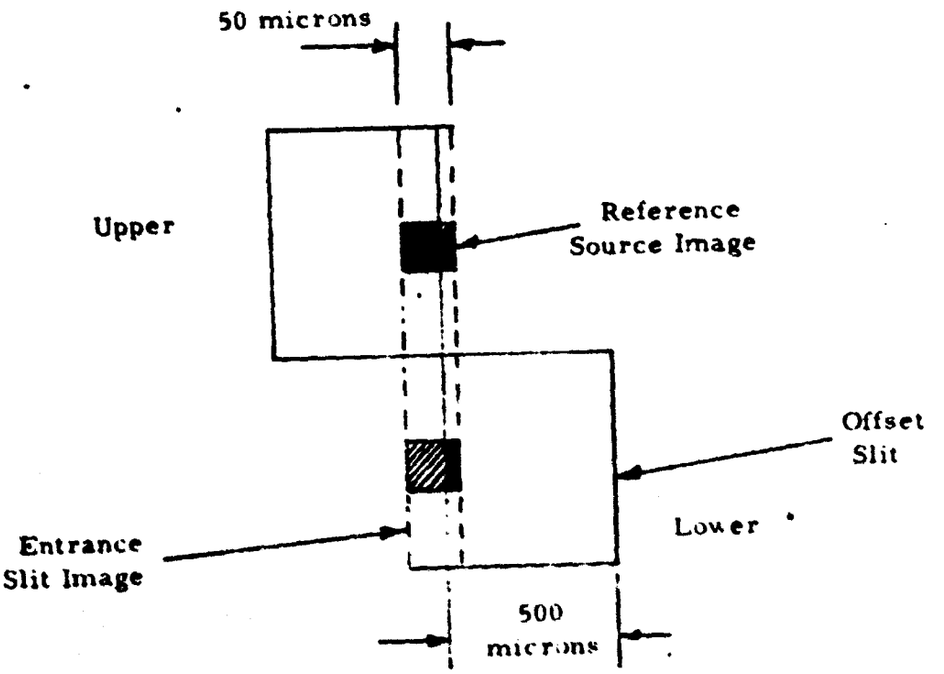

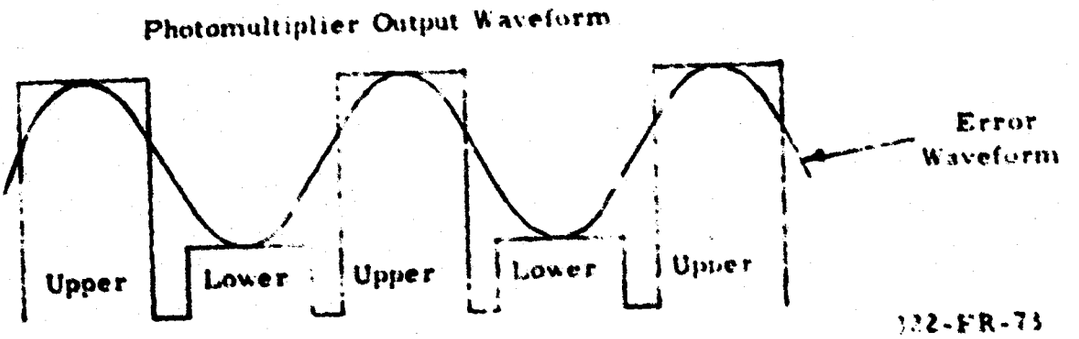

Figure 6-8. Offset Slit with Entrance Slit Image and Source Images Misaligned

6.1.1.2.2 Deflector Plate -- As previously mentioned, the apparent lateral shift of the entrance slit (as "seen" by the offset exit slit) is accomplished optically by rotating an essentially plane parallel plate of transparent refracting material about an axis parallel to the length of the entrance slit, such that the mercury light from the monitor reference source passes through it. In actuality, the deflector is not a true plane parallel plate because one surface has a 3-degree wedge angle with respect to the other parallel side, thus preventing an image of the entrance slit from falling on the grating. However, for the purpose of this discussion, the plate will be regarded as plane and parallel (figure 6-9). Now the amount of displacement d is relate to the angle of rotation θ, the index of refraction n, and the thickness, t, by the formula

$$d = \frac{n\, t \tan \theta' \sin (\theta - \theta')}{\sin \theta} \qquad (6\text{-}1)$$

Since the lateral displacement d is dependent on the index of refraction of the material it is desirable to use a material whose index is uniform over the 2203 A to 4300 A wavelength range. Three materials meet the requirements of uniform index and transparency.

a. Lithium Fluoride
b. Calcium Fluoride
c. Quartz

Lithium fluoride is however unacceptable due to the fact that it discolors upon ultraviolet radiation, thus reducing the material choice to either (b) or (c).

Assuming θ equals 5 degrees and d equals 100 microns and substituting the appropriate index values at 3200 A into equation (6-1), the required thickness of quartz is 3.5 millimeters while that of calcium fluoride is 3.69 millimeters. Now since the index of both materials varies with wavelength, it is necessary to plot displacement, d, against wavelength to establish the possible displacement errors over the wavelength range of interest (figure 6-10).

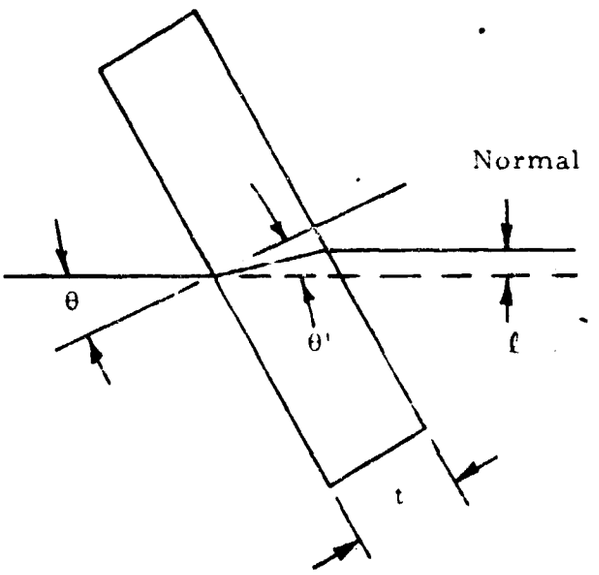

5322-FR-74

Figure 6-9. Deflector Plate, Optical Schematic Diagram

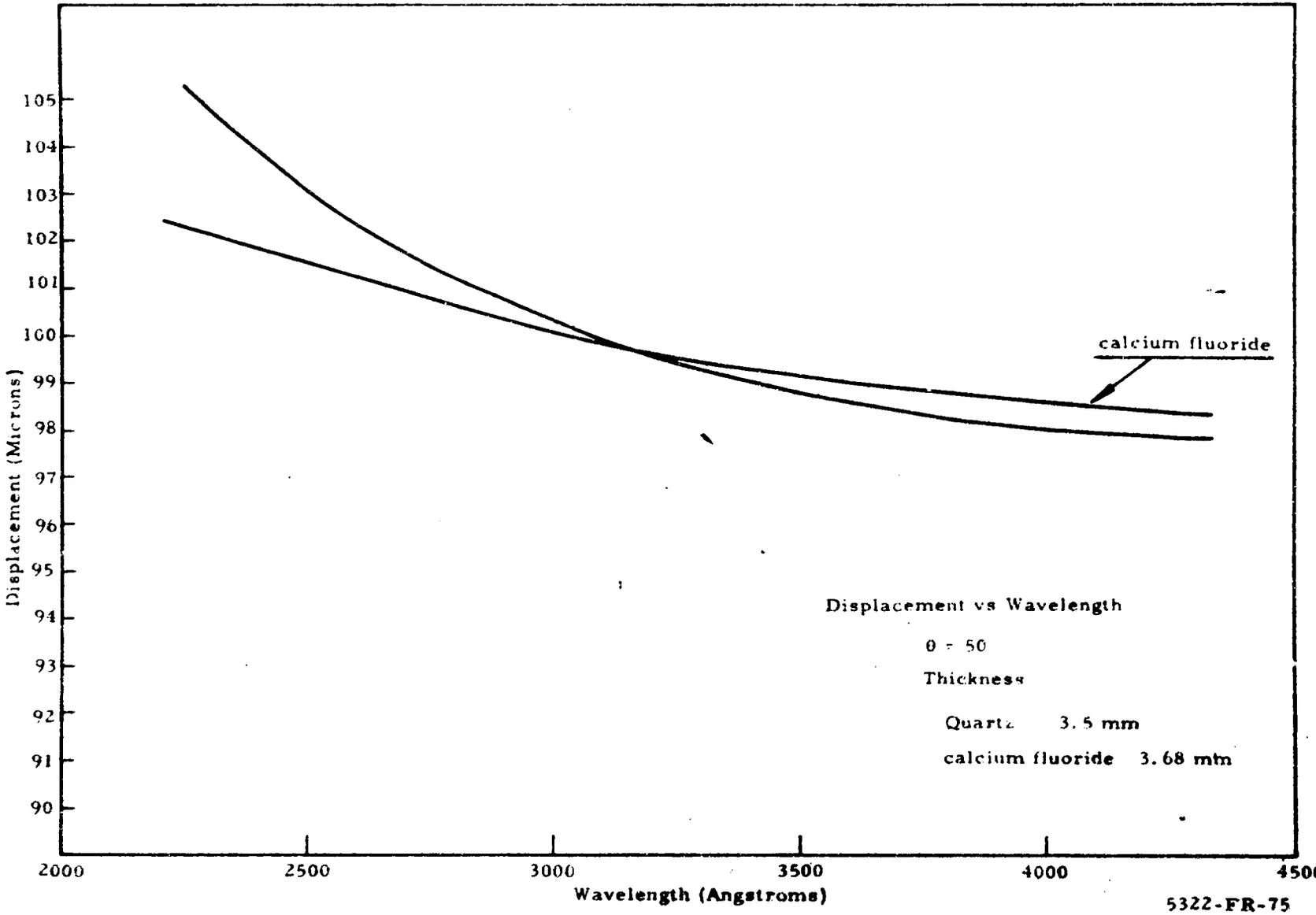

Figure 6-10. Displacement versus Wavelength

From this graph it can be seen that calcium fluoride is much less wavelength dependent that quartz and will therefore give less error over the band. Further consideration of the graph show that the 3126 A mercury line is a suitable choice for the reference line since it minimizes the displacement errors (2.6 microns) over the spectral range of interest and lies approximately in the center of the spectrum.

6.1.1.2.3 Monitor Source Balancing -- As the monitor servo system operates on a light amplitude comparison and balance technique, it is important that all differential gain or amplitude changes be kept to a minimum. This is especially important in the case of the mercury vapor lamp where any differential light output change in the two glow areas can cause an offset error in the servo alignment.

With all filamentary vapor lamps, it is possible to get both differential intensity and positional changes due to aging and heating. A light output balancing circuit (figure 6-11) has therefore been included in the design to maintain glow balance thus improving accuracy and decreasing maintenance.

By means of a beam splitter, a portion of the mercury light aimed at the servo monitor offset slit is directed to a photomultiplier via a 1000-micron wide exit slit. The photomultiplier monitors the mercury light and detects the relative intensities of the glow regions. The output of the photomultiplier then passes through a phase detector. If the two glow regions are of equal intensity, the output of photomultiplier is as in A (figure 6-12) and the phase detector output is zero. However, if one glow region is brighter than the other, the output is as in B (figure 6-12). The phase detector provides a positive d-c output if the detected signal is in phase with the reference and a negative output for an out of phase signal. The d-c signal is amplified in a differential amplifier and fed back to the lamp filament. The output of the d-c amplifier adds to one half of the a-c filament drive and subtracts from the other half offsetting the difference in glow intensities (figure 6-12).

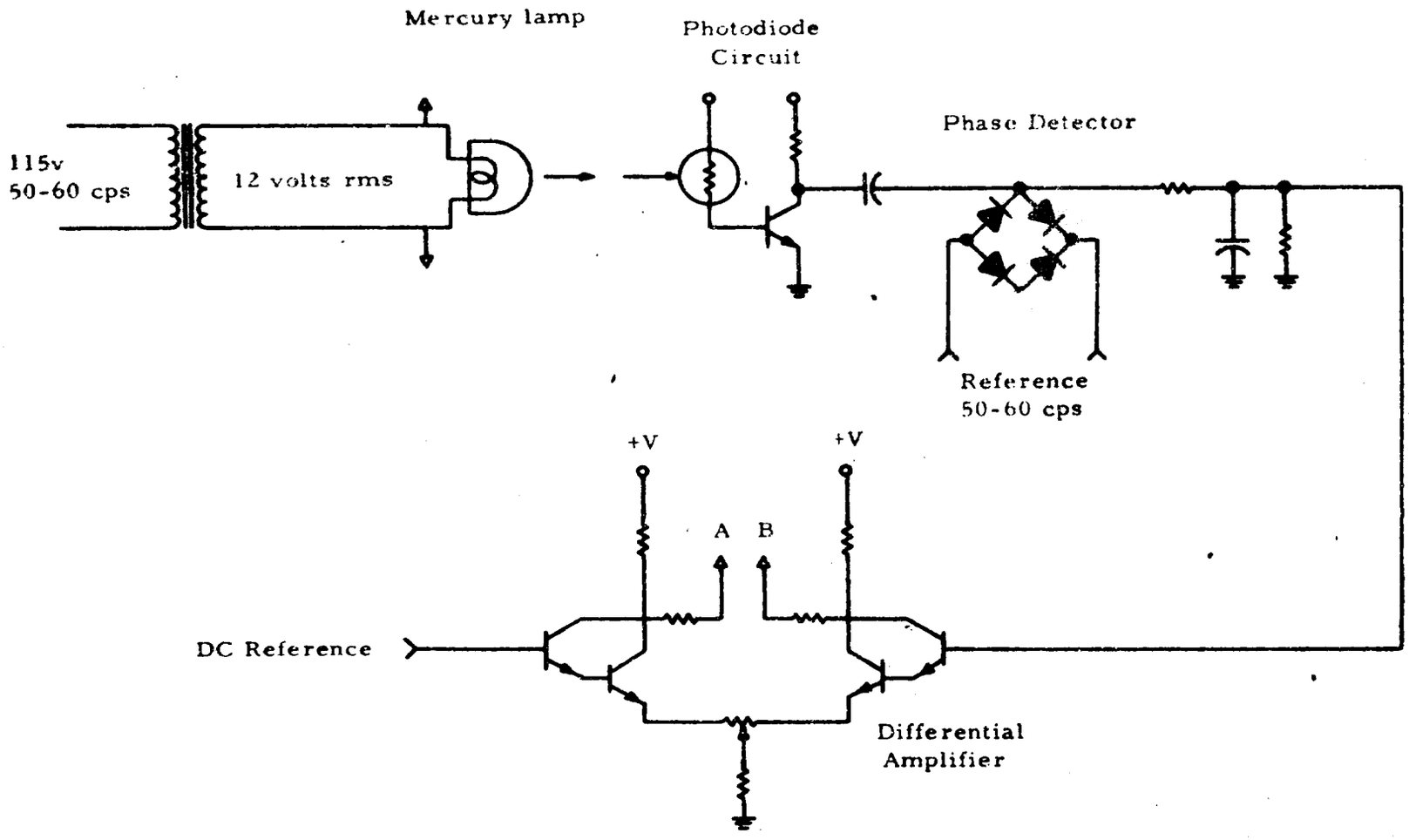

Figure 6-11. Mercury Source Balance Circuit, Alignment Servo

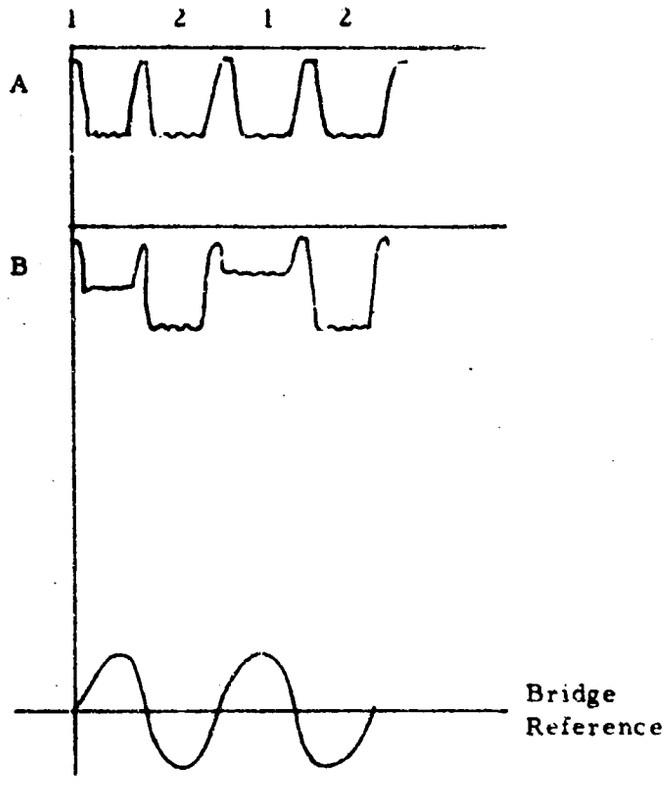

a. With two glow regions equal

5322-FR-89

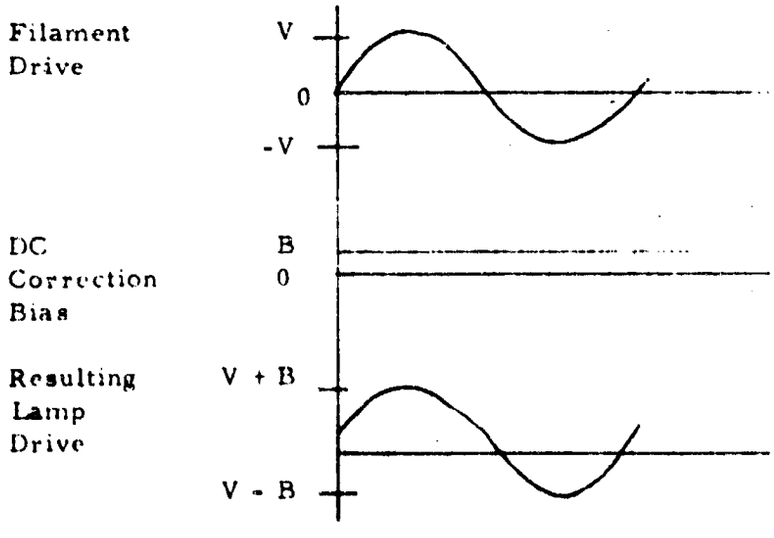

b. With one glow region brighter than other

5322-FR-77

Figure 6-12. Output of Photomultiplier

6.1.1.2.4 Servo Amplifier and Drive -- The electromechanical interconnection of the servo monitor system is shown in figure 6-13. Due to both the low output level of the photomultiplier and the high input level required to drive the Kearfott amplifier, it has been found necessary to include a preamplifier in the design. Because there are no qualified preamplifiers commercially available that meet the design requirements, this unit will be constructed by Baird-Atomic. A schematic of the preamplifier is shown in figure 6-13.

With the exception of the preamplifier, standard "off-the-shelf" hardware will be used throughout.

6.1.1.2.5 Servo Monitor Mechanisms -- The folding mirror is activated through a total travel of 45 degrees by a Ledex rotary solenoid. It is a 2-position operation limited by precision adjustment mechanical stops. The position accuracy is designed within 0.0001 inch. Override for the solenoid is provided by a torsion spring coupling between solenoid and mirror shaft.

The calcium fluoride deflection plate is activated by a Kearfott size 18 servo motor with integral 3230:1 stepdown gearhead.

A maximum travel of ± 25 degrees is provided (capture range) and is read out in microns by a Veeder Root counter driven by the other end of the motor shaft. In order to achieve a readout of the slit image at the focal curve in microns a speed increase is provided between the motor and counter. This is a simple spur gear with a ratio of 1:2.23. The readout accuracy achieved is better than 99.9 percent. Backlash effect from the gearhead is eliminated by torsion spring loading the deflector plate shaft. This is accomplished through "flex-pivots" which also serve as bearings.

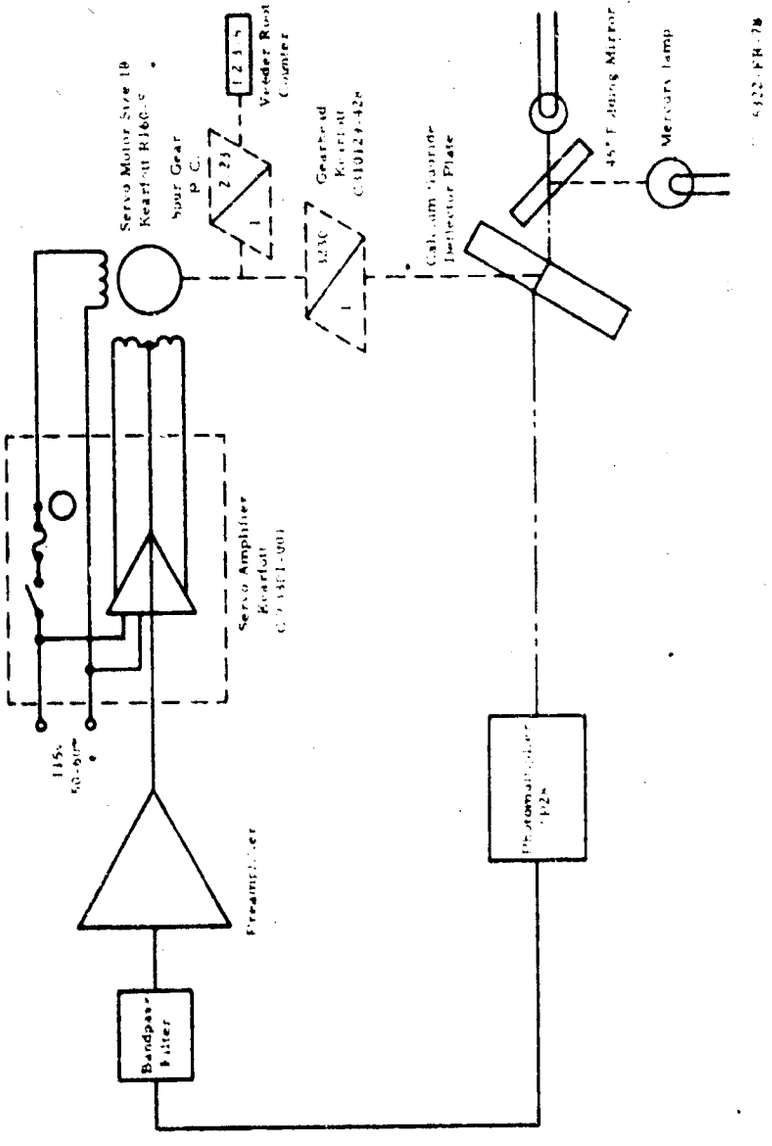

Figure 6-13. Alignment Servo, Functional Schematic Diagram

6.1.1.3 Tilt-Normal Subsystem--A tilt-normal subsystem has been included in the optical head design in order to provide an easy yet foolproof optical calibration and check function. The subsystem is based on the principle of introducing a preset and accurately controlled amount of shift of the 3650A mercury line in the image plane. The consequent misalignment of the line image with its exit slit causes the associated photomultiplier output signal to drop to some predetermined known ratio of the original photomultiplier output level. In the event that the ratio is more than a specified predetermined level it is known that the 3650A line, and hence the entire spectrum, has shifted (figure 6-14). The subsystem itself produces neither the magnitude nor sense of the misalignment just a visual indication that there is indeed misalignment. However, absolute values of optical shift can be determined if the subsystem is used in conjunction with the servo monitor system, Veeder Root readout and the lateral grating mount adjustment. This is achieved by rotating the grating about its vertical axis, first in one direction and then in the other. One direction will increase the tilt-normal ratio while the other will decrease it, thereby providing sense. The magnitude is provided in a similar method. As the grating is rotated the servo monitor on the 3126A line corrects the calcium fluoride deflector plate. The Veeder Root counter indicates directly in microns the amount of correction introduced in order to restore the tilt-normal ratio to its specified value. This subsystem is therefore capable of providing a precise check on the overall optics including the servo. The functional schematic is shown in figure 6-15.

The 3650A mercury line is produced by the servo monitor reference source and was chosen because of its high intensity and the fact that it lay on the opposite side of the mean dispersion angle to that of the 3126A servo monitor line, thereby providing a check and balance on the servo monitor at the longer wavelengths.

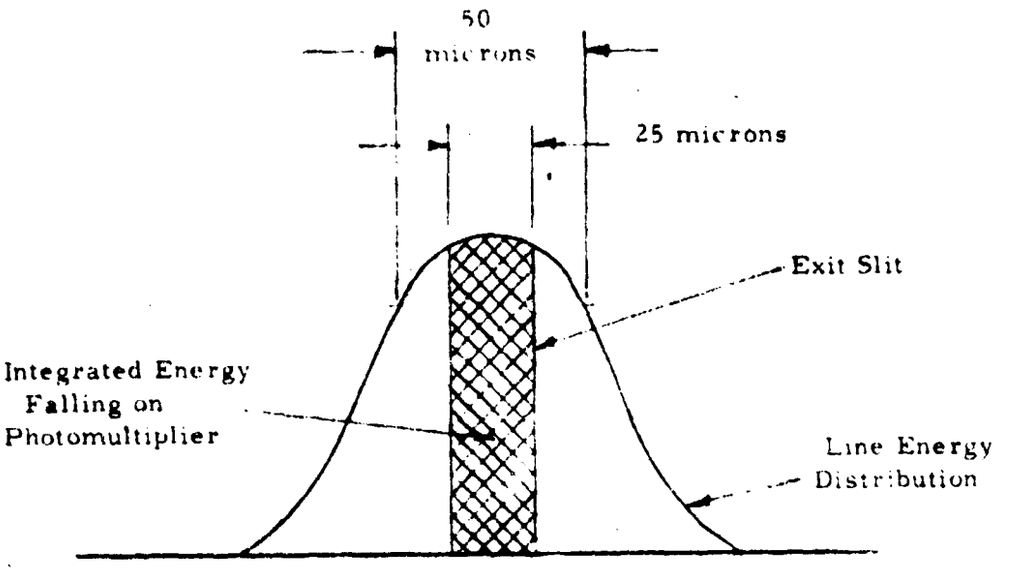

a. 3650 A Line and Exit Slit in Perfect Alignment

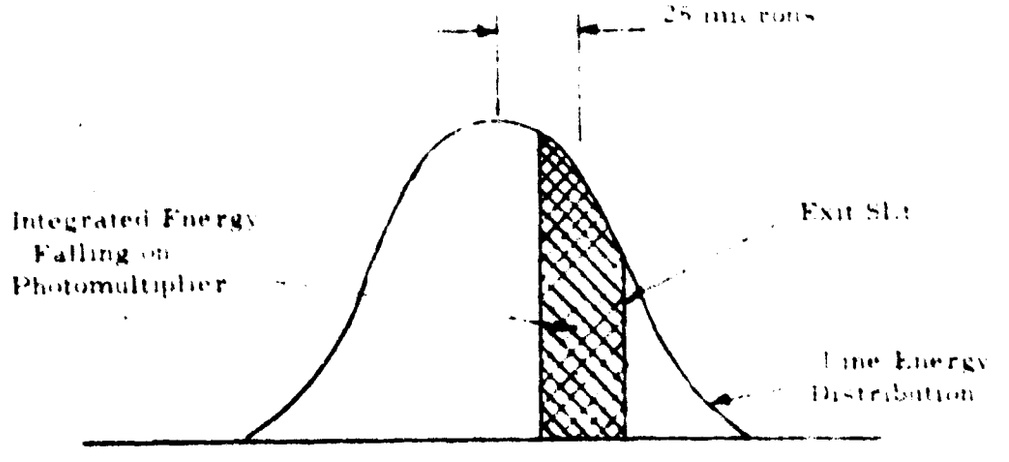

5323-FR-79

b. 3650 A Line Shifted 25 microns with Respect to Exit Slit

Figure 6-14. Alignment of 3650 A Line

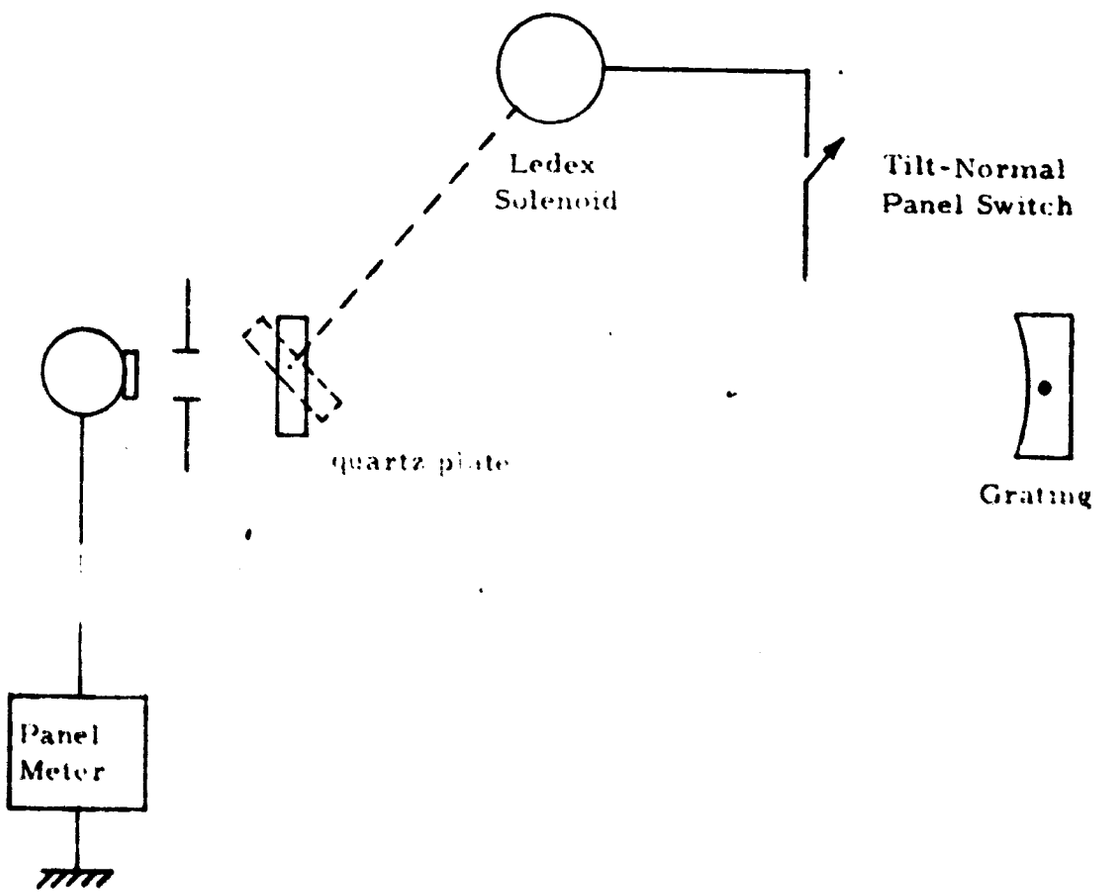

5322-FR-69

Figure 6-15. Tilt-Normal Subsystem, Functional Schematic Diagram

The shift of the 3650A line is achieved by rotating a plane parallel quartz plate through an angle of 3 degrees resulting in a 25-micron shift. The thickness of the plate is derived from

$$t = \frac{\ell \sin \theta}{n \tan \theta' \sin (\theta - \theta')}$$

where

ℓ = 0.025 millimeters

θ = 3 degrees (0.0524 rads)

θ' = angle of reflected ray

n = 1.47456 (at 3650A)

therefore

t = 1.47 millimeters

The quartz plate is mounted just in front of the focal curve and is actuated by means of a Ledex solenoid. The two limit positions of the plate are controlled by precision adjustment mechanical stops. Solenoid override is provided by torsion spring coupling.

6.1.1.4 Focus Servo System

6.1.1.4.1 General -- As previously mentioned in paragraph 4.3.7 there is a ± 0.044 inch change in exit image focal point due to expansion and contraction of the optical base over the specified ± 50°F temperature range. Changes of this magnitude can result in considerable system inaccuracy. The first approach to the solution of this problem was to temperature stabilize the entire optical head assembly by means of electrical heating elements. The maximum operating temperature of the system (130°F) was set as the working temperature of the optical head, thus eliminating the need for a cooling system.

A preliminary thermal analysis was performed resulting in figure 6-16. When this data was reviewed in the light of total system performance there appeared to be many major disadvantages to the technique.

a. Warm-up time of the system was excessive.

b. Power requirements were increased.

c. Life of components in the optical head was reduced.

d. The photomultiplier tubes would be continually used in a degraded condition thereby limiting system accuracy.

e. Added complication to alignment procedures

On the basis of this analysis, this design approach was discarded.

A second approach based upon optical refocusing techniques proved to have none of the previous disadvantages. The principle of this approach is as follows. If a plane parallel transparent plate is placed in a beam of light coming from a point, P, as shown, the apparent plane from which the rays are coming will be shifted by refraction, P' (figure 6-17).

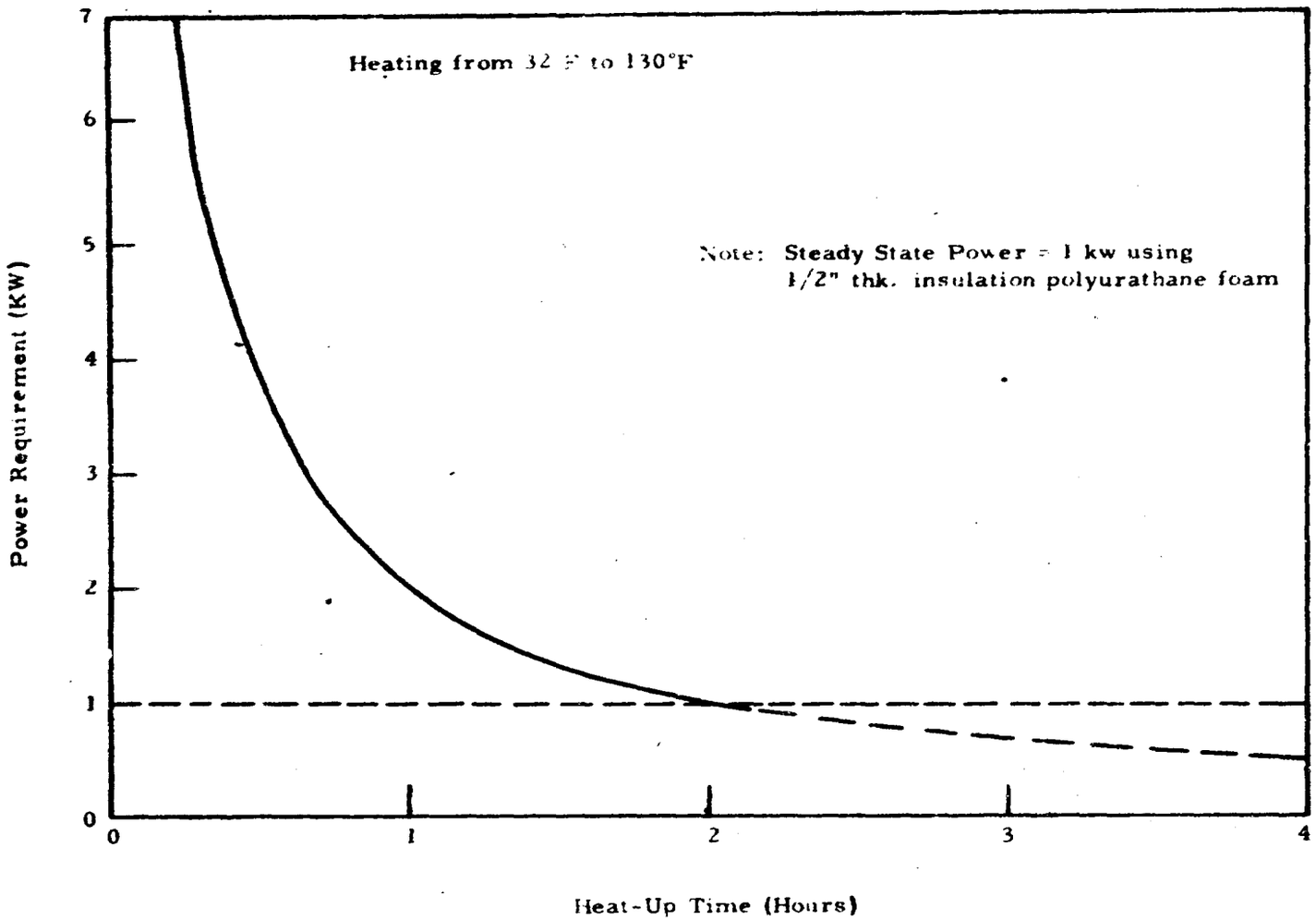

Figure 6-16. Estimated Heating Requirements for the Analyzer Optical Head

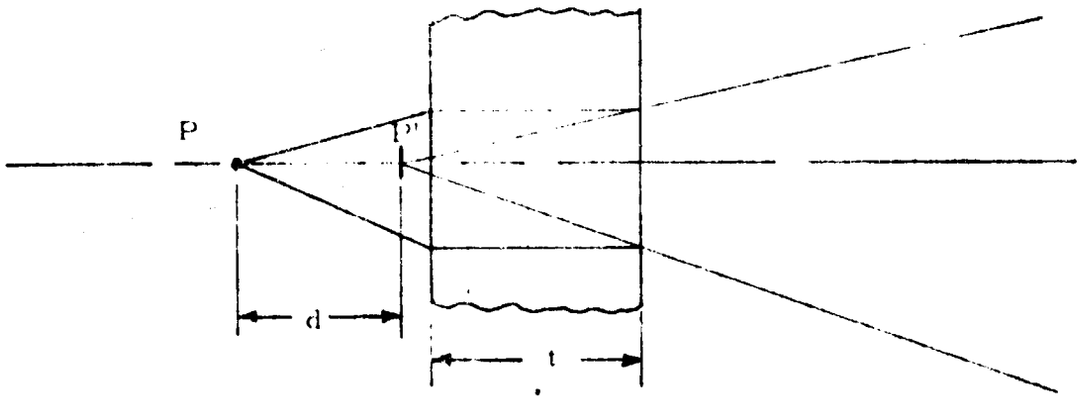

5322-FR-82

Figure 6-17. Change of Optical Pathlength using Plane Parallel Plate

If the index of refraction of the material is n, the distance, d, by which the point is shifted optically is related to the plate thickness by the formula:

$$d = t\left[\frac{n-1}{n}\right]$$

Table 6-1

Value for $\left[\frac{n-1}{n}\right]$

λ	2265A	2573A	3020A	3650A	4340A
Quartz	0.34344	0.3350	0.3278	0.3218	0.31829
Calcium Fluoride	0.32324	0.31739	0.31225	0.30802	0.30554

A method of physically implementing this technique is by utilizing two wedges where one is fixed and the other is movable (figure 6-18).

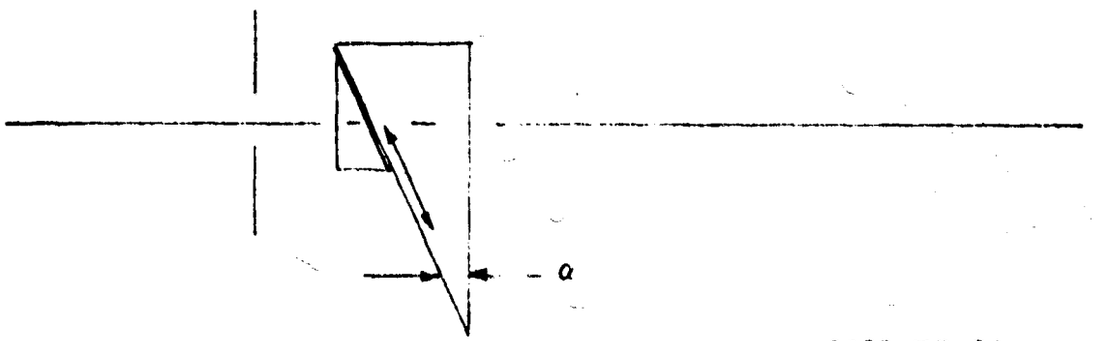

5322-FR-84

Figure 6-18. Focus Servo Optical System

By sliding the long wedge along its hypotenuse, the length of the optical path is continuously variable. Since the entrance and exit faces are perpendicular to the optical axis, no lateral displacement will take place at

these surfaces. However, there is refraction at the internal surfaces of the wedges, the amount of which is dependent on the separation distance and the wavelength. This effect can, however, be neglected if the separation is maintained constant and if the exit slits are correctly set to accommodate the constant offset.

By the simple expedient of driving the long wedge from a temperature-dependent 10-step, open loop servo focus can be maintained This technique has the advantage of precision while being insensitive to lateral motion.

6.1.1.4.2 Focus Servo Optics--Since the amount of optical shift introduced is wavelength dependent, (see table 6-1) it is desirable to use a material which has the least amount of dispersion. For this reason calcium fluoride has been selected. To minimize further the effects of dispersion the focus will be corrected exactly for a wavelength such that the chromatic focusing error is equally divided at the position of maximum correction. To find this, take a value of

$$\left[\frac{n-1}{n}\right] = 0.314$$

or the median value. Using the formula

$$d = t\left[\frac{n-1}{n}\right]$$

This becomes:

$$t = \frac{dn}{n-1} = \frac{0.088}{0.314} = 0.281 \text{ inch}$$

This is the amount of calcium fluoride which must be added between the entrance slit and the grating to shift the focus of the entrance slit by 0.088 inch.

The angle, α, is determined by the length of travel of the wedge:

$$\sin \alpha = \frac{t}{\ell}$$

For mechanical reasons, the travel, ℓ, has been set at 2 inches. Therefore,

$$\sin \alpha = \frac{0.281}{2} = 0.1405$$

$$\alpha = 8° 4\ 6'$$

Since the fixed wedge must be 0.500 inch in length to cover the length of the entrance slit, the minimum thickness is:

$$0.5 \times \tan 8° 4.6' = 0.0[illegible] \text{ inch}$$

An additional 0.080 inch has been added for mechanical strength at the thin end of the wedge to avoid a fragile section.

The total thickness now becomes

Minimum	0.152
Δt	0.281
Maximum	0.433

6.1.1.5 Sample Stand Assembly -- Contained in this assembly are the analytical and auxiliary gaps which comprise the Michigan Tandem air gap. The gaps are located in a cast aluminum housing and are positioned one above the other with the analytical gap being on top. Figure 6-19 . Separating the gaps is a sheet metal baffle which prevents light from the auxiliary gap entering the analytical optical system and also reduces the velocity of the air passing over the analytical gap. The air supply used to stabilize the auxiliary gap enters through the bottom of the housing and is directed up through the analytical gap to scavenge toxic fumes which are ducted out through the top of the housing away from the operator. The analytical gap utilizes the standard

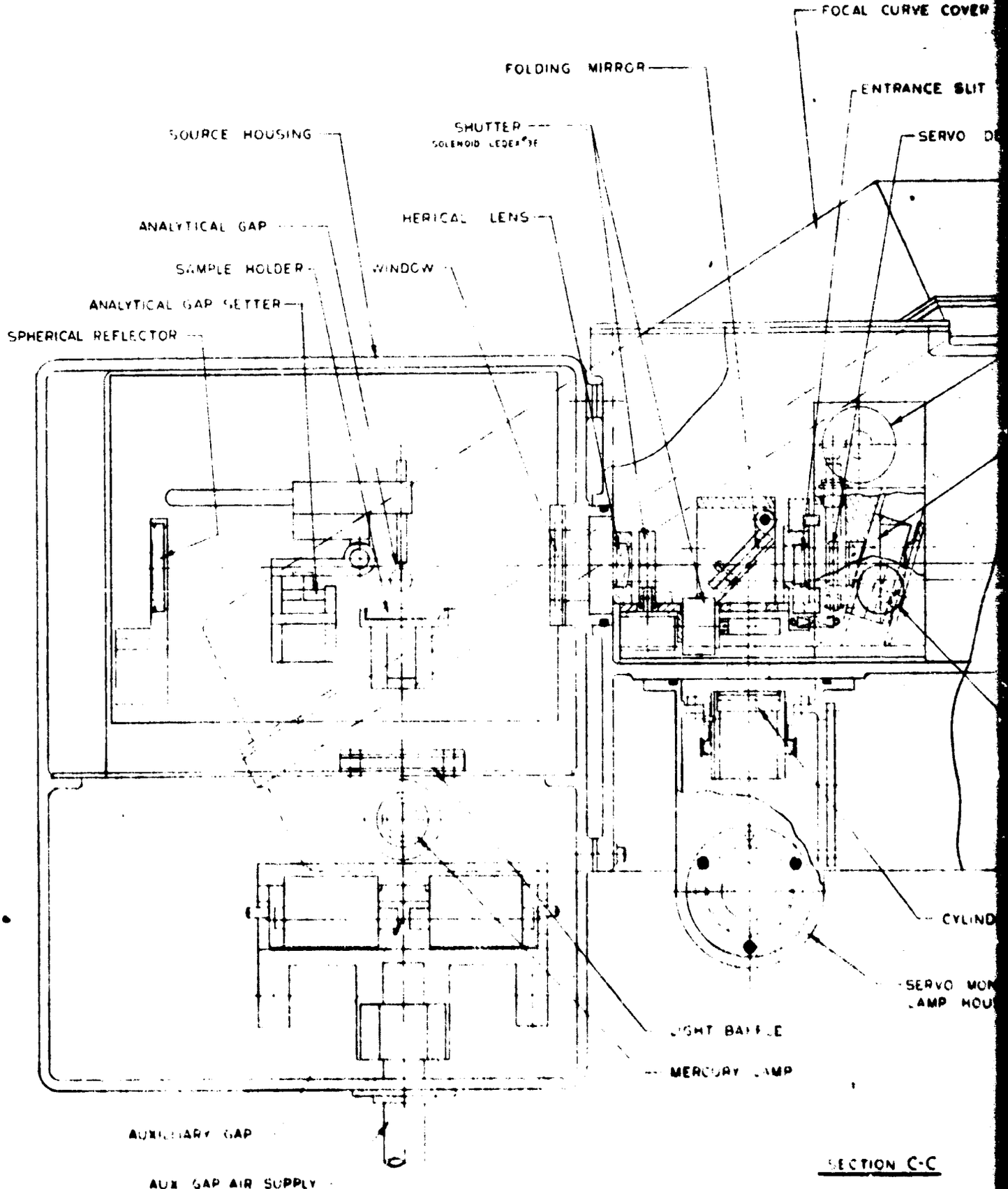
FOCAL CURVE COVER
FOLDING MIRROR
ENTRANCE SLIT
SOURCE HOUSING
SHUTTER
SOLENOID
SERVO
ANALYTICAL GAP
HERICAL LENS
SAMPLE HOLDER
WINDOW
ANALYTICAL GAP SETTER
SPHERICAL REFLECTOR
CYLIND
SERVO MON
LAMP HOU
LIGHT BAFFLE
MERCURY LAMP
AUXILIARY GAP
AUX GAP AIR SUPPLY

SECTION C-C

A

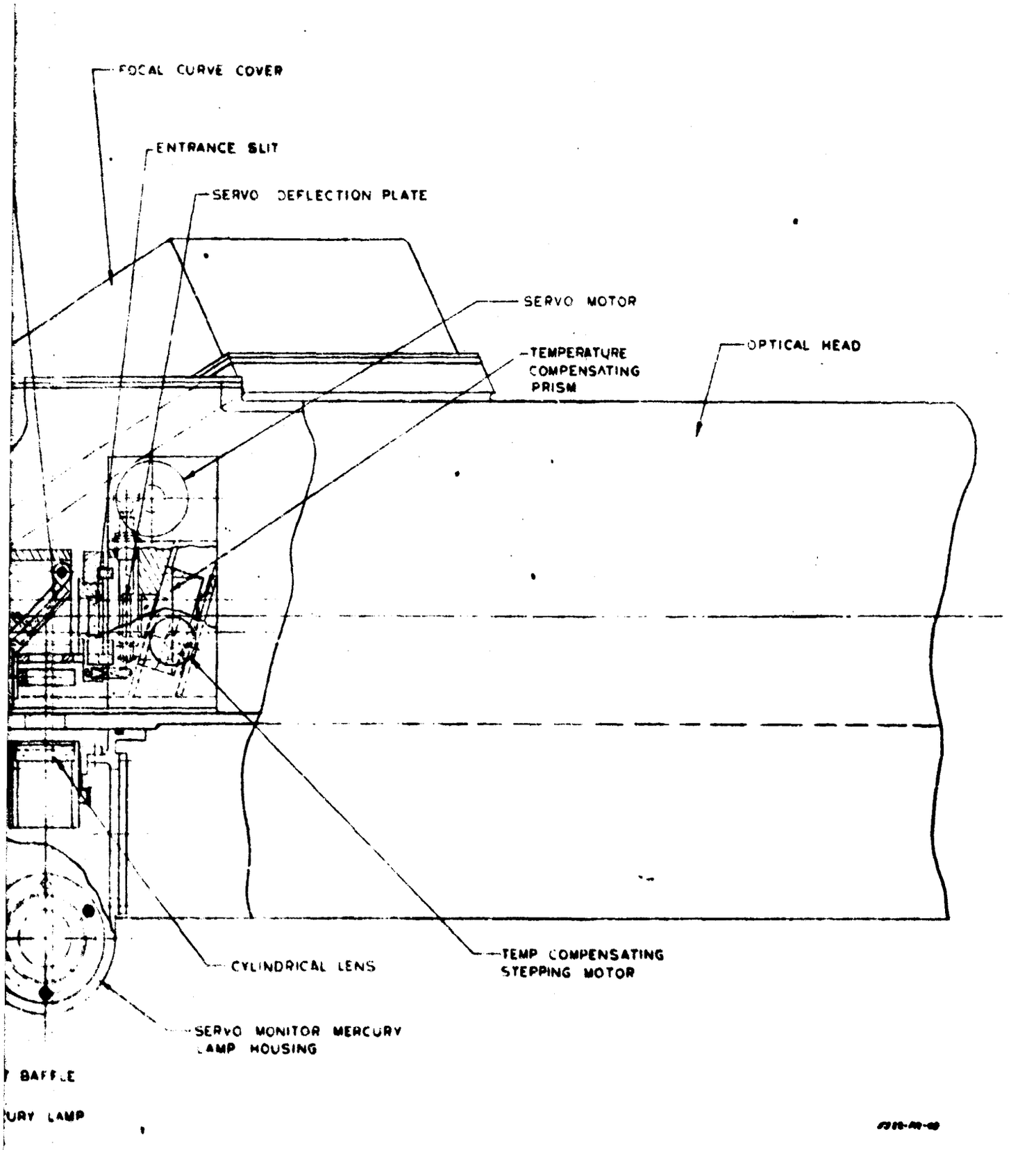

Figure 6-19. Optical Head (Cross Section through the Entrance Optics Axis)

Baird-Atomic gap setting device. After each run, the rotating electrode and fixed electrode are replaced. Once the new electrodes are in place, simply by pressing a lever, the correct gap spacing is set. The auxiliary gap spacing, and hence the breaks per half cycle, are adjusted by means of a shaft coming outside of the housing and connected to a control knob on the front of the console.

The door by which samples are placed in the analytical gap also allows access for servicing the auxiliary gap. Located in the door are two shielded windows for viewing the gaps during operation. The door is fitted with radio frequency interference and humidity control gasketing. To prevent radio frequency interference from radiating to the internal electronics, the separation between the source housing and the cabinet is sealed with a flexible metallic boot. The use of a flexible boot eliminates the need for close alignment of the optical head with the cabinet during assembly and prevents any mechanical stresses being set up between the optical head and the cabinet.

The source assembly is bolted to the optical head and thermally isolated from it to prevent temperature gradients affecting the optical alignment of the system. Vertical and lateral adjustments for lining up the analytical gap with the entrance optics are incorporated into the housing.

In addition to the gaps, the sample stand housing contains two optical components, namely the secondary mirror and the entrance lens. Both of these elements are protected from oil splatter by a quartz window. These slide into place and are easily removed for periodic cleaning.

The procedure for preparing a sample for analysis is as follows:

a. Fill a clean ceramic boat with the sample oil

b. Place the boat on the sample stand.

c. Slide the sample stand up until it is against the stop, which is set to position the rotating electrode at the proper depth in the oil.

6.1.1.6 Relay Network and Integrator Assembly -- The energy derived from the radiant energy in each spectral line is sufficient to cause emission of electrons from the photoemissive surfaces of the photomultiplier tubes. However, a fraction of the total photomultiplier output current is due to dark-current and may be significant at the lower concentration levels. This dark-current is very much a function of the operating temperature of the tube and it is, therefore, desirable to separate this dark-current from the signal current. It is, furthermore, also necessary to measure the average signal current in order to reduce the effect of short term instability in the source. Both functions are obtained by integration which is accomplished by storing a charge on a high quality capacitor.

The charge contribution due to the dark current is cancelled out by reversing the capacitor and integrating the dark-current over the same interval as the exposure period. In order to average out any variations in the dark-current during the sample burn period, it is necessary to repeat the reversal several times. Since the burn time is determined by sampling the voltage on the reference capacitor, (see paragraph 6.1.3.1), the turn off time must necessarily occur some time during the exposure period. Figure 6-20 illustrates the process of integration and dark-current cancellation. Under normal conditions, the radiation will be terminated in the middle of the last exposure period. A quick glance at figure 6-20 reveals that in order to obtain, on the average, complete cancellation of the dark-current, the process must begin with dark-current subtraction for one half of one exposure period. If the burn time is T_R, then

$$T_R = (2N - 1) T_o$$

where

T_o = the exposure period

N = the number of reversals

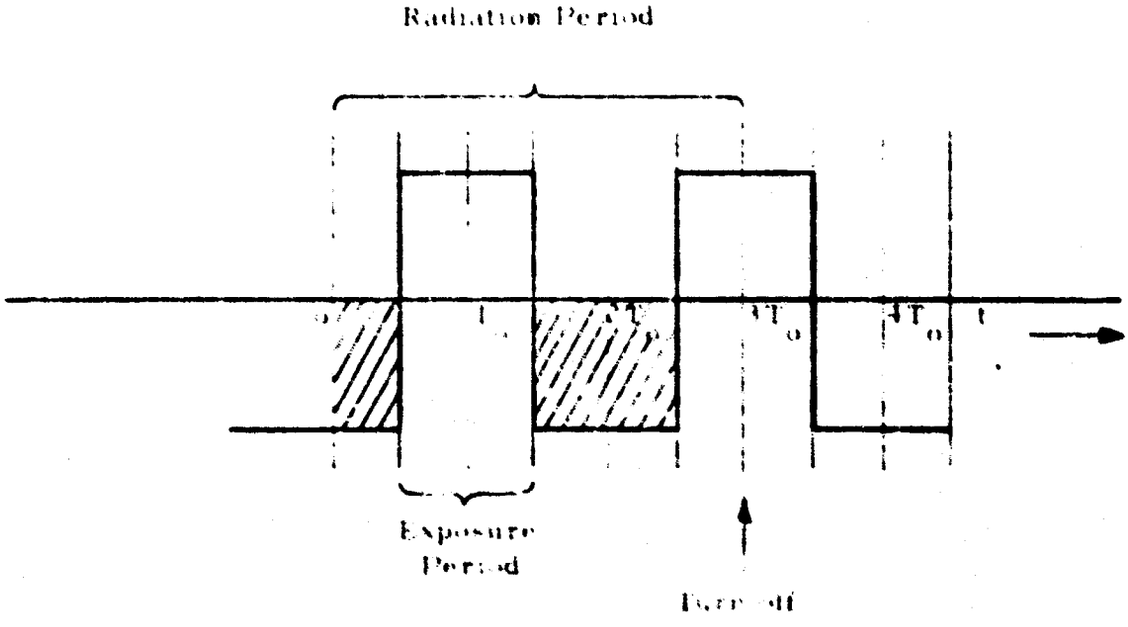

5322-FR-85

Figure 6-20. Integration and Dark-Current Cancellation

In a practical system, the transition times are finite and since the exposure period should be large compared with the transition times, there is an upper limit to the number of reversals. This system is designed for N = 6 and T_o = 2 seconds. Therefore,

$$T_R = 22 \text{ seconds}$$

At the end of this period, the integrating capacitor must be disconnected from the photomultiplier tube to prevent further integration of dark-current.

Perfect integration by a capacitor is only possible if there is no leakage. Any shunt conductance will result in an error in the output voltage. If the time constant, τ, of the integrator can be kept high enough so that the radiation time is small compared to it, the error can be approximated by a linear term

$$\epsilon_i = -\frac{t^2}{2\tau}$$

Using a high quality capacitor with a time constant of 25,000 seconds and assuming an additional shunt conductance of 3×10^{-11} mhos, this error will be approximately 4.2 millivolts. Second order effect are completely negligible. Since the deviation from perfect integration over the range of interest can be very well approximated by a linear term, this is easily compensated for by adjusting the system gain.

In order to maintain a low leakage conductance, the switching networks must necessarily be relay networks. The relays chosen are hermetically sealed in subminiature crystal cans. Figure 6-21 shows a schematic of the relay network and integrator. The 10-element channels and the one reference channel are built on two printed circuit boards and these two boards and two unity gain amplifiers are packaged in one humidity sealed can shown in figure 6-22. The photomultiplier tubes are connected to the respective integrators through miniature, low-noise coaxial cables.

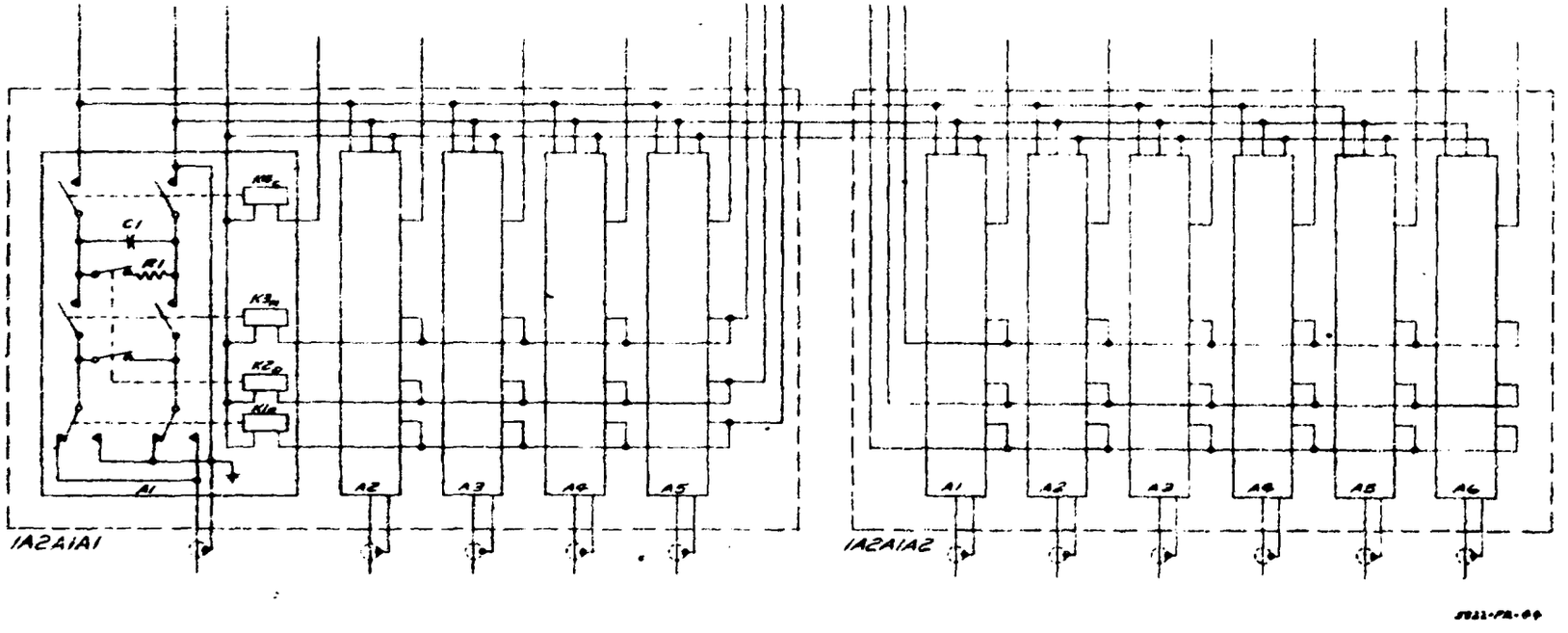

Figure 6-21. Relay Net and Integrator, Block Diagram

See figure 6-35.

Figure 6-22. Enclosures, Relays and Amplifiers

6.1.2 Excitation Source and Power Control

A block diagram of the power distribution system is shown in figure 6-23 with all switches in their off position. The photomultiplier supply switch S12 and the monitor servo switch S21 are normally closed so that the photomultiplier tubes and the monitor servo are working normally as long as the main circuit breaker is closed. It is desirable to maintain the high voltage across the photomultipliers so as to improve the aging characteristics of the tubes. An elapsed time indicator is located in the photomultiplier power branch showing the total time that the equipment has operated.

When the analyzer is turned off, three vents are closed to prevent humid air from entering the system. These vents are opened by the motors, B1, B2, and B3, as soon as the power switch is turned on. Power is supplied to the system, however, if and only if all three vents are completely open. A ready light indicates when the vents have opened. The load current is carried by a set of relay contacts on K1 which is activated by three normally open limit switches on the vents. Any one of the ten access panel interlocks may remove power to the system, but only three particular high voltage interlocks will turn off the photomultipliers.

Unregulated power is supplied to the disc electrode motor, the scope, and the blower motor after the temperature inside the analyzer reaches a predetermined temperature. Regulated power is supplied to the servo mercury lamp and to all the electronic power supplies through another ON-OFF switch S20. Regulated power is further supplied to the high voltage supply for the source through the contacts of relay, K2. This relay may be activated by a source setup switch for the purpose of adjusting the number of breaks per half cycle without having to turn on the electronics. The program timer will also control this relay. If the electronic test switch is opened, the electronics will function normally without power to the source.

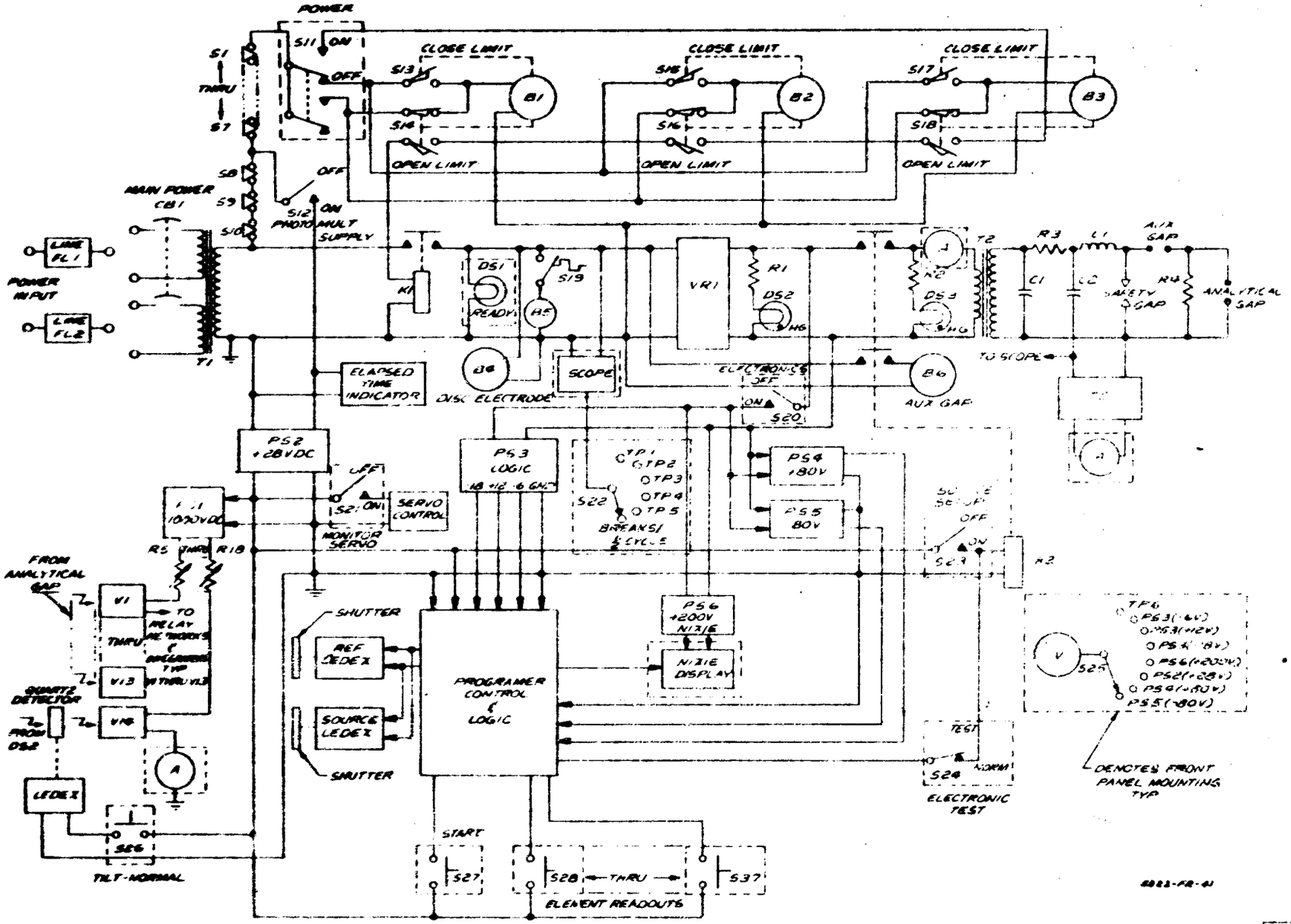

Figure 6-23. Power Distribution, Block Diagram

When the power "OFF" switch is pressed, power is immediately removed from the operational system but is continued to be supplied to the three vent motors through normally closed limit switches. These motors will now close the vents again and then turn themselves off.

Other functions indicated on the drawing are line filters, photomultipliers, tilt-normal, monitor servo, source and reference Ledex, and program timer and control. Since all these functions have been discussed thoroughly in other paragraphs, they will not be covered here.

6.1.2.1 Power Budget -- The calculated maximum power for the Base Level Analyzer design is shown in figure 6-24.

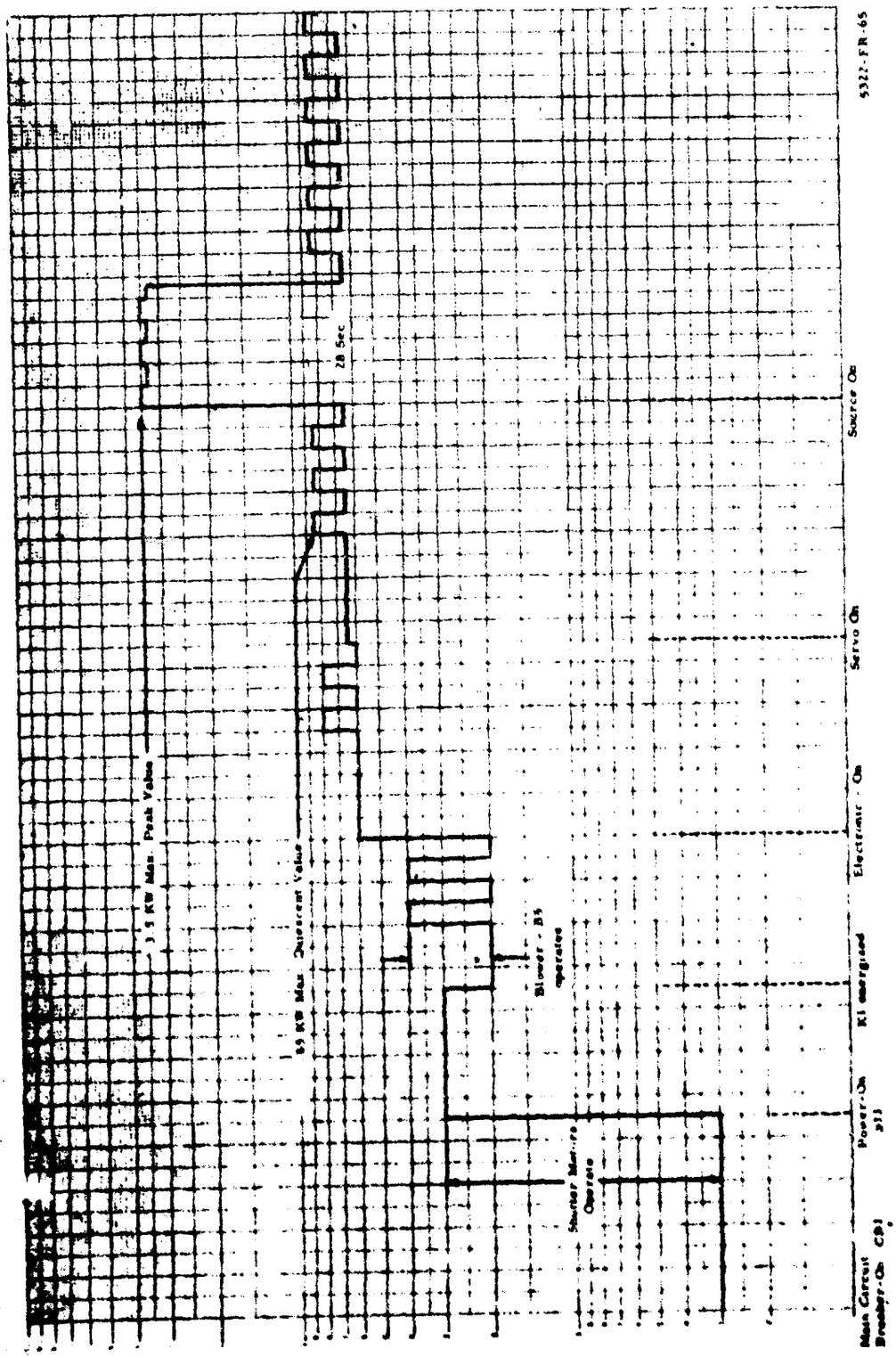

Figure 6-24. Power Profile

6.1.3 Electronic Signal Processing System

The specifications for the analyzer require that the concentration levels be presented in digital readout directly in parts per million. Since ten or more contaminants are to be analyzed simultaneously, ten or more 3-digit readouts are required unless the information is placed in temporary storage and read out one at a time under the direction of the operator. It was decided that the temporary storage approach had many advantages, namely an instrument with only one display would be much easier to read and since this approach also would demand fewer electronic components, the system would be smaller and more economical. A system of this kind would also be more flexible for future modifications. It is possible to expand to more than 10 elements without having to add another display for each element and with the information readily available in serial form, the system may very easily be modified for completely automatic readout.

Due to the fact that nearly all the elemental photomultiplier outputs are nonlinear with respect to concentration, there is a need for some nonlinear compensation in the system transfer function. This compensation is readily obtainable by inclusions of semiconductor diodes in the feedback loop of an operational amplifier. From statistical data on 7808 oil, it is apparent that no more than three diodes will be needed in any one channel. Since every channel requires different amounts of compensation and different amounts of gain due to changes in photomultiplier sensitivity with respect to line wavelength, there is a separate shaping network for every channel. However, these networks may be switched across one operational amplifier in a sequential manner, since only one integrator is read at one time.

In order to minimize the error due to leakage across the integrators, it is desirable to convert and store the information in digital form as soon as possible. For the same reason, it is desirable to maintain as low a leakage as possible.

The impedance level of the feedback networks across the operational amplifier are finite and in order to minimize an error due to the input leakage current, the driving source impedance must be rather low. In order to minimize both sources of error, it is necessary to include a high input impedance, unity gain buffer amplifier between the integrator and the operational amplifier. The error due to leakage may now be approximated by a linear term again,

$$\epsilon_c = -\frac{t}{T}$$

Assuming the same time constant as that for the reference channel and allotting a generous time of one second for all conversions, this error is only 7 microvolts and may hence be ignored.

A separate unity gain buffer amplifier has been included for the reference channel since the input impedance of the analog-to-digital converter is also rather low. It may be possible, in the final system, to combine these two buffer amplifiers since only one amplifier need work at one time. As mentioned earlier, both unity gain amplifiers and the integrators are packaged together in one humidity sealed box This was done to keep all high impedance circuits free of moisture.

Figure 6-25shows a block diagram of the electronic system for the analyzer. In what follows, a short description of the operation is given, more detailed description of the important subsystems are given in the subsequent sections. The radiant energy reaching the photomultiplier tubes cause emission of electrons from the photo-emissive surfaces of the tubes and the output currents will be functions of the concentration of the respective contaminants in the oil. These currents are integrated and stored temporarily on high quality capacitors. The voltage on the reference capacitor is continuously sampled and analog-to-digital converted. When this voltage reads 9.92 volts, a pulse is generated which stops all further integration and gives a signal to the program

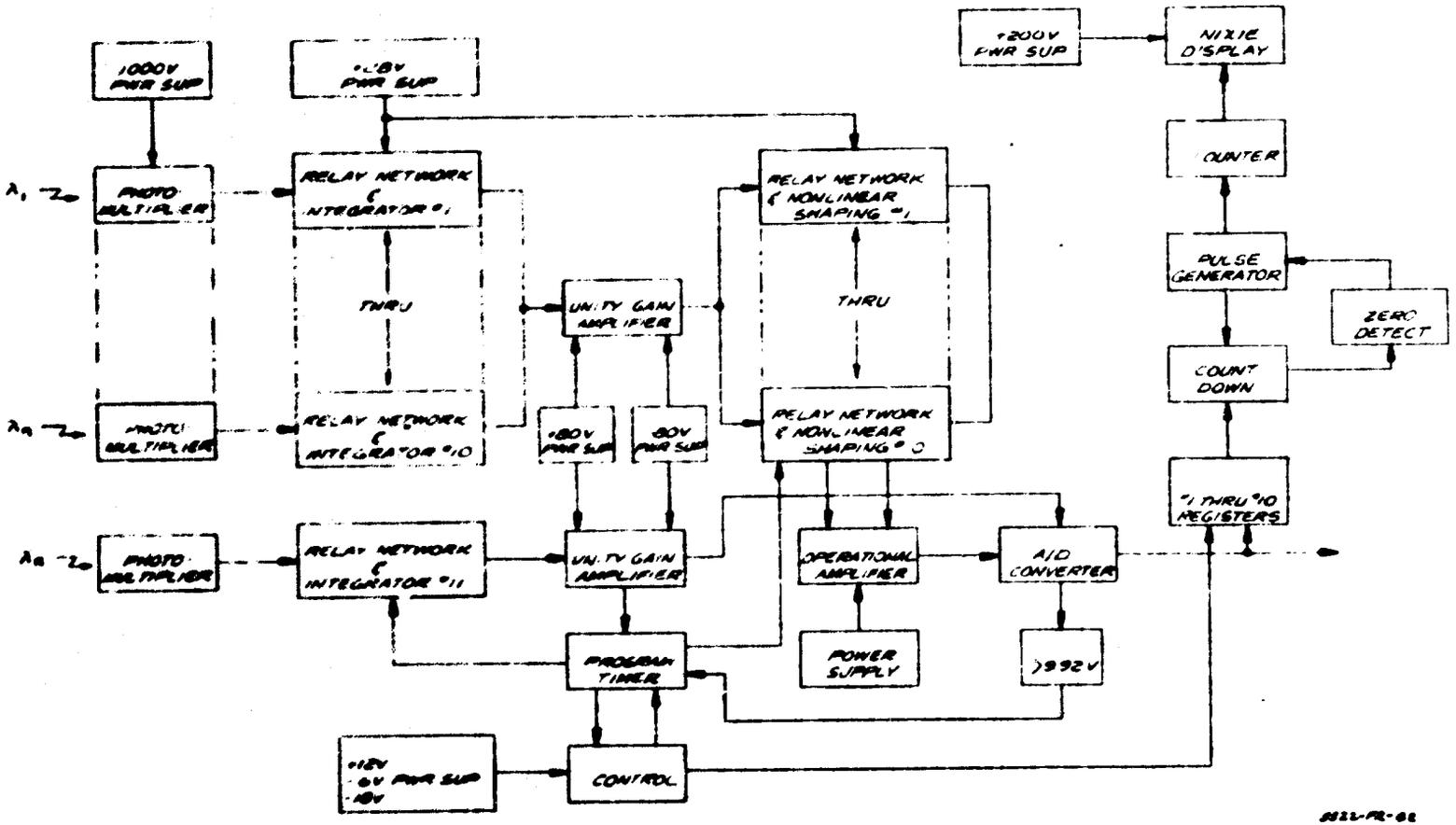

Figure 6-25. Base Level Analyzer, Block Diagram

timer to start digitizing the ten integrator outputs. The program timer also controls the transfer of the digital words to the correct register. After one second, all information has been stored in the registers and the program timer turns itself off. From now on the readout is under the control of the operator. Any one of the registers may be loaded into a countdown accumulator by depressing a button on the control panel. A zero detector turns the pulse generator off when the accumulator is empty. In less than 50 milliseconds the information is displayed on a 3-digit Nixie display. The same information may be read out any number of times since the registers are not reset until a new cycle has been started.

6.1.3.1 Program Timer -- The electronic brain of the system (figure 6-26 is the program timer. All timing and switching depend upon the proper operation of this subsystem. Fortunately, the program timer is not very complex. The sample analysis begins when the start button, S27, is depressed and at this time it is important that all digital circuits are in their proper state. Since the first eight seconds after start is allocated for preburn period, the start button is used to reset all registers and readout circuits. The decoding matrix and its associated 4-bit counter automatically resets itself after one second and hence presents no problem. It is necessary, however, to reset the first 3-bit counter and two RS flip-flops, A1A1 and A1A3, after the power is first turned on and before the start button is depressed. The system clear, shown in figure 6-27, automatically resets these circuits a few seconds after the power is first turned on. The system will continue to be in its proper state as long as the power is on.

The servo monitor system, described in paragraph 6.1.1.2, has an actuated folding mirror in front of the entrance slit which is controlled by a Ledex switch. Normally this mirror is in the open position and is closed during the burning process. Another Ledex switch which controls the dark-current cancellation shutter in front of the source is normally closed and is opened only during the exposure periods. When the start button is depressed,

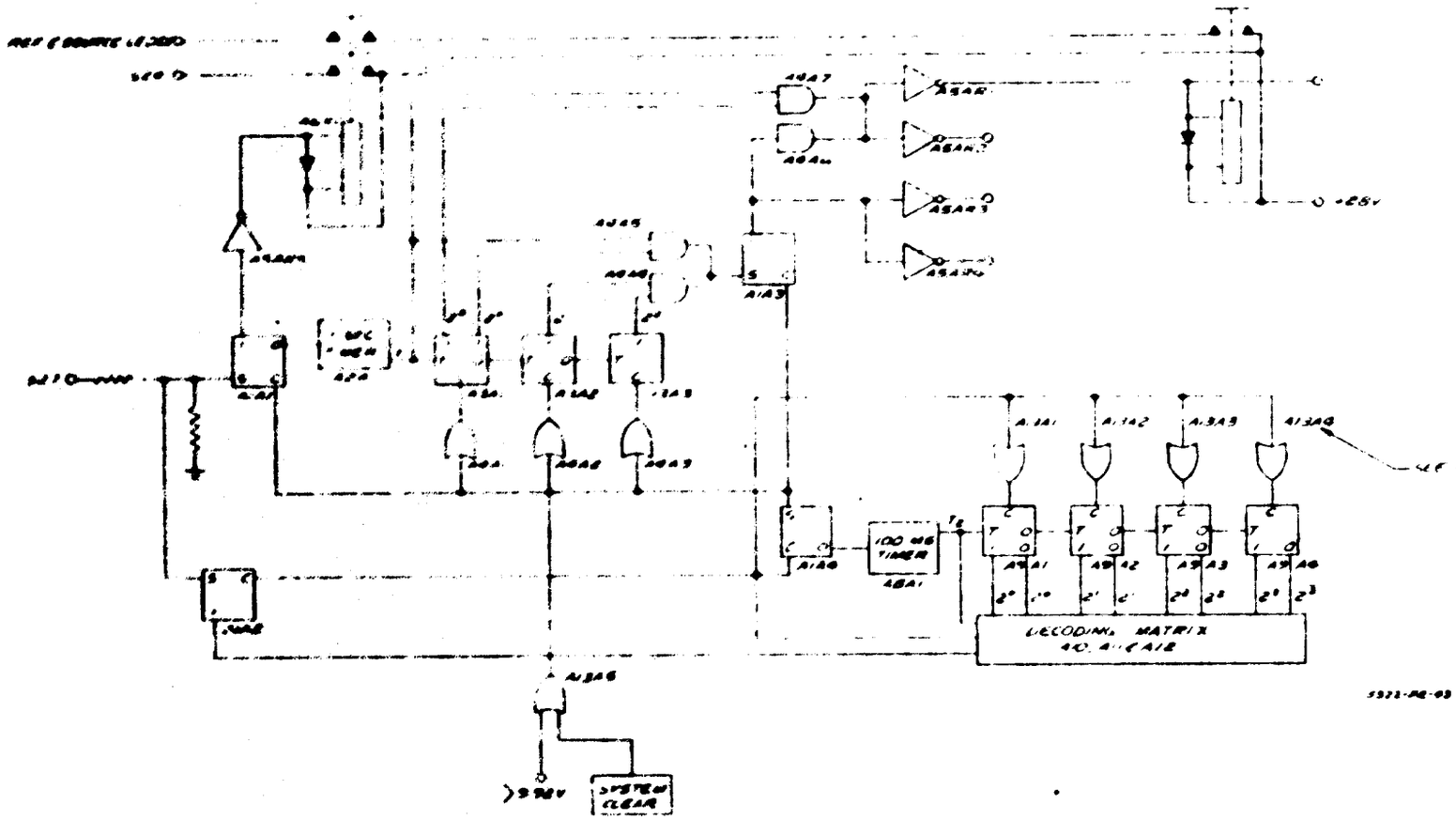

Figure 6-26. Program Timer and Control

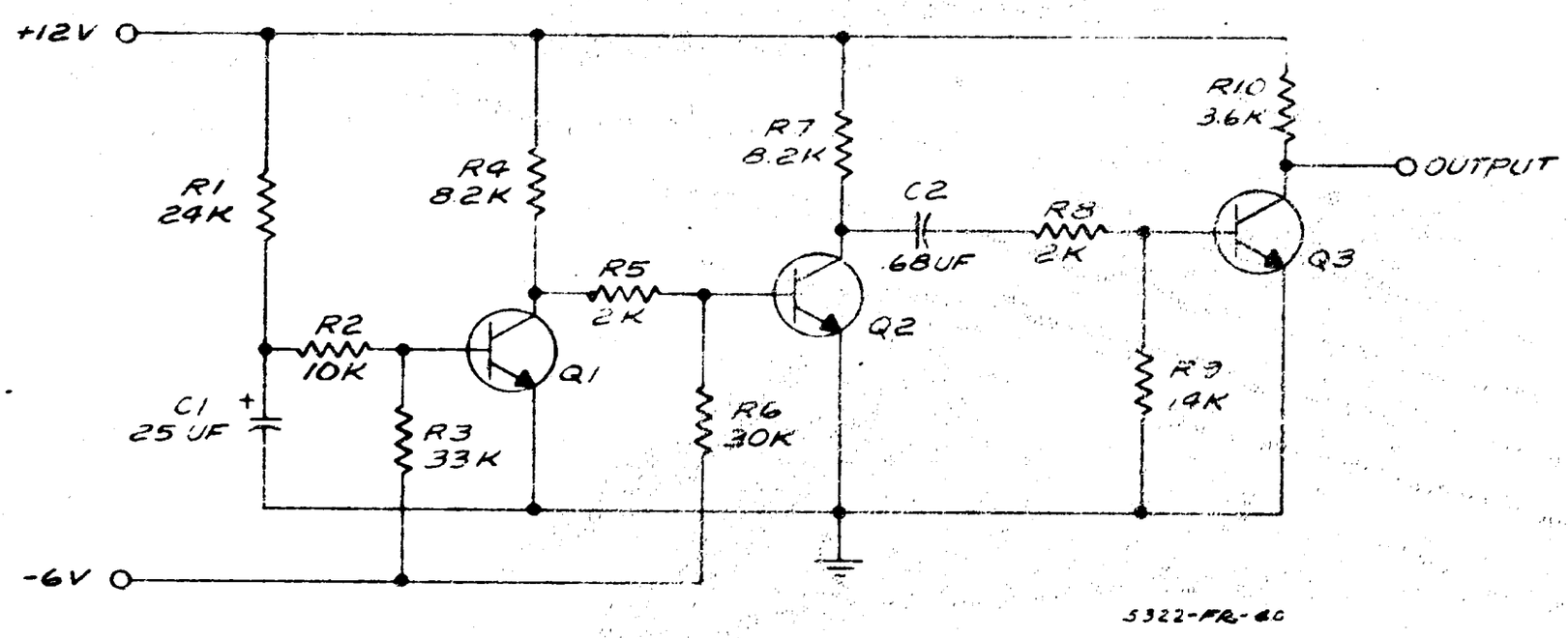

Figure 6-27. System Clear, Schematic Diagram

both flip-flops, A1A1 and A1A2, are set up. Flip-flop A1A1 starts the 1-second timer and energizes relay A6K1 which in turn supplies power to switch S24 and the source Ledex switch. It should be noted, however, that power is supplied to the source Ledex switch if and only if relay A6K2 is energized. This relay is only energized only during exposure periods under the control of the 3-bit counter. Since S24 is normally closed, application of power to this switch causes the arc-like spark to be ignited. Flip-flop A1A2 energizes all D relays which remove the shorts across the integrating capacitors during the burning period. At the end of the preburn period, eight seconds, flip-flop A1A3 is set up. This flip-flop energizes all M relays which connect the integrating capacitors to the photomultiplier tubes via reversing relays, and also enables the AND gates such that a 2-second square wave will energize the R relays and A6K2 during every exposure period. A decoder in the analog-to-digital converter detects when the voltage on the reference capacitor reaches 9.92 volts and generates a pulse which resets flip-flops A1A1 and A1A3, and the 3-bit counter and also sets up flip-flop A1A4. At this time all integrating capacitors are completely disconnected from other circuits and the two Ledex switches are restored to their normal position. Flip-flop A1A4 starts the 100-millisecond timer and the decoding matrix in conjunction with the 4-bit counter will operate the C relays sequentially. The C relays connect the integrating capacitors to the buffer amplifier, connect appropriate feed-back networks to the operational amplifier, and select the correct storage register. When all capacitors have been sampled and analog-to-digital converted, a pulse is generated which resets the rest of the program timer. The system is now under control of the operator for manual readout.

The logic diagram for the decoding matrix is shown in figure 6-28 and is self-explanatory. Circuit diagrams for the two timers are shown in figure 6-29.

The timing is controlled by a unijunction transistor relaxation oscillator which has been designed to be very temperature stable.

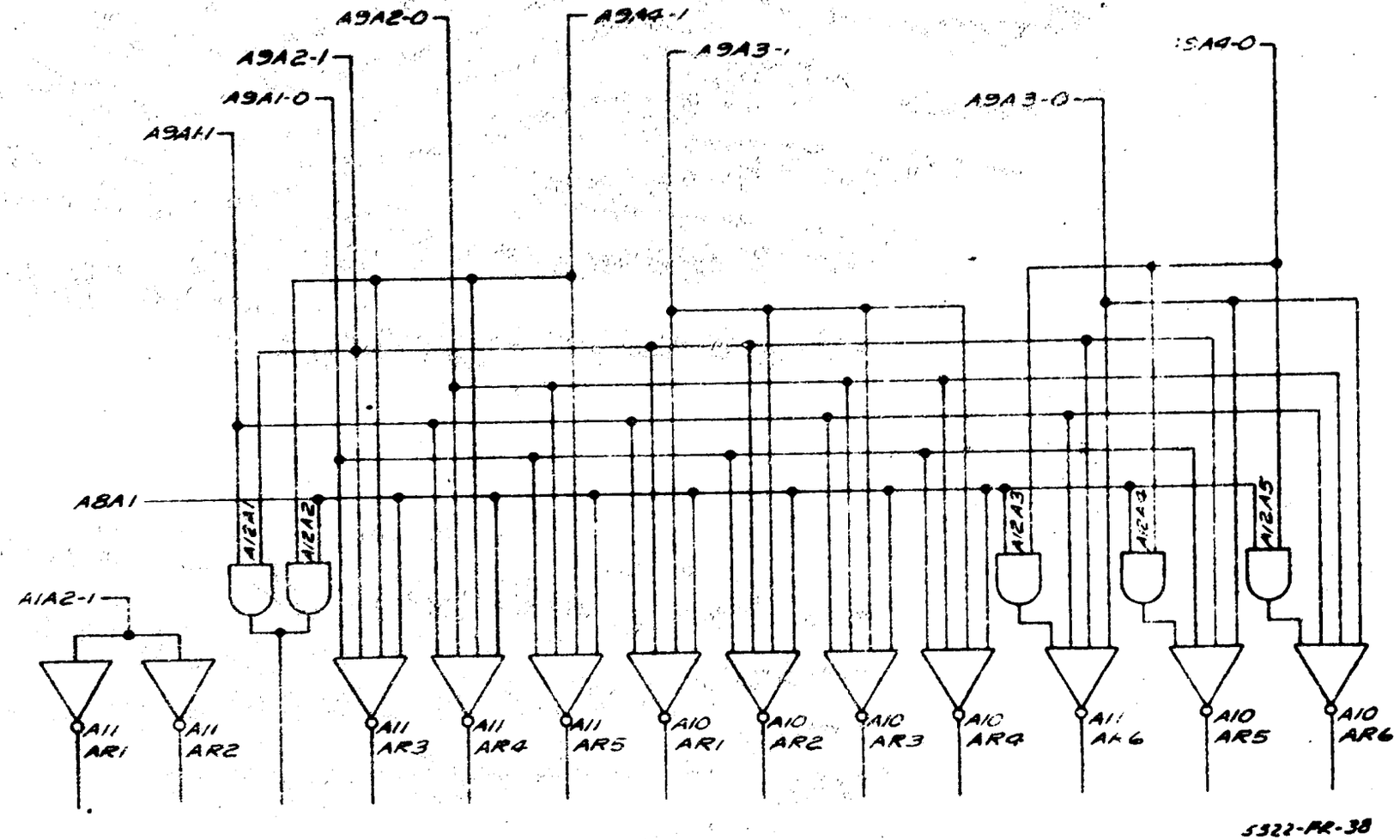

Figure 6-28. Decoding Matrix 1A1A1

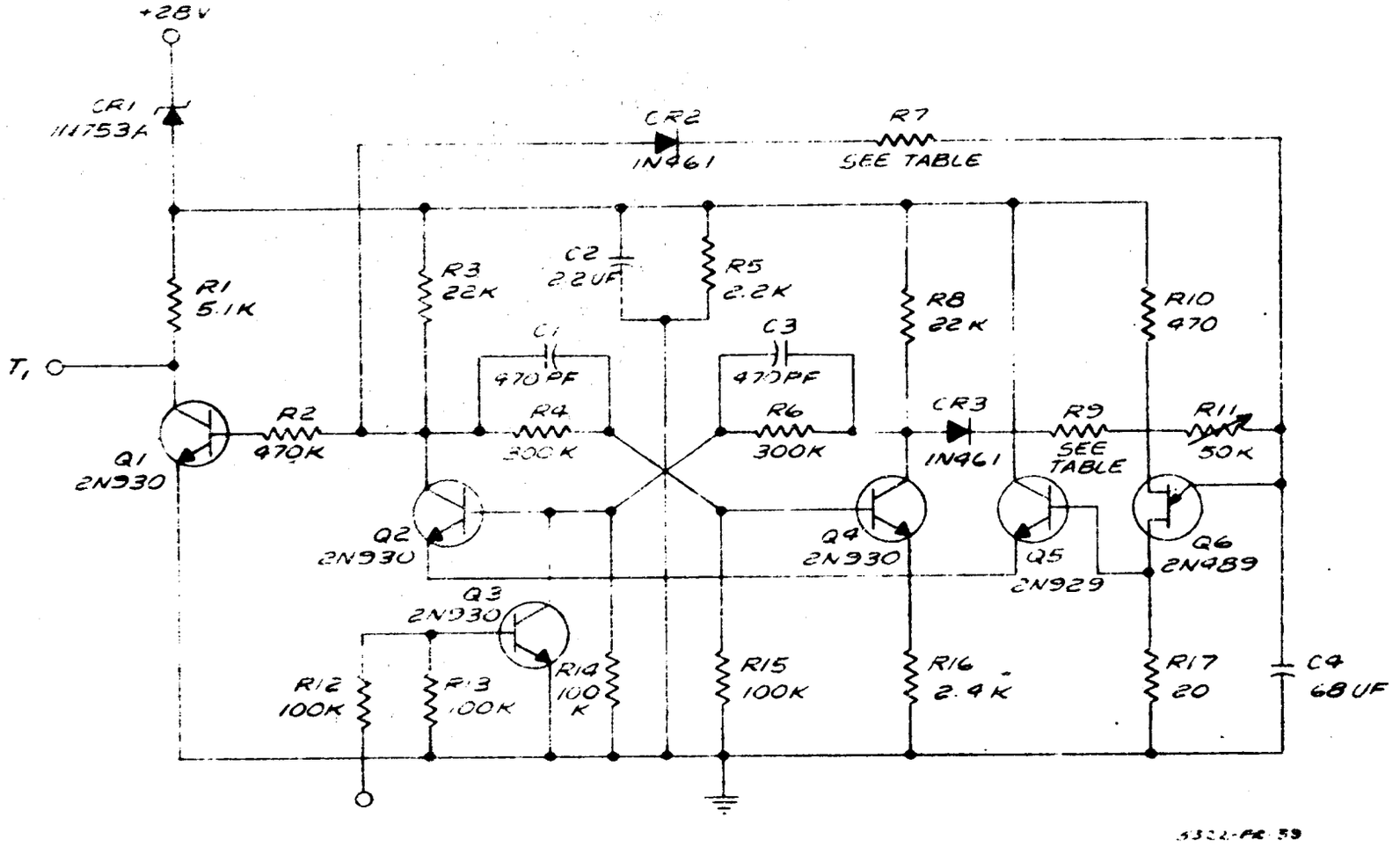

Figure 6-29. Timer, Schematic Diagram

6.1.3.2 Relay Network and Shaping -- The gain of a photomultiplier tube is a very sensitive function of the dynode voltage. For a 9-dynode tube, (like those used in the analyzer), it is easy to show that the sensitivity is

$$\frac{dG}{G} = 9\frac{dV}{V}$$

where

G = the nominal gain with a dynode voltage V

Even though the supply voltage may be regulated to a small fraction of one percent, the percent change in gain will be approximately nine times higher. For example, if the supply voltage is regulated to within 0.03 percent, the gain will change by approximately 0.27 percent. For an output voltage of 10 volts, this means an error of 27 millivolts and, as will be shown in the section on analog-to-digital converter, this is equivalent to one part per million. Even more serious is the change in gain with age. Over the lifetime of the tube the nominal gain may change by more than two.

Since the voltage on the integrating capacitors represent the concentration of the contaminants, it is important that the system transfer function be independent of the photomultiplier gain. For this reason a reference channel has been added which integrates the current due to fixed background radiant energy. The voltage across the reference capacitor is then

$$V_R = \frac{Q_R}{C_R} = \frac{I_R T}{C_R} = \frac{K_R G_R T}{C_R}$$

where

K_R includes the quantum efficiency and the sensitivity of the photoemissive surface to the particular wavelength in question

G_R = the multiplier tube gain

T = the total time of integration

Solving for this time,

$$T = \frac{V_R C_R}{K_R G_R}$$

For a fixed value of V_R, it is seen that the time of integration varies directly as the gain. For any of the other channels, the output voltage is

$$V_x = \frac{Q_x}{C_x} = \frac{I_x T}{C_x} = \frac{K_x G_x V_R C_R}{C_x K_R G_R}$$

This equation shows that the unknown value of the voltages depend on the ratio of the photomultiplier tube gains and the accuracy has been greatly increased. Each photomultiplier has its own gain control so that all photomultipliers can be set to have equal gain. It may be necessary to readjust these gains at infrequent intervals over the lifetime of the tubes. The output voltage may now be written

$$V_x = K_N \; (N = 1, 2, \text{-----}, 10)$$

where K_N depends only on the radiant energy of the particular line and the sensitivity of the photoemissive surface to the wavelength of the line. For this analyzer the wavelength varies from 2203 to 4300 A and over this band the sensitivity varies approximately 30 percent. Furthermore, the radiant energy of any line is not only dependent upon the concentration but also upon the chemical element being analyzed. These factors demand that the gain of each channel be different. This is readily accomplished by switching in appropriate resistive networks across an operational amplifier. These networks are, unfortunately, further complicated due to the fact that for some elements, K_N is not a linear function of concentration. For these elements diodes are incorporated in the feedback loop to achieve non-linear compensation. Figure 6-30 shows a typical network. Resistors, R1 and R2, adjust the break points

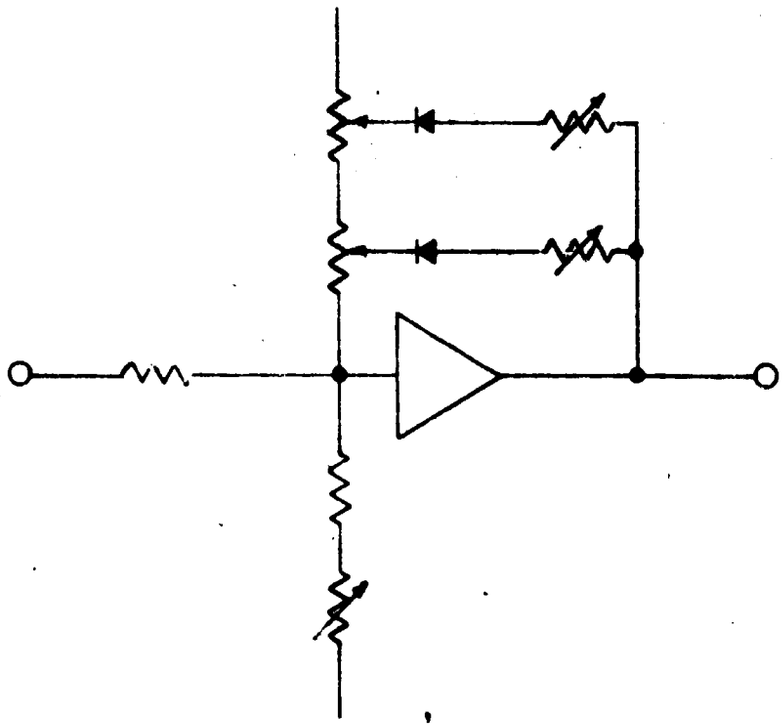

5322-FR-96

Figure 6-30. Nonlinear Compensation

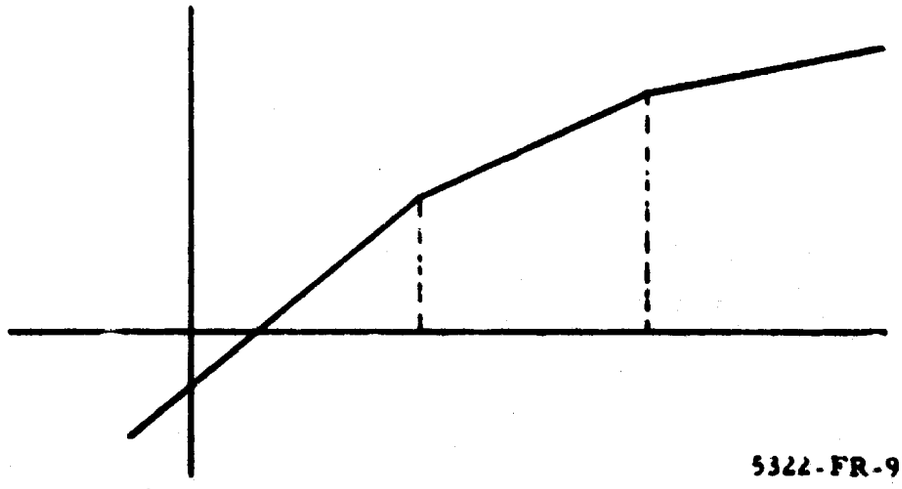

5322-FR-97

Figure 6-31. Typical Transfer Function

of the transfer function shown on figure 6-31. Resistor, R3, adjusts the quiescent input voltage V_{IN} such that it not only compensates for the amplifier input offset voltage in each channel. Figure 6-31 indicates that it requires a finite input voltage before the output goes through zero. The only things this simple network does not compensate for are the temperature dependent terms of the input offset voltage and leakage current. Over the operating temperature, 0 to 50°C the input offset voltage changes typically ± 75 microvolts with a maximum of ± 300 microvolts. With a driving point impedance of 20 kilohms, the input voltage changes typically ± 100 microvolts with a maximum of ± 300 microvolts due to input leakage current.

6.1.3.3 Analog-to-Digital Converter -- The data which has been stored temporarily as charge on high quality capacitors must be digitized and stored in flip-flop registers as soon as possible in order to reduce errors due to leakage. It has been shown in paragraph 6.1.3 that a total conversion time of 1-second results in a maximum voltage change of seven microvolts which is negligible. In order to provide a 1-part-per-million resolution, a 9-bit analog-to-digital converter is required. The system transfer function has been adjusted such that a maximum concentration of 500 parts per million of any element will result in a 10-volt output. The quantizing steps are then 20 millivolts.

In order to make sure that all transients have died out after the capacitors have been switched in, a 30-millisecond delay has been included in the analog-to-digital converter leaving 70 milliseconds for one conversion. A 7-kilocycle oscillator is all that is needed to complete the 9-bit conversion in this time, but in order to maintain sufficient margin, a 50-kilocycle clock rate was selected. Even 50 kilocycle rate is very slow in digital machines and it makes it possible to choose the simplest counter type converter for this project. A logic diagram is shown in figure 6-32. The 10-volt reference supply is very stable and has a drift over the temperature range of less than one millivolts. The comparator itself is accurate to one millivolt, thus, providing an analog-to-digital converter with 1 part per million resolution and 0.1 part per million accuracy.

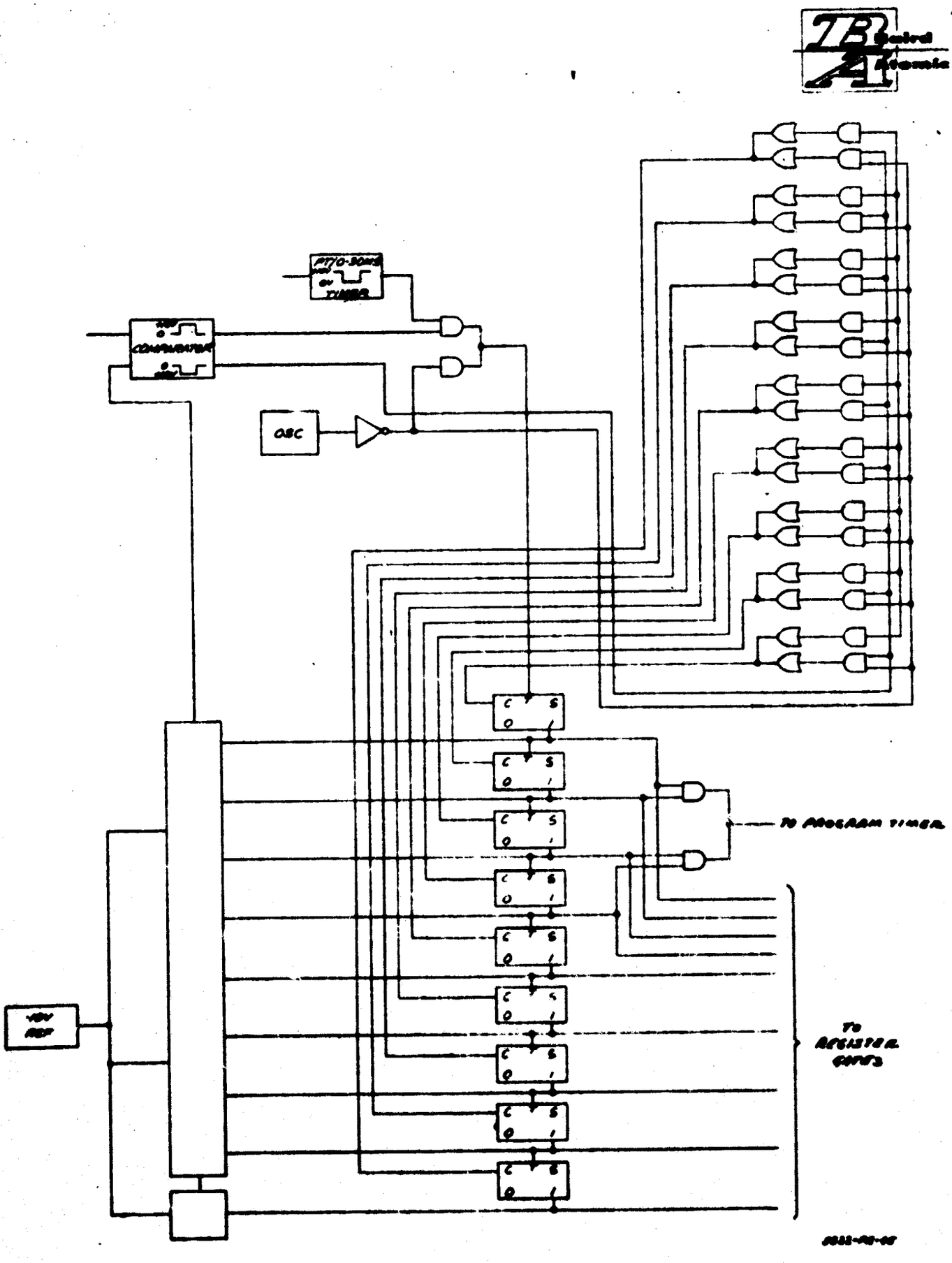

Figure 6-32. Analog-to-Digital Converter, Logic Diagram

6.1.3.4 Data Storage -- To provide a compatible system, the storage device for the analyzer data will be 10 9-bit flip-flop registers. The digitized word in the analog-to-digital converter is wired to the input gates of all 10 registers in parallel. The decoding matrix in the program timer provides pulses to transfer the data to the appropriate register. Figure 6-33 shows a logic diagram of the registers. This drawing is self-explanatory.

6.1.3.5 Readout -- Any one of the registers may be transferred to the countdown accumulator by depressing a button on the control panel. When a button is depressed, a gating voltage is applied to the appropriate transfer gate as indicated in figure 6-34. At the same time a gate is opened for the pulse generator to start the countdown. When the accumulator reaches zero, a pulse is generated which turns off the pulse generator. A decade counter has counted the number of pulses necessary to clear the accumulator and at the completion, which takes less than 10 milliseconds, the result is displayed on 3 Nixie tubes directly in parts per million. This circuit is also self-explanatory.

6.1.3.6 Electronic Packaging -- The electronic system is divided into three mechanical assemblies:

a. Relay Network and Integrator Assembly
b. Signal Shaping, Analog-to-Digital Converter and Readout Logic Assembly
c. Power Supply Chassis

The relay network and integrator assembly electronics will be mounted on four 5-inch x 8-inch printed circuit cards. The cards will be placed in a sealed housing purged of all air and filled with dry nitrogen to minimize the affects of humidity on the storage capacitors. The assembly will be located directly beneath the photomultiplier tubes, keeping lead lengths from the tubes to the storage capacitors to a minimum (figure 6-35).

Signal shaping, analog-to-digital converter and readout logic assembly consists of a rectangular open frame box formed from extruded angle, to which

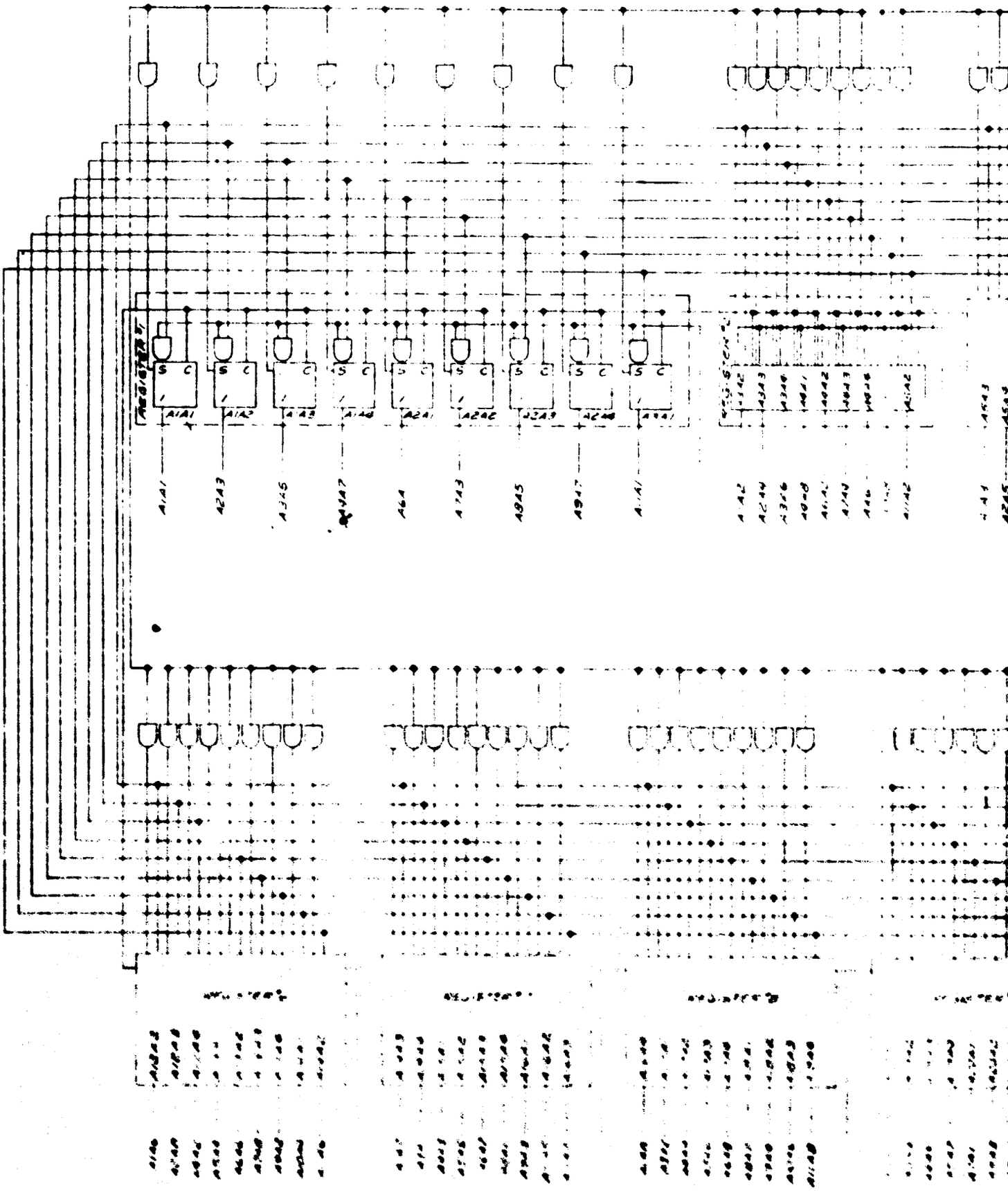

A

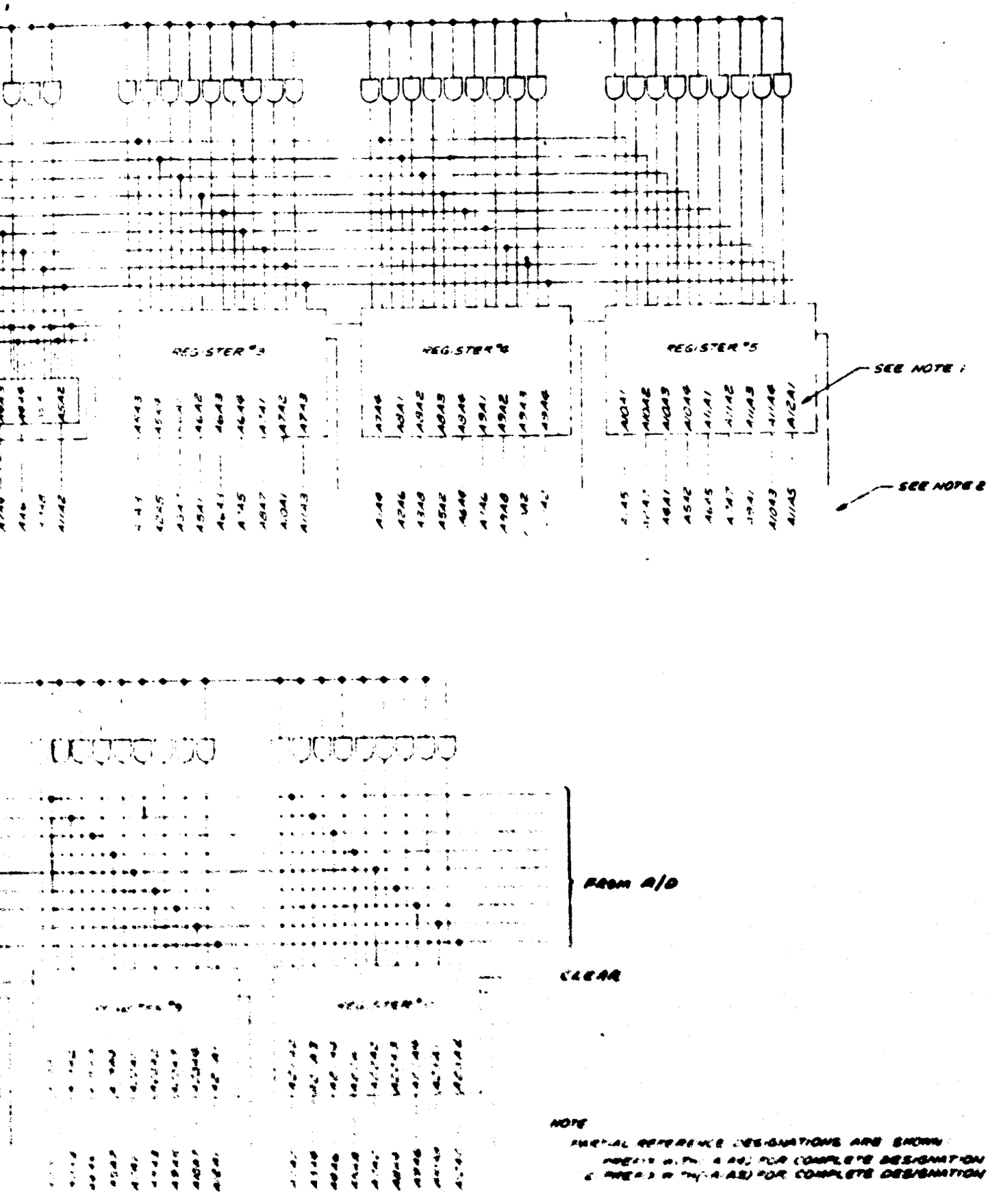

Figure 6-33. Element Register, Logic Diagram

B

A

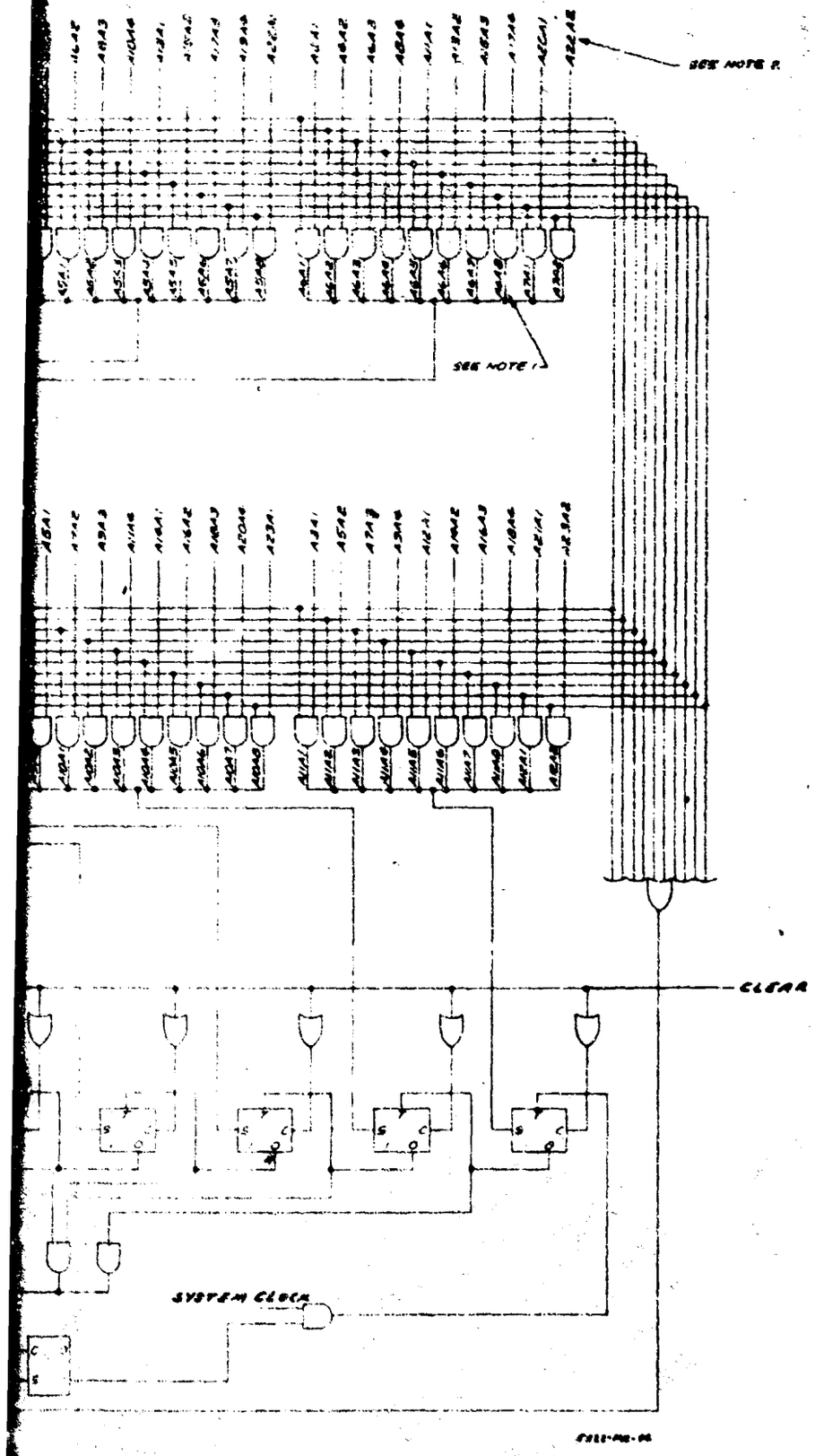

NOTE
PARTIAL REFERENCE DESIGNATIONS ARE SHOWN:
1 PREFIX WITH (1A1A5) FOR COMPLETE DESIGNATION
2 PREFIX WITH (1A1A6) FOR COMPLETE DESIGNATION

Figure 6-34. Register Readout, Logic Diagram

B

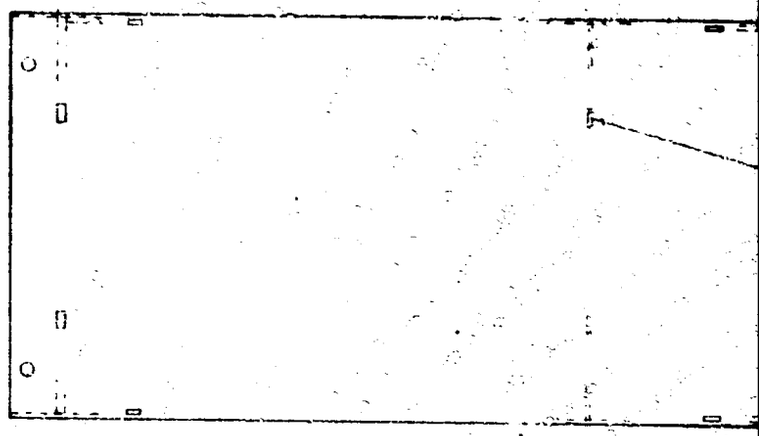

VIEW B-B

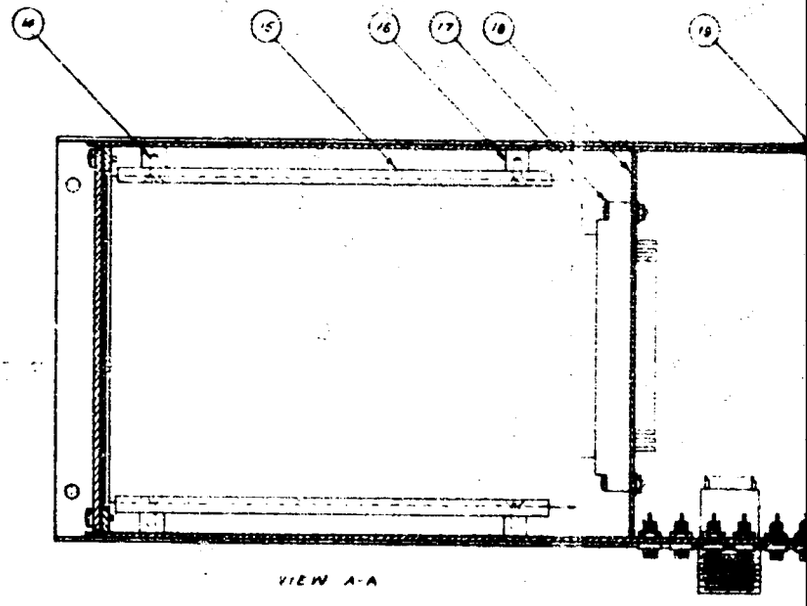

VIEW A-A

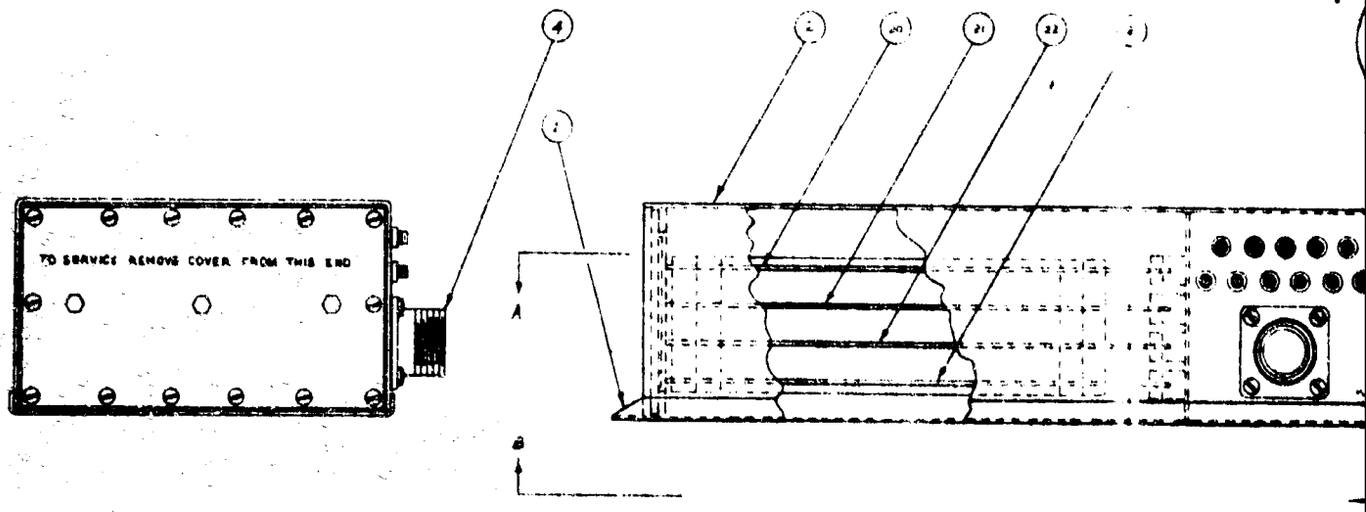

A

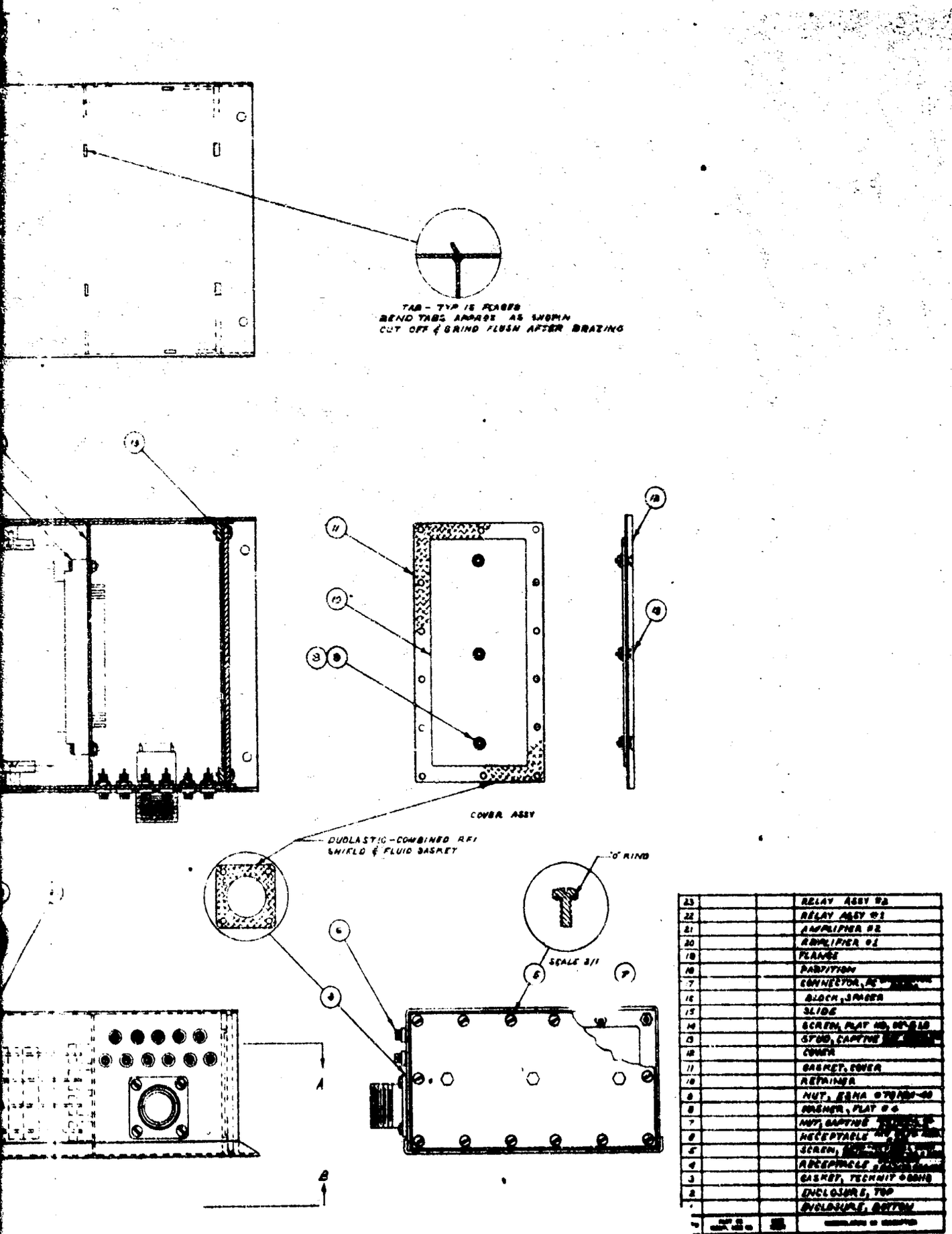

23			RELAY ASSY #2
22			RELAY ASSY #1
21			AMPLIFIER #2
20			AMPLIFIER #1
19			FLANGE
18			PARTITION
17			CONNECTOR, RF
16			BLOCK, SPACER
15			SLIDE
14			SCREW, FLAT HD, 82° SLD
13			STUD, CAPTIVE
12			COVER
11			GASKET, COVER
10			RETAINER
9			NUT, ESNA 8-32 UNC-2B
8			WASHER, FLAT #4
7			NUT, CAPTIVE
6			RECEPTACLE
5			SCREW,
4			RECEPTACLE
3			GASKET, TECHNIT #8616
2			ENCLOSURE, TOP
1			ENCLOSURE, BOTTOM

Figure 6-35. Relay Network and Integrator Assembly

standard printed circuit card hardware is added, sufficient for accepting 100 3-1/2-inch x 5-inch plug-in cards. When the access panel is removed, the connector end of the card is exposed. The terminals on the connector will be marked and can be used as test points. To remove a card or get at the signal shaping potentiometer, the entire assembly swings out by means of a hinge about a vertical axis. Two snap slide fasteners hold the assembly in the retracted position (figure 6-36).

All the power supplies are mounted on a single chassis and can be removed as a unit. Power supply test points are located behind the same access panel which covers the signal shaping electronics assembly (figure 6-37).

6.1.4 System Mechanical Design

The principal mechanical design criteria are:

a. MIL-Specification Requirements for Ground Support Equipment
b. Isolation from Environmental Influence
c. Simple Operation Servicing and Maintenance

6.1.4.1 Design Considerations Based on Environmental Conditions -- All components are designed to withstand MIL-Specification conditions for Class III sheltered electronic ground support equipment per MIL-STD-810 which specifies:

a. Humidity (Method 507)

   Relative humidity of 95 percent at 71°C (nonoperating)

b. Temperature (Method 501 and 502)

   Operating: 0°C to 55°C

   Survival: 62°C to 71°C

c. Shock (Method 516, Procedure II)

   30 g's in both directions along three perpendicular axes.

d. Vibration (Method 514)

   15 to 26 cps at 1.3 g's

   26 to 50 cps at 0.036 double amplitude

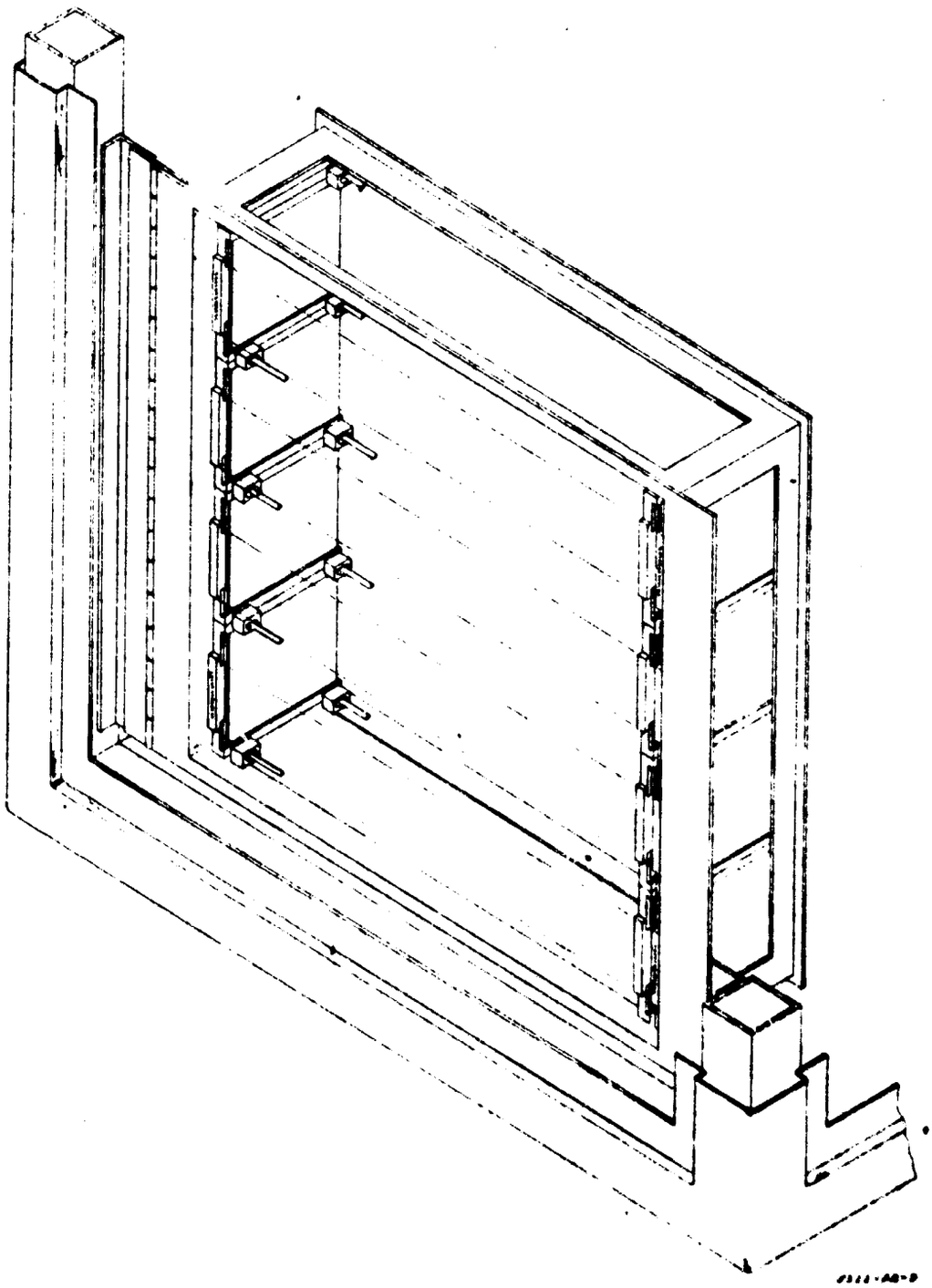

Figure 6-36. Electronic Plug-In Rack

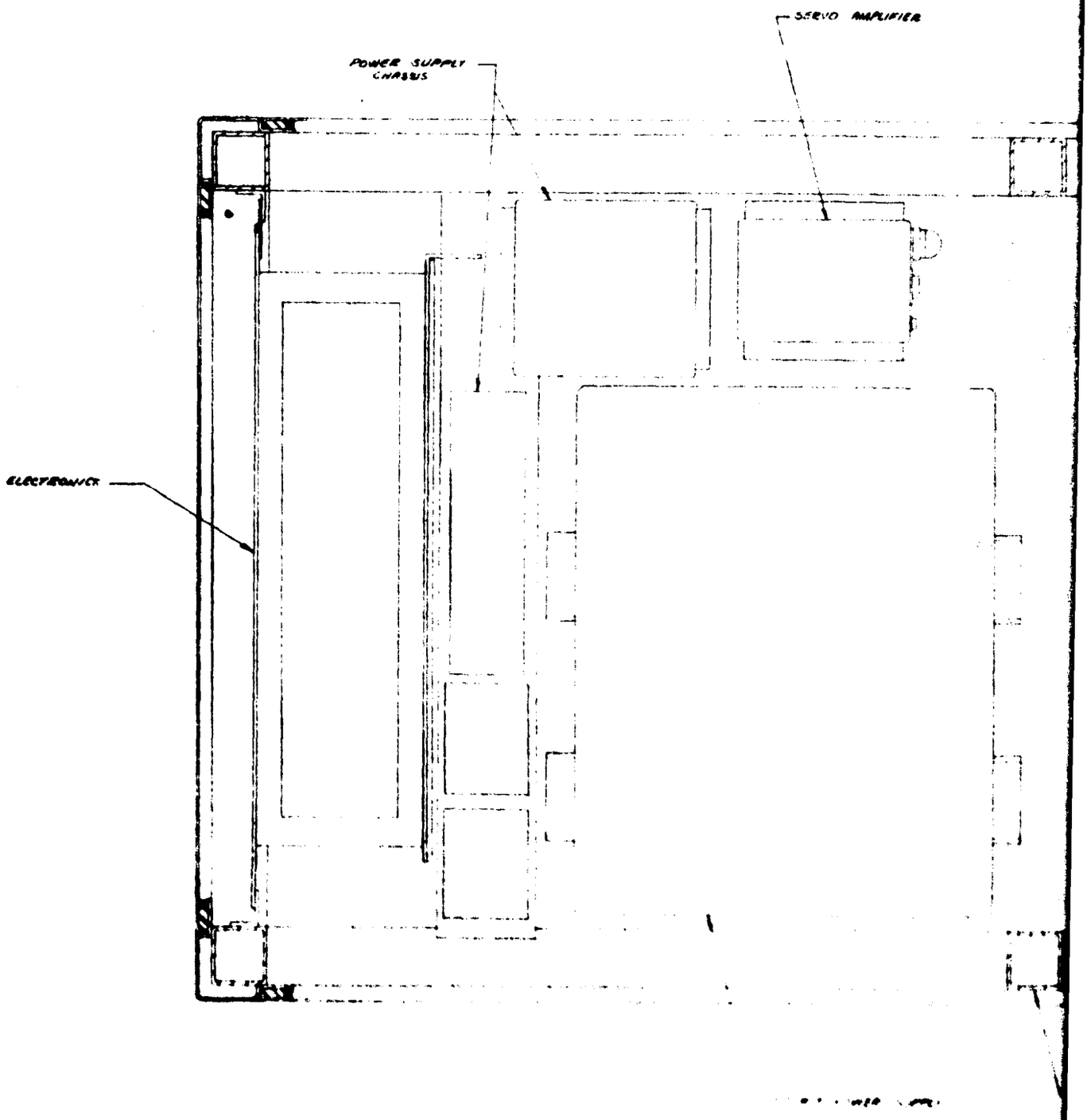

A

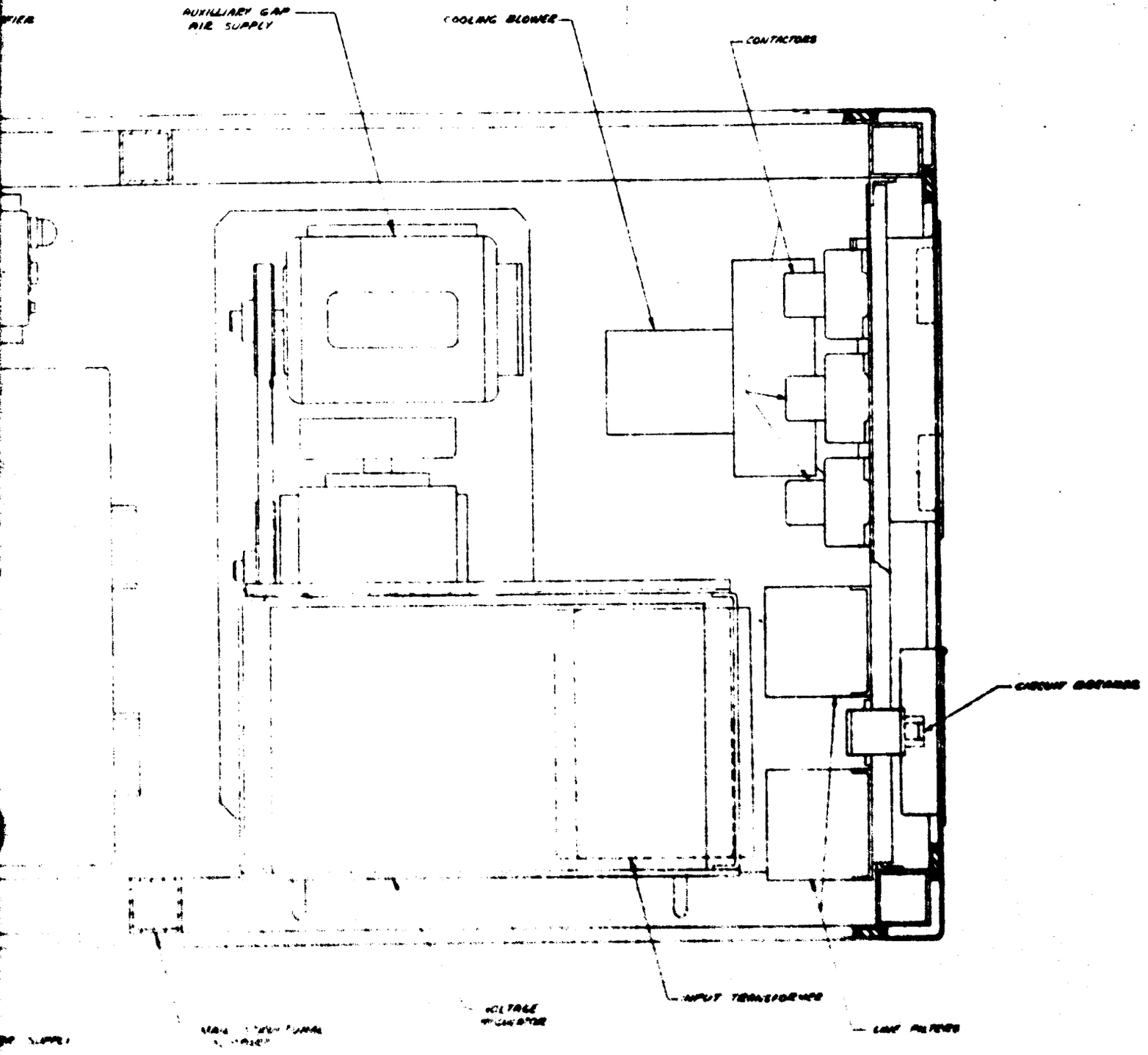

Figure 6-37. Base Level Analyzer (Cross Section to Support Equipment Area)

6.1.4.1.1 Humidity -- Humidity is only a problem in that condensation on the optical elements and certain electronic components would seriously impair their performance. In some installations it may be necessary to draw upon exterior air for both the auxiliary gap air supply and general cooling in order to comply with the explosion hazard requirements. Humidity control is especially critical under this condition. Several approaches are possible.

Dehumidifiers are a logical approach. Two types are available: absorption and cold coil. The standard absorption equipment heats the air under some conditions which obviously reduces its cooling capacity. The cold coil type requires either a cold water supply or an active refrigeration system with attendant maintenance problems, complexity, and cost, further a condensate drain is required.

Sealing the equipment and enclosing an air conditioner as a closed loop system is another solution but maintenance, complexity, weight, and cost are disadvantages here also.

The design used was selected for simplicity and effectiveness throughout the operating requirements. It is based on temperature control combined with a desiccant which is automatically reconstituted. The cooling fan operates only when the equipment temperature exceeds 90°F which maintains equipment at temperatures above the dewpoint of intake air at 130°F and 25 percent relative humidity (the apparent worst case condition).

Formulation of condensation in the equipment when shut down is averted by automatic close off of all ports. Desiccant containers are strategically located within the cabinet to absorb entrapped moisture during shut down. Their placement is such that they effectively protect the vital components and also are in the hottest sections of the cooling air so that they are regenerated during operation. If necessary they will be electrically regenerated with automatic control.

6.1.4.1.2 Temperature -- There are two areas which, due to different temperature control requirements, must be treated separately:

a. Optical Head Area

b. Support Equipment Area

Physically, the optical head area consists of the entire upper half of the console and the support equipment area is the lower half of the console (figure 3-3).

In the optical head, temperature gradients are the major design concern, whereas in the support equipment area the temperature must be kept within the designed operating range of the components.

Thermal control of the optical head consists of minimizing heat sources that would impart mechanical distortions into the optical housing, thus disturbing the optical alignment of the system. It is not necessary that the temperature of the optical head be kept fixed, but that thermal gradients must be held at a minimum over the entire optical head.

These effects are controlled by:

a. The high thermal conductivity of the aluminum as the housing material allows the optical head to reach thermal equilibrium rapidly.

b. Since the thermal mass of the optical housing is large, its thermal time constant is high. This results in slow change in housing temperature for large shifts in surrounding air temperature.

c. In order to minimize rapid changes of air temperature around the head, both the optical head and the cabinet interior are thermally insulated so as to isolate the optical head.

The average heat generated in the support equipment area is about 1000 watts. Considering the maximum operating temperature of 130°F and limiting the temperature of the exhaust air to 150°F, the volume of air required for cooling purposes is approximately:

Cubic feet per minute (CFM) $= \frac{3170 \times KW}{\Delta T}$

$\Delta T = 150°F - 130°F = 20°F$

$KW = 1$

$CFM = \frac{3170 \times 1}{20}$

$CFM = 158.5$

In order to overcome back pressures caused by the restricted air intake and ducting requirements, a centrifugal type blower is used. The Rotron Model D type blower is best suited for this application.

As discussed in the humidity control section, the blower will be thermostatically controlled to go "on and off" at a specific temperature.

Cooling air will be brought in through the right side of the console, across a dust filter, circulated in the support equipment area, past the desiccant and out through an exhaust port on the left side of the console.

6.1.4.1.3 Shock and Vibration -- Test conditions prescribed in MIL-STD-810 specify for this weight equipment:

Shock - (per Method 516, paragraph 4, Procedure II)

30 g half-sine 11 millisecond duration pulse applied in both directions along three mutually perpendicular axes.

Vibration - (per Method 514, Class 6, mounting "B", paragraph 5.6)

15 to 26 cps at 1.3 g
26 to 50 cps at 0.036 double amplitude

A fragility level of 10 g's was set as a design guide for maximum shock transmission.

In order to withstand these specifications, a study showed that mounts with a natural frequency of 8 to 10 cps loaded, transmissibility below four, and a deflection of 1-1/2 inches would be required.

A set of isolators, one in each corner of the base of the console, is sufficient to meet the specification. However, since the center of gravity of the unit must be located high above the mounts, clearances for large excursions must be allowed for in the trarsit case size, especially in console depth. In order to reduce these excursions, a set of supplementary isolators are located on the rear of the console (figure 6-38).

Supplementary isolators are functioning only when the oil analyzer is in a transit condition with the shroud in place. During operation, only the base isolators are functioning.

In order to support the loads imposed by the optical head, because of its weight and location in the system, a welded structural frame of square aluminum tubing was designed. All the loads are transferred to the isolators through the structural frame (figure 6-39).

6.1.4.2 Radio Frequency Interference -- To provide effective radio frequency interference control, shielding for both internal and external electronics was carefully designed. To reduce the radiation to the levels required in MIL-I-26600, double shielding was required. A ground terminal sufficiently large to accept a 1-inch wide grounding strap is provided as part of the equipment.

A good ground is absolutely essential to radio frequency interference control.

All possible leakage paths in the console are shielded, in addition the source supply is double shielded (figure 6-40). Two sides are replaced with wire mesh to allow for circulation of cooling air. The analytical and auxiliary gap housing is shielded from the internal electronics and the viewing windows are covered back and front with mesh. All intakes and exhaust parts are shielded with metal honeycomb and the back of the control panel is fitted with a cover which reduces radio frequency interferernce leakage through the controls.

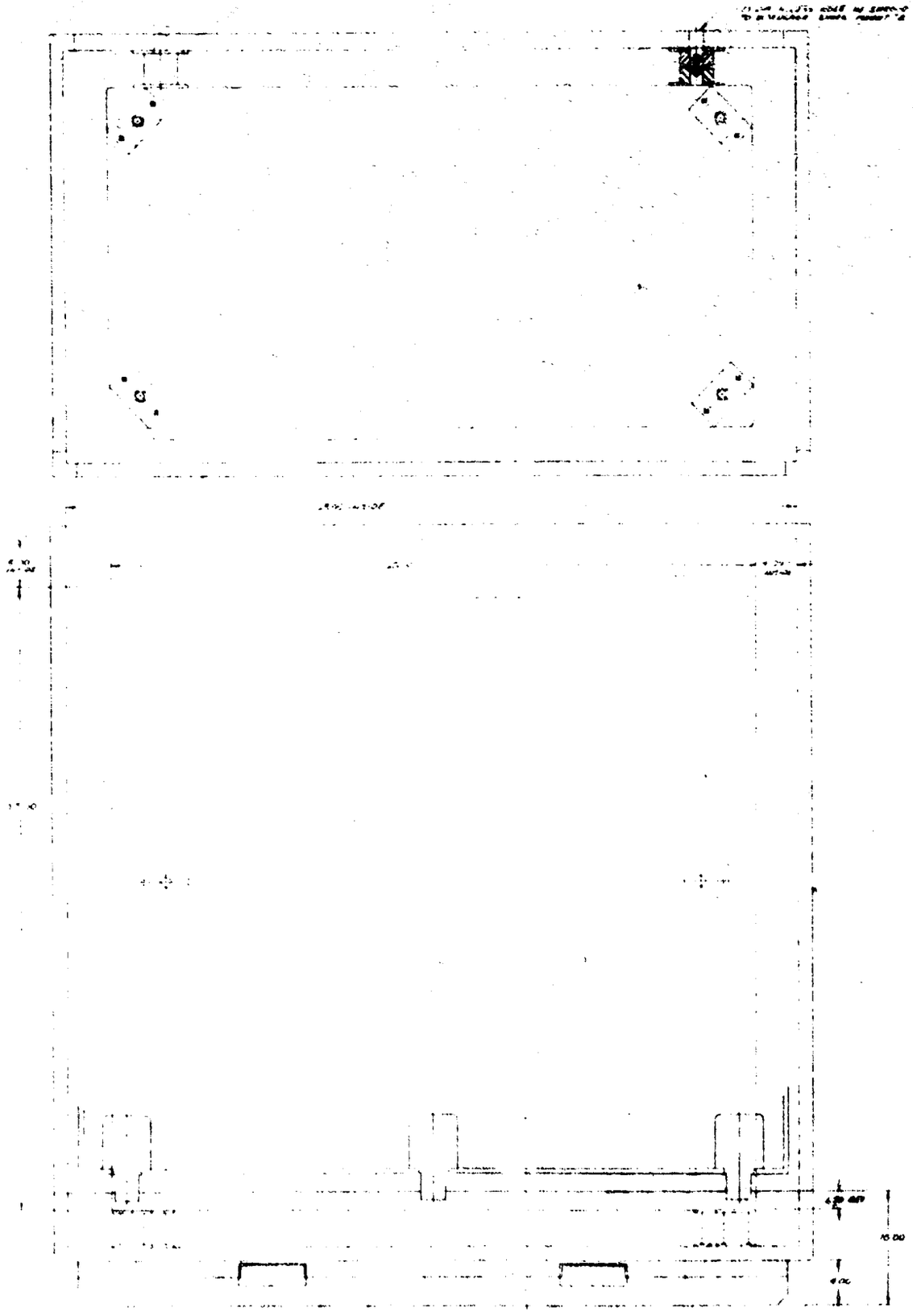

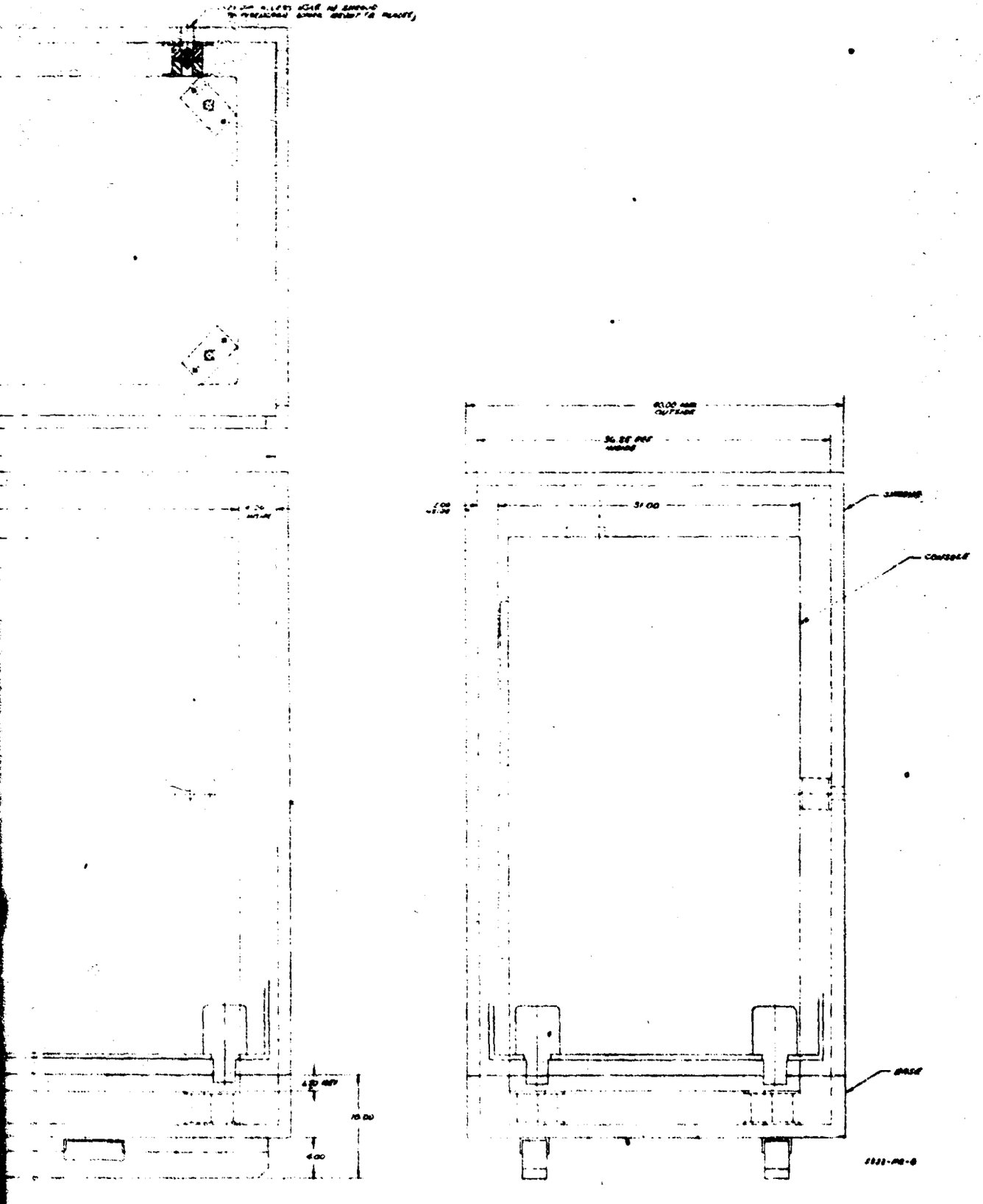

Figure 6-38. Transit Case Assembly

B

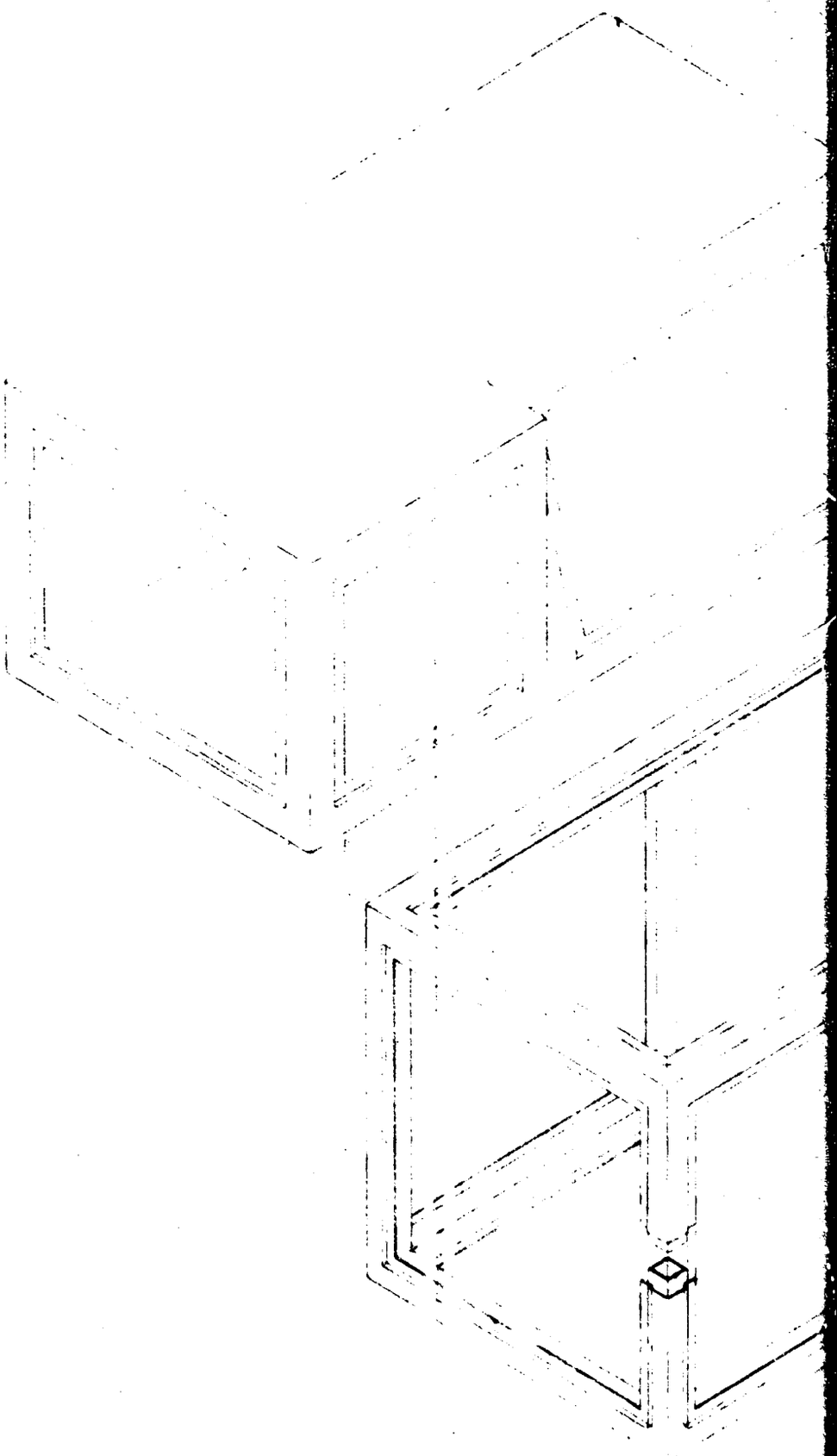

A

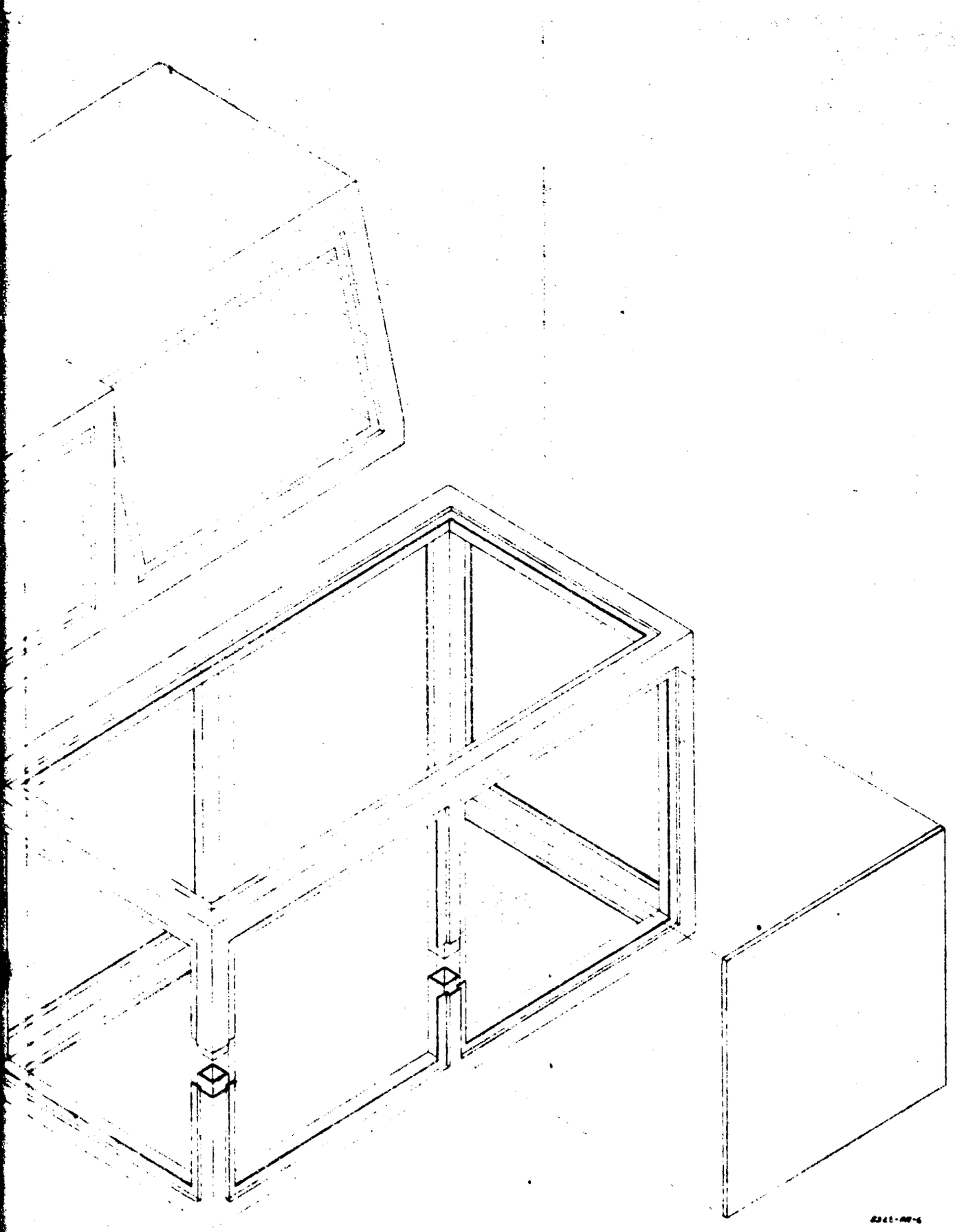

Figure 6-39. Cabinet

B

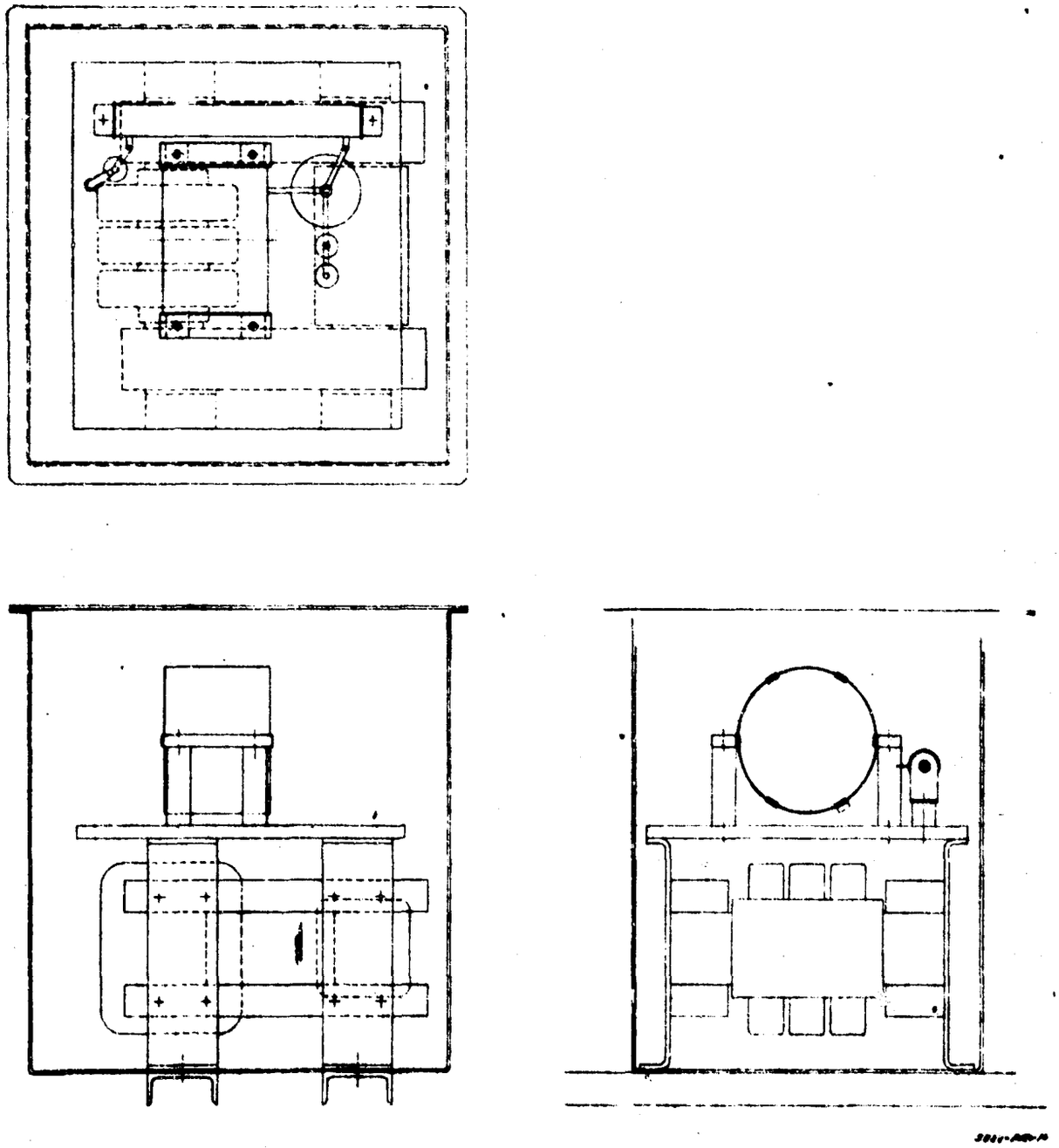

Figure 6-40. Source Power Supply Assembly

Access panels and doors are fitted with combination radio frequency interference and fluid gasketing. It is important that radio frequency interference gasket seals be free of oxidation and that they be good electrical conductors.

All aluminum surfaces will be coated with Iridite no. 14 which is an excellent corrosion inhibition for aluminum and a very good electrical conductor.

6.1.4.3 Mechanical Description -- The console has been designed to conform as closely as possible to the human engineering design criteria set forth in MIL-STD-803A-1.

After reviewing the procedure for preparing, analyzing, and recording an oil sample test, a sit/stand console height was considered to be the most practical and expeditious position for operating the analyzer. The instrument grouping on the control panel is arranged so that all calibrating and system test functions are together on one side and the sample analyzing functions on the other. A writing surface the length of the console is provided. The area in front of the control panel is used for recording sample data and the area in front of the analytical gap access door for preparing and storing samples for analysis (figure 3-1).

The console is laid out so that all optics, analytical and auxiliary gaps, signal storage, and relay switching assembly are located in the upper half of the console. The supporting equipment, such as electronics, power supplies, filters, blowers, etc., are located in the lower half of the console.

In order to simplify installation and transportation problems, the console need not be removed from the skid. The console has been designed so that all maintenance and operating procedures can be efficiently carried out with the console on the skid.

The entire system is contained in one console and can be shipped in one transit case (figure 6-38). Size of shipping container: 71 inches in height, 72 inches in width, 40 inches in depth, maximum dimensions.

6.1.4.4 Weight Budget

Analytical and Auxiliary Gap Housing	30.0 pounds	
Optical Head	160.0	
Cabinet	150.0	
Power Supplies	10.0	
Electronics	12.0	
Line Filters	25.0	
Line Transformer	53.0	
Air Supply (Auxiliary Gap)	81.0	
Blower	10.0	
Source Supply	75.0	
Contactors	5.0	
Oscilloscope	9.0	
Cabling	10.0	
Miscellaneous	20.0	
Relay Integrator Assembly	3.0	
Console		653 pounds
Transit Case (skid and transit case)		340
Total		993 pounds